TAMPEREEN TEKNILLINEN YLIOPISTO
TAMPERE UNIVERSITY OF TECHNOLOGY
Julkaisu 677 • Publication 677

Yuan Yang

Filter Bank Based Channel Equalization in Broadband Wireless Single-Carrier Systems

Tampere 2007

Tampereen teknillinen yliopisto. Julkaisu 677
Tampere University of Technology. Publication 677

Yuan Yang

Filter Bank Based Channel Equalization in Broadband Wireless Single-Carrier Systems

Thesis for the degree of Doctor of Technology to be presented with due permission for public examination and criticism in Tietotalo Building, Auditorium TB109, at Tampere University of Technology, on the 19th of October 2007, at 12 noon.

Tampereen teknillinen yliopisto - Tampere University of Technology
Tampere 2007

ISBN 978-952-15-1844-7 (printed)
ISBN 978-952-15-1877-5 (PDF)
ISSN 1459-2045

Abstract

Channel equalization is a very important anti-multipath technique in broadband communication systems and it has received much attention during the era of digital communications. Frequency selective fading arises whenever the bandwidth of the transmitted signals is comparable to, or larger than the channel delay spread. In the absence of any suitable signal processing in the receiver, this leads to significant distortion of the signal due to intersymbol interference, which is a major barrier to high-speed digital transmission over wireless channels. This thesis considers frequency-domain signal processing techniques to combat intersymbol interference effects in the context of single-carrier broadband wireless transmission. Meanwhile, it has been recognized that filter bank transforms with high frequency selectivity can offer many advantages over the current discrete Fourier transform based approaches for frequency-domain processing. The main objective of this thesis is to establish a novel single-carrier frequency-domain equalization model utilizing perfect reconstruction, orthogonal, complex modulated filter banks.

An introduction to modulated filter banks and common channel equalization techniques is first given. The main research work presented in this thesis can be separated into two topic areas: *frequency-domain channel equalization* and *combined equalization/decoding schemes* for coded transmission. First, compared to the discrete Fourier transform approach, the important property of filter bank based equalization is that the channel subband response is not flat anymore. The subband equalizer responses are designed to cope with the channel response within each subband, by utilizing a low-complexity frequency sampling based approach. This is in contrast with the discrete Fourier transform approaches where channel equalization is done with a single complex multiplier per subband. One merit of using the filter bank approach is the absence of cyclic prefix preceding the data block, improving the data rate accordingly. Furthermore, this scheme can be used for any communications waveform and it exhibits improved tolerance against narrowband interference. The same filter banks can be used to provide a significant part of the channel filtering, thus relieving the receiver front-end complexity and leading to a very flexible receiver structure.

Second, in the case of coded transmission, the optimal way for equalization/decoding is to use the maximum a posteriori probability equalizer. The problematic issue of such an optimal method would be the high calculation complexity involved, especially when high-order modulation is applied and long channel delay spread may be encountered. This motivates to develop low-complexity solutions for the equalization/decoding loop. A brief introduction of well-known turbo equalization is given in this thesis and two low-complexity

equalization/decoding methods are developed. Our approach is based on the decision feedback equalization concept utilizing the noise prediction model and decoding in the feedback loop.

Preface

The research work for the thesis has been carried out during the years 2001-2006 at the institute of Communications Engineering (ICE), former Telecommunications Laboratory of Tampere University of Technology, Tampere, Finland. This thesis is the result of work whereby I have been supported by many people.

Deep thanks and appreciation are not enough to express my gratitude toward my supervisor Prof. Markku Renfors for his kind supervision, valuable comments and infinite tolerance throughout the stages of this research, which helped to propel my research work and to prepare this dissertation.

I would like to express my thanks to Prof. Phillip Regalia from Department of Electrical Engineering and Computer Science, Catholic University of America and Dr. Nikolai Nefedov from Nokia Research Center, Switzerland, the reviewers of this thesis, for their valuable and constructive feedback.

I certainly like to thank all ICE members for creating such a cheerful working environment. In addition, I would like to deeply thank my colleagues, Tero Ihalainen and Tobias Hidalgo Stitz, for always giving clear and full answers to my questions and fruitful cooperation, to Mika Rinne from Nokia Research Center for his constructive comments on the publications. Separate words of gratitude go to Ali Hazmi, Ari Viholainen, Juuso Alhava, Monaem Lakhzouri and Toni Levanen for pleasant support and discussion during the work. Much thanks are due to Tarja Erälaukko, Sari Kinnari, Ulla Siltaloppi and Elina Orava for their kind help with practical things.

I am really grateful to all my friends in Finland for spending a great time together, especial to our Chinese community in Tampere area.

This thesis was financially supported by Nokia, Academy of Finland (project: Advanced Multicarrier Techniques for Wireless Communications), and National Technology Agency of Finland (Tekes, project: Digital and Analog Techniques for Flexible Receivers), which are gratefully acknowledged.

Finally, I want to express my deep gratitude to my parents, to my brother for their understanding, even though they are at a far distance. My warmest thanks go to my wife, Lu Li, for her endless love, continuous encouragement during these years.

YUAN YANG

Tampere, September 19, 2007

Contents

List of Publications **vii**

List of Symbols and Acronyms **xi**

1 Introduction **1**
1.1 Background and motivation 1
1.2 Scope and organization 3

2 Modulated Filter Bank Systems **7**
2.1 Introduction 7
2.1.1 Analysis filter banks 8
2.1.2 Synthesis filter banks 8
2.1.3 Filter bank systems 9
2.2 Modulated filter banks 10
2.2.1 Cosine/sine modulated filter banks 10
2.2.2 Complex modulated filter banks 12
2.3 Efficient implementation of PR cosine modulated filter banks 14
2.4 Programmable digital signal processor based implementation 17

3 Channel Equalization **21**
3.1 A discrete-time system model 21
3.2 Equalizer design criteria 24
3.3 Time-domain equalizer 27
3.3.1 Maximum likelihood equalizer 27
3.3.2 Linear equalizer 28
3.3.3 Decision-feedback equalizer 28
3.3.4 Interference cancelation equalizer 29
3.4 Frequency-domain equalizer 31

3.4.1 FFT-FDE 32
3.4.2 Noise prediction DFE 33
3.5 Our studies 34

4 On Combined Equalization and Decoding **37**
4.1 Introduction 37
4.2 Transmission scheme 38
4.3 Turbo equalization 39
4.3.1 MAP equalizer 40
4.3.2 MAP decoder 41
4.3.3 Turbo equalization using MSE equalizer 41
4.4 Our studies 42

5 Summary of Publications **45**
5.1 Overview of studies 45
5.2 Author's contributions to the Publications 46

6 Conclusions and Future Work **49**

References **51**

List of Publications

[P1] Y. Yang, T. Ihalainen, M. Rinne and M. Renfors, "Frequency-domain equalization in single-carrier transmission: Filter bank approach," *EURASIP Journal on Advances in Signal Processing*, vol. 2007, Article ID 10438, 16 pages, 2007.

[P2] Y. Yang, M. Rinne and M. Renfors, "Filter bank based frequency-domain equalization with noise prediction," *in Proc. 17th Annual IEEE International Symposium on Personal, Indoor and Mobile Radio Communications,* PIMRC'06, Helsinki, Finland, 2006.

[P3] Y. Yang, T. Ihalainen, M. Rinne and M. Renfors, "Noise predictive Turbo equalization for a filter bank based receiver in SC transmission system," *in Proc. IEEE 65th Vehicular Technology Conference Spring*, VTC'07, Dublin, Ireland, April 2007, pp. 2389-2393.

[P4] Y. Yang and M. Renfors, "Channel equalization in wideband single-carrier transmission using a filter bank transform and a block interleaved DFE," *in Proc. IEEE 8th Workshop on Signal Processing Advances for Wireless Communications*, SPAWC'07, Helsinki, Finland, June 2007.

[P5] Y. Yang, M. Rinne and M. Renfors, "Mitigation of narrowband interference in single carrier transmission with filter bank equalization," *in Proc. IEEE Asia Pacific Conference on Circuits and Systems*, APCCAS'06, Singapore, December 2006, pp. 748-751.

[P6] Y. Yang, T. Ihalainen, J. Alhava and M. Renfors, "DSP implementation of low-complexity equalizer for multicarrier systems," *in Proc. IEEE 7th International Symposium on Signal Processing and Its Applications*, ISSPA'03, Paris, France, July 2003, vol. 2, pp. 271-274.

[P7] Y. Yang, T. H. Stitz and M. Renfors, "Implementation of a filter bank based narrowband interference suppression algorithm on a DSP processor," *in Proc. IEEE International Conference on Telecommunications*, ICT'02, Beijing, China, June 2002, pp. 608-611.

List of Figures

2.1 Basic blocks of analysis-synthesis filter bank system. 8

2.2 Magnitude response of the filters in the case of cosine modulation. 10

2.3 Comparison of the subband frequency responses of DFT and EMFB (the roll-off factor $\rho = 1$ and overlapping factor $K = 5$). 13

2.4 Efficient implementation for exponentially modulated filter bank. 13

2.5 Channel equalization with oversampled EMFB structure using two CMFBs and SMFBs. 15

2.6 Fast implementation of the cosine modulated filter bank. 16

2.7 Functional block diagram of a GSM phone. 18

3.1 Multipath environment in wireless channel. 22

3.2 Discrete-time baseband equivalent channel model. 23

3.3 An ISI channel modeled as an FIR filter with AWGN. 24

3.4 System model with channel equalization. 25

3.5 Signal spectra in the cases of SSE and FSE. 25

3.6 Frequency-domain SSE and FSE performance comparison in the ITU-R Vechicular A channel model with 20 MHz bandwidth (uncoded cases). . . . 26

3.7 Block diagram of decision-feedback equalizer. 29

3.8 Block diagram of the interference cancelation equalizer. 30

3.9 Performance comparison among the traditional equalizers; Uncoded QPSK modulation in Proakis type B channel. 31

3.10 FFT-FDE and noise prediction type DFE. 34

4.1 Transmitter side in the coded modulation. 38
4.2 An example of block interleaver with parameters (4,3). 39
4.3 A receiver diagram of turbo equalization using MAP equalizer. 40
4.4 A receiver diagram of turbo equalization using MSE filter equalizer. 42

List of Symbols and Acronyms

SYMBOLS

$(.)^*$	Complex conjugation
$\|.\|$	Absolute value
E_b	Average energy of a bit
E_s	Average energy of a symbol
$E\{.\}$	Statistical expectation
$L(.)$	Log-likelihood function
$H_{eq}(.)$	Discrete-time baseband equivalent channel
$H_0(.)$	Continuous-time baseband equivalent channel
N_0	Noise power spectral density
$P(.)$	Apriori probability
T	Symbol interval
f_s	Sampling frequency
g_l	Feedback equalizer coefficients
$h_C(.)$	Channel impulse response
$h_T(.)$	Transmitter filter impulse response
$h_R(.)$	Receiver filter impulse response
j	Imaginary unit ($j = \sqrt{-1}$)
$p(.\|.)$	Conditional probability density function
v_m	Discrete noise samples
w_l	Forward equalizer coefficients
x_m	Discrete transmitted symbols
$\hat{x}_m$	Discrete estimate symbols

y_m	Discrete received samples
$\bar{y}_m$	Discrete equalized samples

ACRONYMS

3G	3rd Generation wireless system
3GPP	3rd Generation Partnership Project
ARQ	Automatic Retransmission Request
ASIC	Application-Specific Integrated Circuit
AWGN	Additive White Gaussian Noise
BER	Bit Error Rate
BPSK	Binary Phase Shift Keying
BWA	Broadband Wireless Access
CDMA	Code Division Multiple Access
CMFB	Cosine Modulated Filter Bank
CP	Cyclic Prefix
DCT	Discrete Cosine Transform
DFE	Decision Feedback Equalizer
DFT	Discrete Fourier Transform
DST	Discrete Sine Transform
DS-SS	Direct Sequence Spread Spectrum
ELT	Extended Lapped Transform
EMFB	Exponentially Modulated Filter Bank
FB	Filter Bank
FBF	Feed Back Filter
FDE	Frequency-domain equalization
FDMA	Frequency Division Multiple Access
FER	Frame Error Rate
FFT	Fast Fourier Transform
FFF	Feed Forward Filter
FIR	Finite Impulse Response
FSE	Fractionally-spaced Equalizer
GSM	Global System for Mobile communications
IBI	Interblock Interference

IC	Interference Cancelation
ISI	Intersymbol Interference
LAN	Local Area Network
LE	Linear Equalizer
LDPC	Low-density Parity-check Code
LLR	Log-likelihood Ratio
ITU	International Telecommunication Union
MAP	Maximum A Posteriori
ML	Maximum Likelihood
MLSE	Maximum Likelihood Sequence Estimation
MSE	Mean Square Error
NBI	Narrowband Interference
NLOS	Non-Line Of Sight
NPR	Nearly Perfect Reconstruction
OFDM	Orthogonal Frequency Division Multiplexing
PAM	Pulse Amplitude Modulation
PN	Pseudo-random Number
PR	Perfect Reconstruction
QAM	Quadrature Amplitude Modulation
QPSK	Quadrature Phase Shift Keying
RF	Radio Frequency
RRC	Root Raised Cosine
SISO	Soft-Input Soft-Output
SMFB	Sine Modulated Filter Bank
SNR	Signal-to-Noise Ratio
SSE	Symbol-Spaced Equalizer
TDMA	Time Division Multiple Access
TMUX	Transmultiplexer
UTRAN	Universal Terrestrial Radio Access Network
WMF	Whitened Match Filter
ZF	Zero Forcing

Chapter 1

Introduction

1.1 BACKGROUND AND MOTIVATION

Broadband wireless access (BWA) techniques have become a focus of worldwide research and commercial activities. Next generation mobile radio systems will provide a wide variety of integrated multimedia services, supported by greatly increased system capacity. Compared to today's cellular systems, the next generation mobile and fixed wireless systems will have a much higher channel bit rate capability, e.g., to provide over 10 Mb/s multimedia services to multiple users within each coverage area. BWA techniques will be required to overcome the effects of multipath delay spread over mobile radio channels.

Due to the distortion characteristics of the wireless propagation environment, the transmitted data symbols in bandlimited channels will spread out in time and interfere with each other. A phenomenon named intersymbol interference (ISI) has been recognized as the major obstacle to high-speed data transmission [Proa 01, Falc 02a, Gold 05]. Generally, the degree of ISI depends on the data rate; the higher the data rate, the more ISI is introduced. Therefore, ISI mitigation schemes constitute a major challenge in current and future broadband wireless communication systems.

In broad sense, the ISI mitigation schemes can be applied both on the transmitter side and on the receiver side. Here we focus on processing techniques at the receiver end, which are generally regarded as channel equalization. Frequency-domain equalization (FDE) utilizing filter bank (FB) transforms in the case of single-carrier (SC) modulation is the main scope of this thesis.

Spread spectrum

Spread spectrum [Turi 80, Proa 01, Faze 03] is a modulation technique which increases the transmit signal bandwidth. There are two common forms of spread spectrum: direct sequence and frequency hopping. In direct sequence spread spectrum (DS-SS), information symbols are modulated by a pseudo-random (PN) sequence, which is also named as spreading code. Moreover, the autocorrelation properties of the spreading code determine

the multipath rejection capability. In conjunction with a RAKE receiver with ideal spreading codes, the energy in different multipath signal components can be collected and combined coherently through simple correlation processing. However, in practical multiuser environment with fading multipath channels, more elaborate receiver structures are needed for maximizing the system performance.

Multi-carrier modulation

The basic principle of multi-carrier (MC) modulation [Bing 90, Baha 99, Faze 03] relies on the transmission of data by dividing a high-rate data stream into a number of low-rate subchannel streams. These data sequences are modulated on different sub-carriers. By using a large number of sub-carriers, high immunity against multipath dispersion can be provided, because the sub-channel data symbol duration becomes much larger than the channel time dispersion. Hence, the effects of ISI will be minimized. It has been described in [Wein 71, Czyl 97, Falc 02a] that if the data blocks are cyclically extended prior to transmission and a sufficient number of subchannels are used, a complex-valued single-tap coefficient per subchannel provides ideal equalization.

Single-carrier systems with channel equalizer

A large amount of research work has been done in the area of single-carrier channel equalization over the last decades and several well-known techniques have been established. Among these, maximum likelihood sequence estimation (MLSE) is an optimal equalization technique. The common algorithm for MLSE is the Viterbi algorithm. Unfortunately, the complexity grows exponentially with channel delay spread and this approach is utilized only when the number of significant channel delay taps is small enough. Therefore, it is impractical in the context of broadband wireless transmission channels, which normally have longer dispersion length. Other commonly adopted techniques are based on symbol-by-symbol estimation, which can be basically divided into two broad categories: linear and nonlinear. The linear approaches are generally realized by a transversal filter, which has rather low-complexity as a linear function of the channel dispersion length. However, they typically suffer from noise enhancement for severely distorted wireless channels, such as channels with spectral nulls [Belf 79, Proa 01]. The advantage of nonlinear approaches, e.g., decision feedback equalization (DFE), is the reduction of ISI effect with lower noise enhancement, which result in better performance over linear equalizers. Meanwhile, with low signal-to-noise ratio (SNR), the nonlinear equalizers suffer from error propagation, due to wrong feedback decisions.

As data rates increase, the ISI distorts the transmitted signal even more. The difficulty of channel equalization in single-carrier broadband systems is thus regarded as a major challenge to high-speed transmission over mobile radio channels. Meanwhile, time-domain equalization solutions become unfavorable, because the transversal filters need to have a high number of taps to cover the maximum channel delay spread and result in high computational complexity [Clar 98]. This motivates the development of novel low-complexity solutions for broadband wireless transmission.

As an example, the wireless LAN systems described in the IEEE 802.11a and the HiperLan2 standards use orthogonal frequency-division multiplexing (OFDM) technique in the

physical layer. OFDM provides an effective, low-complexity way for wireless systems operated in the radio channels with high frequency selectivity in the transmission band. An alternative solution is the concept of single-carrier transmission with frequency-domain equalization (SC-FDE). It has been adopted by the IEEE 802.16 wireless metropolitan area network standard as an alternative technique to OFDM in the physical layer. Moreover, single-carrier frequency division multiple access (SC-FDMA) system adopted for the uplink of the UTRAN (Universal Terrestrial Radio Access Network) Long Term Evolution under standardization by 3GPP [3GPP] is based on SC-FDE processing on the receiver side.

SC-FDE is characterized by block-wise transmission, where equalization tasks are performed in frequency-domain. This leads to a remarkable complexity reduction compared to its time-domain counterpart when long delay spread channels are encountered [Kade 97, Clar 98, Falc 02a]. Interestingly, SC-FDE may be derived from OFDM by shifting the synthesis part from the transmitter to the receiver, thereby moving complexity to the receiver side. Then the overall complexity of SC-FDE is very similar to the OFDM systems. SC-FDE has two main well-known advantages over OFDM, namely, lower peak-to-average ratio and reduced sensitivity to carrier frequency errors [Sari 95, Falc 02a]. In [Kade 97, Gusm 03], it has been demonstrated that the SC-FDE systems have performance advantage, more diversity benefits compared with OFDM system. In [Sari 95, Czyl 97], SC-FDE has been shown to be more robust without heavy interleaving and error correction coding, and less sensitive to nonlinear distortion and carrier synchronization difficulties. Since the complexity in SC-FDE systems is concentrated on the receiver end, this concept is a good candidate for uplink transmission in future broadband wireless networks. Moreover, SC-FDE provides a possibility for hardware re-use with multicarrier-based downlink processing.

1.2 SCOPE AND ORGANIZATION

Filter banks provide an alternative way to perform time-frequency transforms with clearly better frequency selectivity than discrete Fourier transforms (DFTs). They have been used in traditional frequency division multiplexing telecommunication systems for long, and multirate digital filter banks were originally proposed for application in speech compression more than 20 years ago [Croc 83]. They have been used extensively in high-quality audio compression. In recent years, there has been growing interest in the use of filter banks in the context of multicarrier modulation [Hiro 80, Tzan 94, Sand 95, Alha 01, Sioh 02, Ihal 07]. Frequency-domain adaptive signal processing has also become an important field of study in broader application areas beyond communications [Shyn 92, Petr 00].

The goal of this thesis is to explore filter bank based multirate signal processing in broadband wireless communications, emphasizing on frequency-domain channel equalization. It consists of two major subjects, along with one minor subject related to digital signal processor based implementation. The studies are carried out in the context of broadband frequency-selective wireless channels.

1. Subband signal processing for channel equalization: The SC-FDE has been widely studied for over a decade. While the research on filter bank based multicarrier sys-

tems is gaining momentum in the wireless communications context, there is practically no earlier literature on the use of filter banks in the frequency-domain channel equalization context. This is surprising, since subband signal processing utilizing filter banks has been studied in some extent in other application areas [Shyn 92]. In the literature, there are a few contributions focusing on cyclic prefix (CP)-free methods based on overlapped FFT processing [Falc 02b, Mart 03, Schn 04], which can be seen as low-complexity filter banks. Our aim is to explore efficient combinations of filter bank systems and subband-wise equalizers, as an alternative way for performing the SC-FDE task. In addition, it has been shown that filter bank based narrowband interference mitigation provides clearly better performance than DFT based methods [Hara 96, Medl 97, Stit 04], due to filter banks' ability to compactly represent the interfering signal energy in the transform domain. Enhanced frequency-domain narrowband interference mitigation utilizing the proposed FB-FDE structure is also addressed. Here only a minor additional calculations are introduced, compared to the basic FB-FDE.

We start our studies in filter bank based frequency-domain equalization from the linear equalizer case, focusing on the fractionally-spaced equalizer model. In the next step, non-linear equalization based on decision feedback (DFE) model is considered. It turns out that the DFE model based on noise prediction is particularly useful in our application. The considered DFE structure includes a fractionally-spaced, filter bank based frequency domain equalizer as the feedforward filter and noise predictor as the feedback filter.

2. Combined equalization/decoding schemes in the coded transmission: Ideally, DFE can achieve significant performance gain over linear equalizer in frequency-selective wireless channels. However, error propagation occurs when wrong feedback decisions are used for prediction. This will result in great performance degradation, and the performance gain of DFE may become marginal, unless the reliability of the feedback decisions is improved through the use of error control decoding in the feedback loop. In general, error control codes have been devised for increasing the reliability of transmission, and they also result in significant performance improvement. In order to secure reliable bandwidth-efficient data transmission over frequency-selective channels, a combination of equalization and decoding functions is needed at the receiver side. The optimal receiver should perform equalization and decoding jointly, but this leads to a huge amount of calculation complexity in the case of frequency-selective wireless channel. This leads to the development of low-complexity solutions, such as iterative equalization/decoding schemes, namely, turbo equalization. In this thesis, turbo equalization is constructed by including error control decoding in the noise prediction feedback loop of the DFE, and iterating the decoding feedback loop. In this context we utilize low-density parity-check (LDPC) codes. Also an alternative scheme is developed which doesn't require the iteration of the outer loop.

3. Digital signal processor based implementation of filter bank applications: The programmable digital signal processor becomes more and more popular solution for baseband digital signal processing algorithm, due to its high performance and high

flexibility. The possibilities to implement some selected algorithms of this work using digital signal processors are also briefly discussed.

This thesis is comprised of two parts, where Part I is the introduction and summary of the work. Part II includes seven original research publications, which are referred in the text as [P1],[P2],[P3],...,[P7].

In Part I, after the introduction in Chapter 1, Chapter 2 reviews the basic concepts of multirate filter banks. Complex modulated perfect reconstruction (PR) filter banks, namely exponentially modulated filter bank, are presented, along with efficient implementation using cosine and sine modulated filter banks. Chapter 3 addressed the equivalent baseband channel model and several commonly-used channel equalizer structures. In Chapter 4, we study combined equalization/decoding methods in coded modulation, presenting the turbo equalization approaches with maximum a posteriori (MAP) equalizer and mean square error (MSE) equalizer. The summary of publications and author's contributions are described in Chapter 5. Finally, conclusion and future research topics are stated in Chapter 6.

Chapter 2

Modulated Filter Bank Systems

Filter banks provide an alternative way to perform the signal transforms between time and frequency domains with more frequency selectivity, instead of DFT/IDFT. This chapter concentrates on a subclass of filter banks, namely, orthogonal modulated filter banks, which are very efficient from both the design and implementation points of view. All the subband filters can be generated from a single prototype filter by using cosine, sine, or exponential modulation [Malv 92b, Vaid 93, Viho 04]. Cosine modulated filter banks (CMFBs) are widely used to process real-valued signals, whereas exponentially modulated filter bank (EMFB) systems are very suitable for the processing of complex-valued signals. In addition, EMFBs can be realized using CMFBs and sine modulated filter banks (SMFBs), and thus resulting in efficient implementation using, e.g., the extended lapped transform (ELT) structure [Malv 92a].

Many practical applications use both the analysis and synthesis filter banks, and they can be cascaded to form two different configurations. One is synthesis-analysis filter bank system, also called as transmultiplexer (TMUX), which can be used for multicarrier transmission purposes, another is analysis-synthesis system which provides means for subband signal processing in frequency-domain. The latter configuration will be mainly addressed in this thesis and it will be utilized for a number of multirate signal processing algorithms. Publications [P5] and [P7] are concerned with interference mitigation techniques. Channel equalization techniques were studied in Publications [P1], [P2], [P3], [P4], and [P6]. EMFBs with good frequency-selectivity were applied in most of these studies.

2.1 INTRODUCTION

Filter banks can be viewed as groups of filters used for the spectral decomposition and composition of signals. They play an important role in many signal processing applications, such as audio and image coding [Stra 96, Cvet 03, Chen 05]. Filter banks have also been used in digital communication systems in many applications [Vaid 01], like discrete multitone modulation [Star 99, Vaid 00], digital transmultiplexer and channel equalization [Bell 74, Sand 95, Gian 97, Alha 01, Ihal 07]. The reason for their popularity is the

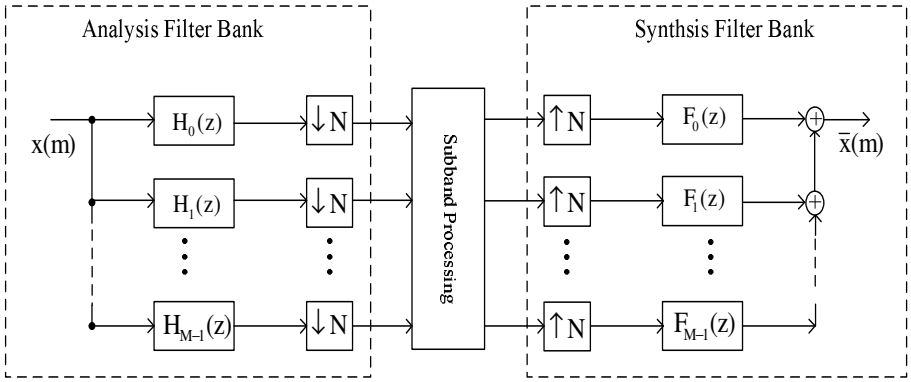

Fig. 2.1 Basic blocks of analysis-synthesis filter bank system.

fact that they allow flexible extraction and processing of different spectral components of a signal while providing very efficient implementation. Since most filter banks involve various sampling rates, they are also referred to as multirate systems. The basic blocks of filter bank systems are known as analysis filter bank and synthesis filter bank, as shown in Figure 2.1.

2.1.1 Analysis filter banks

An analysis filter bank consists of a set of filters and a set of down-samplers as shown in Figure 2.1. Each analysis filter $H_i(z)$ covers a certain frequency band and they are organized in such a manner that $H_0(z)$ is a lowpass filter, $H_1(z), ..., H_{M-2}(z)$ are bandpass filters and H_{M-1} is a highpass filter [Viho 04]. Downsampling by N means that only every Nth sample is taken. This operation is to reduce or eliminate redundancies in the M subband signals. Thus each of the subband signals carries information of a particular frequency bin. If all the filters have equal bandwidth and the corresponding down-sampling factors are also the same, then the filter bank is called uniform filter bank. An M-subband analysis filter bank is called critically sampled or maximally decimated if the total sum-up rate of the low-rate subband signals is equal to the sample rate of the high-rate input signal. In the case of real-valued signals, this means that $N = M$. If $N < M$, then the total sum-up rate is higher than the input sample rate, and the filter bank is called oversampled filter bank.

2.1.2 Synthesis filter banks

Figure 2.1 also shows a synthesis filter bank on the right side. It consists of a set of upsamplers and lowpass, bandpass, and highpass filters. The input signals are upsampled by the factor of N and filtered with the synthesis filters $\{F_k(z)\}$. Upsampling by N means the insertion of $N - 1$ consecutive zeros between the samples. This allows us to recover the original sampling rate. The samplers are followed by filters which replace the inserted zeros with meaningful values. Finally, the outputs are summed in order to obtain the output signal $\bar{x}_m$. In the case of real-valued signals, the M-subband synthesis filter bank is called critically sampled or minimally interpolated if $N = M$.

2.1.3 Filter bank systems

The basic blocks of a filter bank system, including the analysis filter bank, subband processing, and the synthesis filter bank, are depicted in Figure 2.1. The analysis filter bank is to decompose the signal into a number of low-rate signal components accurately, while the synthesis filter bank constructs them back to a single high-rate signal with sufficient accuracy. The subband signals between analysis and synthesis filter banks can be processed independently or jointly by application dependent algorithms. The aim of this thesis is to apply subband signal processing for channel equalization. In this thesis, we focus on modulated filter banks satisfying PR conditions.

The input and output relation for an analysis-synthesis system can be given in the z-domain

$$\bar{x}(z) = \frac{1}{M} \sum_{k=0}^{M-1} F_k(z) \sum_{i=0}^{M-1} H_k(zW_M^i) X(zW_M^i), \tag{2.1}$$

where W_M is the Mth root of unity, $W_M^i = e^{-j2\pi i/M}$ and $j = \sqrt{-1}$. The equation can be rewritten as

$$\bar{x}(z) = T_0(z)X_(z) + \sum_{i=1}^{M-1} T_i(z) X(zW_M^i), \tag{2.2}$$

where

$$T_0(z) = \frac{1}{M} \sum_{k=0}^{M-1} F_k(z) H_k(z) \tag{2.3}$$

and

$$T_i(z) = \frac{1}{M} \sum_{k=0}^{M-1} F_k(z) H_k(zW_M^i). \tag{2.4}$$

The transfer functions $T_0(z)$ and $T_i(z)$ for $i = 1, 2, ..., M-1$ are the distortion component and the aliasing component, respectively. The PR conditions are satisfied when $T_0(z) = z^{-D}$, where D is the system delay, and $T_i(z) = 0$ for $i = 1, 2, ..., M-1$. Thus, the output signal is just a delayed version of the input signal, i.e., $\bar{x}(m) = x(m-D)$. The system is near PR (NPR) system, if those conditions are only approximately fulfilled.

Critically sampled PR filter banks typically allow some amount of aliasing in the subband signals, but these aliasing components are canceled by the synthesis filter bank. Therefore, critically sampled filter banks are practical solutions in subband processing applications when aliasing in the subbands is not troublesome [Viho 04]. A solution for avoiding or reducing the unwanted aliasing in subband signals is by oversampling. The oversampling can also obtain some additional freedom for the filter design process. Other advantages of the oversampled system are improved noise immunity and noise shaping capability [Bolc 97, Bolc 98]. All these improvements are achieved at the expense of increased computational complexity, since a higher number of subband signal samples have to be processed.

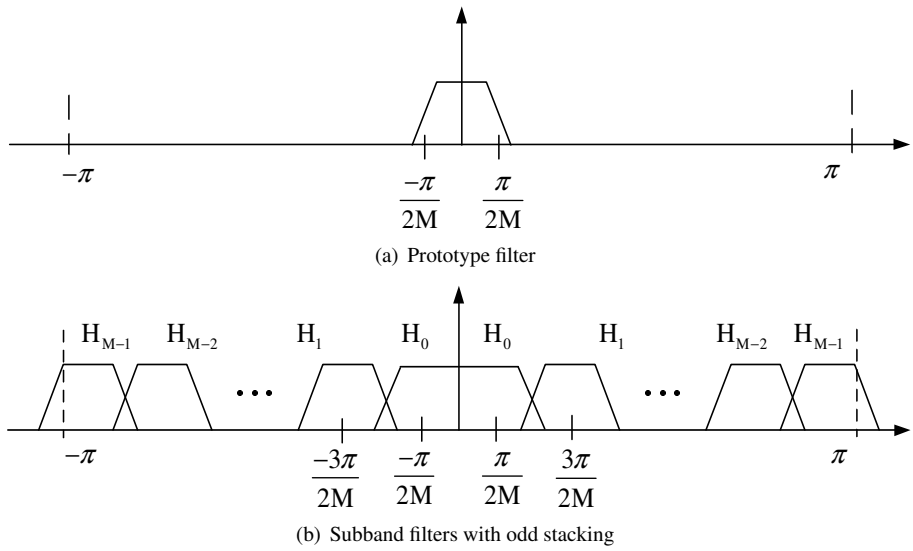

Fig. 2.2 Magnitude response of the filters in the case of cosine modulation.

2.2 MODULATED FILTER BANKS

Modulated filter banks are widely used because of easily-derived, efficient realization of subband filters, i.e., all analysis and synthesis filters can be obtained from a single real-valued linear-phase lowpass prototype filter by using cosine, sine, or exponential modulation [Malv 92b, Vaid 93, Viho 04]. This chapter will present an overview of cosine, sine, and exponentially modulated filter banks with PR condition, which will be utilized throughout this thesis.

2.2.1 Cosine/sine modulated filter banks

Cosine/sine modulated filter banks have real-valued subband filters, which transform real-valued input signals into real-valued subband signals. They are very attractive from both the design and implementation point of view, because all the analysis filters and synthesis filters are generated by using a single lowpass prototype filter and a discrete cosine/sine transforms (DCT/DST).

A very typical way to obtain an orthogonal cosine modulated filter bank is to use a linear-phase lowpass FIR prototype filter $h_p(m)$. If the order of the prototype filter is N, its transfer function is

$$H_p(z) = \sum_{m=0}^{N} h_p(m) z^{-m}, \tag{2.5}$$

where $h_p(N-m) = h_p(m)$. In many applications, it is wanted that each subband filter has a bandwidth of π/M. Therefore, the prototype filter should be a good frequency-selective

lowpass filter with cutoff frequency of $\pi/(2M)$ and its stopband edge is defined as

$$\omega_s = \frac{(1+\rho)\pi}{2M}, \tag{2.6}$$

where $\rho > 0$ is the roll-off factor. It controls the trade-off between the stopband attenuation and the transition bandwidth. Moreover, it determines how much adjacent channels overlap.

Generally, the quality of a modulated filter bank system depends mainly on the properties of the prototype filter. Long and smooth prototype filters tend to provide good stopband attenuation, thus resulting in highly frequency-selective subband filters. The works in [Koil 92, Malv 92b, Malv 92a, Sara 92] show that highly frequency-selective PR cosine modulated filter banks can be designed when the order of the prototype filter is set to be $N = 2KM - 1$, and we assume this choice for the filter order in the continuation. The K is a positive integer, known as overlapping factor, and M is the number of subbands, usually chosen to be a power of two, which enables an efficient implementation. More on the prototype filter design can be found in [Malv 92b, Sara 92, Viho 04].

2.2.1.1 Odd-stacked cosine modulated filter banks Generally, there are four types of DCT/DST, i.e., types I, II, III, IV [Wang 84]. The use of different schemes would result in different channel stacking arrangements.

The use of DCT-IV (or DCT-II) type of modulation leads to the odd-stacked filter banks [Croc 83]. All the M subbands filters have equal bandwidth of π/M and their center frequencies are located at $w_k = (k + 1/2)\frac{\pi}{M}$, for $k = 0, 1, ..., M - 1$, as can be seen in Figure 2.2.

The kth subband analysis filter impulse response is [Malv 92b, Malv 92a, Viho 04]

$$h_k^c = \sqrt{\frac{2}{M}} \cos((k + \frac{1}{2})\frac{\pi}{M}(N - n + \frac{M+1}{2})), \tag{2.7}$$

and the kth subband synthesis filter is simply the time-reversed version of the corresponding analysis filter $f_k^c = h_k^c(N - n)$, obtained as

$$f_k^c = \sqrt{\frac{2}{M}} \cos((k + \frac{1}{2})\frac{\pi}{M}(n + \frac{M+1}{2})). \tag{2.8}$$

The definitions for sine modulated subband filters are

$$h_k^s = \sqrt{\frac{2}{M}} \sin((k + \frac{1}{2})\frac{\pi}{M}(N - n + \frac{M+1}{2})), \tag{2.9}$$

and

$$f_k^s = \sqrt{\frac{2}{M}} \sin((k + \frac{1}{2})\frac{\pi}{M}(n + \frac{M+1}{2})). \tag{2.10}$$

The following relations between cosine and sine modulated subband filters can be found

$$h_k^s(n) = (-1)^{k+K} f_k^c(n), \tag{2.11}$$

and

$$f_k^s(n) = (-1)^{k+K} h_k^c(n). \tag{2.12}$$

This shows that the sine modulated analysis and synthesis filter bank can be obtained from the corresponding cosine modulated synthesis and analysis filters, respectively.

2.2.2 Complex modulated filter banks

Complex modulated filter banks are often used for the processing of complex-valued input signals. This is especially needed in spectrally efficient radio communications. It was stated in [Hell 99, Karp 99, Viho 04] that the frequency-selective prototype filters for an M-subband CMFB/SMFB can be used also for $2M$-subband complex modulated filter banks.

2.2.2.1 DFT-FB DFT-FBs were the first modulated filter banks introduced in the literature, and originally they were proposed for communication purposes [Bell 74, Wein 71]. The use of the DFT as a modulation function leads to a uniform even-stacked filter bank. It is well known that the critically sampled $2M$-subband DFT-FB with FIR analysis and synthesis filters satisfies the PR property if the prototype filter $h_p(n)$ and $f_p(n)$ are simple $2M$-length rectangular windows [Croc 83]. Because of this, the stopband attenuation of the resulting subband filters is only 13dB. They have also wide transition bands and, therefore, adjacent subband overlap significantly. This results in significant amount of aliasing in the subband signals after downsampling.

The exponentially modulated filter bank is motivated by the fact that DFT-FB have poor stopband attenuation and wide transition band. Figure 2.3 illustrates EMFB frequency-selectivity advantage compared to a DFT-FB. It is clear that EMFB provides better spectral selectivity, and stopband attenuation compared to DFT-FB.

2.2.2.2 Exponentially modulated filter banks The analysis and synthesis subband filters can be obtained in the same way as in Equation (2.7) and (2.8), and the exponential modulation is applied instead of cosine modulation.

$$h_k^e = \sqrt{\frac{2}{M}} \exp(-j\frac{\pi}{M}(k+\frac{1}{2})(N-n+\frac{M+1}{2})) \tag{2.13}$$

and

$$f_k^e = \sqrt{\frac{2}{M}} \exp(j\frac{\pi}{M}(k+\frac{1}{2})(n+\frac{M+1}{2})), \tag{2.14}$$

where $k = 0, 1, ..., 2M-1$ and $n = 0, 1, ..., N$. Due to modulation, all the analysis and synthesis filters are linear-phase filters and their impulse responses are complex-valued. The EMFB is used for complex-valued high-rate signals, and therefore, it covers the whole signal frequency range $[-f_s/2, f_s/2]$, where f_s is the sampling rate.

In a critically sampled cosine/sine modulated analysis filter bank with M-subbands, the input signal bandwidth of $f_s/2$ is divided into M low rate subband signals with a bandwidth of $f_s/2M$. A straightforward approach to critically sampled complex modulated filter banks is to divide the signal into $2M$ complex subbands with a bandwidth of $f_s/2M$ using a down-sampling factor of $2M$. In [Viho 02], Viholainen et al. have demonstrated that no aliasing cancelation is possible for this kind of complex modulated filter bank with

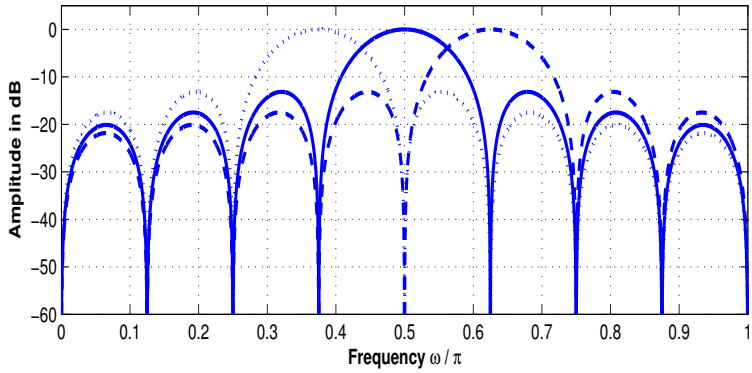

(a) DFT-FB

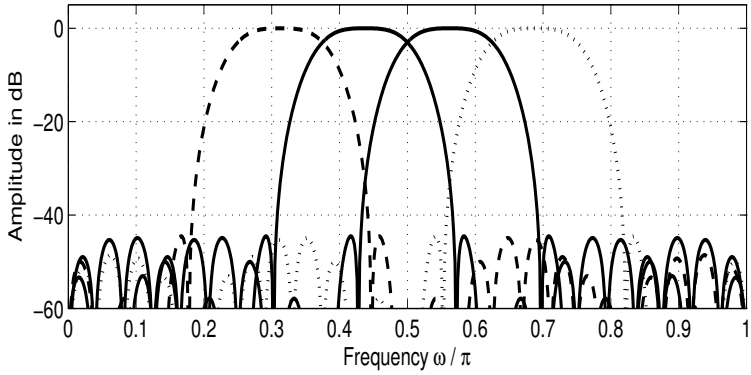

(b) EMFB

Fig. 2.3 Comparison of the subband frequency responses of DFT and EMFB (the roll-off factor $\rho = 1$ and overlapping factor $K = 5$).

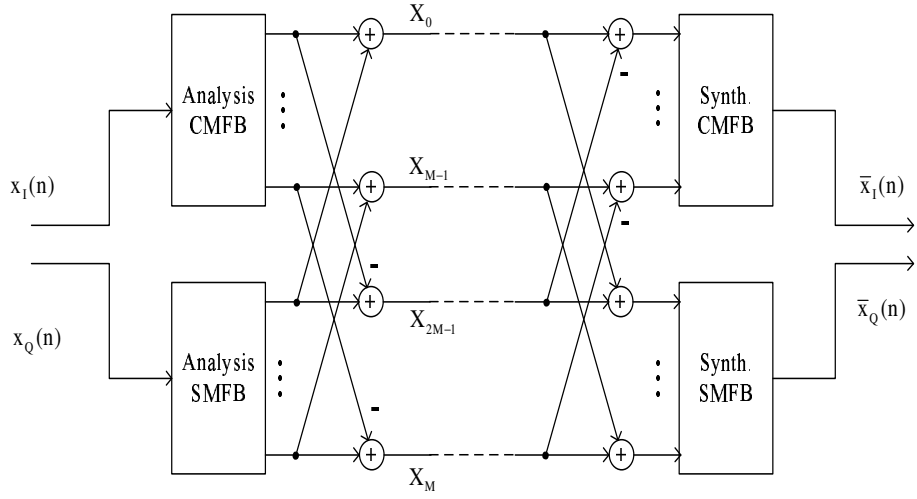

Fig. 2.4 Efficient implementation for exponentially modulated filter bank.

$2M$ subbands and downsampling factor of $2M$. They proposed a $2M$-subband complex modulated analysis-synthesis PR filter bank structure where the sampling rate conversion factor is M, but only the real part of the subband signals are utilized. This structure can be implemented using M-subband cosine and sine modulated filter banks as building blocks, as shown Figure 2.4.

The connection between $2M$-subband exponentially modulated filter banks and M-subband cosine modulated and sine modulated filter banks can be expressed as follows,

$$f_k^e(n) = \begin{cases} f_k^c(n) + jf_k^s(n), & k \in [0, M-1] \\ -(f_{2M-1-k}^c(n) - jf_{2M-1-k}^s(n)), & k \in [M, 2M-1] \end{cases} \tag{2.15}$$

and

$$g_k^e(n) = \begin{cases} g_k^c(n) - jg_k^s(n), & k \in [0, M-1] \\ -(g_{2M-1-k}^c(n) + jg_{2M-1-k}^s(n)), & k \in [M, 2M-1]. \end{cases} \tag{2.16}$$

All operations, shown in Figure 2.4, are carried out with real-valued critically sampled modulated filter banks. This results in efficient implementations based on polyphase structures [Malv 92b, Vaid 93], lattice structures [Koil 92, Vaid 93], or fast ELT structures [Malv 92a, Malv 92b]. A short overview of cosine modulated filter banks implementation will be present in Section 2.3, together with complexity comparison with other implementation structures.

2.2.2.3 Oversampled exponentially modulated filter banks

For each block of M complex input samples, $2M$ complex subband samples are generated in 2x-oversampled case. This can be achieved by using two CMFBs and SMFBs, as depicted in Figure 2.5 [Alha 01, Ihal 05, Viho 06a]. This 2x-oversampled filter bank was applied in our studies for channel equalization purpose.

The advantage of using 2x-oversampled analysis filter bank is that the channel equalization can be done within each subband independently of the other subbands. Assuming roll-off $\rho = 1.0$ or less in the filter bank design, the complex subband signals of the analysis bank are essentially alias-free. This is because the aliasing signal components are attenuated by the stopband attenuation of the subband responses. Subband-wise equalization compensates the channel frequency response over the whole subband bandwidth, including the passband and transition bands. The imaginary parts of the subband signals are needed only for equalization. The real parts of the subband equalizer outputs are sufficient for reconstructing signal, using a critically sampled synthesis filter bank.

2.3 EFFICIENT IMPLEMENTATION OF PR COSINE MODULATED FILTER BANKS

The main disadvantage of direct implementation of cosine and sine modulated filter banks is the computational complexity. A straightforward implementation does lots of useless computation because only every Mth sample is saved and $M-1$ of computed samples are discarded due to the downsampling operation. A more efficient implementation can avoid

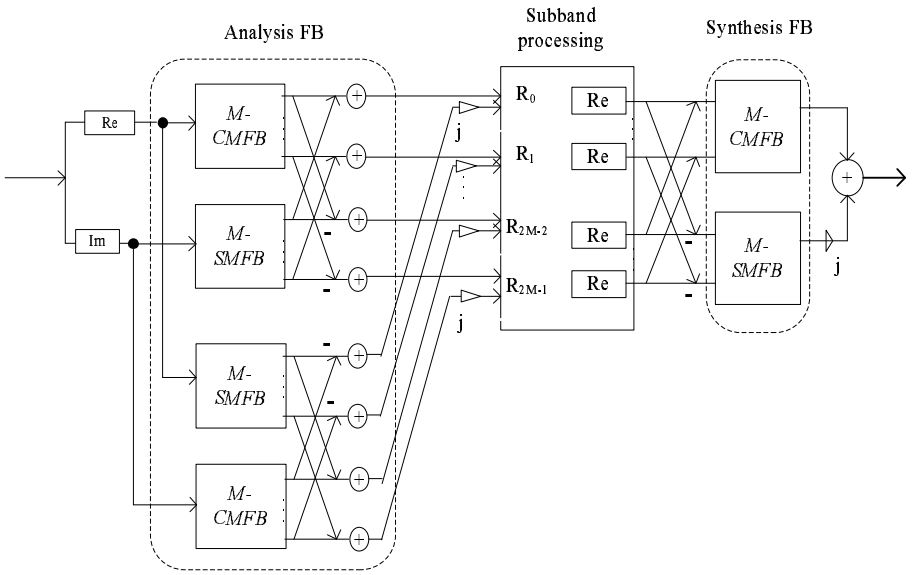

Fig. 2.5 Channel equalization with oversampled EMFB structure using two CMFBs and SMFBs.

useless computation. Nevertheless, in order to obtain a new output sample from one subband filter, $2KM$ multiplications and $2KM-1$ additions are needed. This results in the total computational complexity of $2KM^2$ multiplications and $2KM^2 - M$ additions for analysis or synthesis filter bank.

Fast ELT algorithm

Cosine modulated filter banks with PR condition have an efficient implementation structure based on the structure of ELT [Malv 92a]. The basic idea behind a fast ELT algorithm is to implement the polyphase component matrix as a cascade of two kinds of matrices, zero-delay orthogonal factor and pure delays. The structures for the fast direct ELT and inverse ELT are shown in Figure 2.6. The basic elements of the fast ELT structure are the symmetrical $M \times M$ butterfly matrices D_k^c, which are described by

$$D_k^c = \begin{bmatrix} -C_k & S_k J \\ J S_k & C_k \end{bmatrix}, \tag{2.17}$$

where

$$C_k = \text{diag}(\cos\theta_{0k}, \ \cos\theta_{1k}, \ ..., \ \cos\theta_{(M/2-1)k}), \tag{2.18}$$

and

$$S_k = \text{diag}(\sin\theta_{0k}, \ \sin\theta_{1k}, \ ..., \ \sin\theta_{(M/2-1)k}). \tag{2.19}$$

J is the reversal matrix, performing a reversing operation. The last element of the fast ELT structure is the cosine modulation block which can be directly implemented with the DCT-IV transform. The relationship between the prototype filter coefficients and the but-

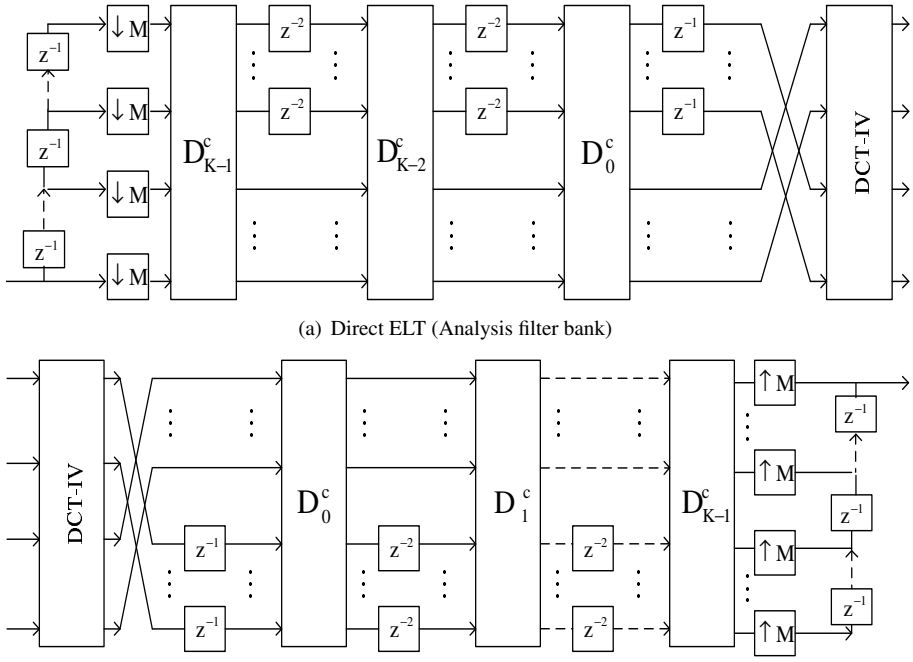

Fig. 2.6 Fast implementation of the cosine modulated filter bank.

terfly angles θ_k can be found in [Malv 92a]. The direct ELT and inverse ELT actually have identical butterflies and DCT-IV matrix. It should be noted that the ELT structure can not be used for filter banks with NPR conditions because of the prototype filter for NPR filter bank cannot be represented using butterfly angles.

The calculational complexity of fast ELT can be further reduced by two methods. One is to scale the butterfly matrices D_k so that their diagonal (or anti-diagonal) entries are equal to unity [Malv 92a], as follows

$$D_k^c = \begin{bmatrix} -\cos\theta_k & \sin\theta_k \\ \sin\theta_k & \cos\theta_k \end{bmatrix} = \cos\theta_k \begin{bmatrix} -1 & \tan\theta_k \\ \tan\theta_k & 1 \end{bmatrix} = \sin\theta_k \begin{bmatrix} -\mathrm{ctan}\theta_k & 1 \\ 1 & \mathrm{ctan}\theta_k \end{bmatrix}. \tag{2.20}$$

Here $\tan\theta_k = \frac{\sin\theta_k}{\cos\theta_k}$ and $\mathrm{ctan}\theta_k = \frac{\cos\theta_k}{\sin\theta_k}$. Another complexity reduction method is to use the trick where complex multiplication can be done with three real multiplications and three additions [Malv 92a]. The total computational complexity of the fast ELT algorithm, along with other implementation structures, is given in Table 2.1. The same computational complexities are also valid for the corresponding synthesis filter bank structures, as well as for sine modulated filter banks.

The fast ELT algorithm has the lowest number of multiplications and delay elements, and at the same time, it offers a computationally efficient implementation structure as discussed above. In Publications [P6] and [P7], this fast ELT algorithm was applied to implement cosine and sine modulated filter banks on two different Texas Instruments pro-

Table 2.1 Computational complexities of efficient analysis/synthesis cosine modulated filter bank structures.

	$\mu(M)$	$\alpha(M)$
Direct Form	$2KM^2$	$2KM^2 - M$
Polyphase	$\frac{M}{2}(4K + \log_2 M + 2)$	$\frac{M}{2}(4K + 3\log_2 M - 2)$
Lattice	$\frac{M}{2}(4K + \log_2 M - 2)$	$\frac{M}{2}(4K + 3\log_2 M - 2)$
Fast ELT	$\frac{M}{2}(2K + \log_2 M + 3)$	$\frac{M}{2}(2K + 3\log_2 M + 1)$

grammable digital signal processors, so as to evaluate the feasibility of filter banks for practical hardware implementation.

2.4 PROGRAMMABLE DIGITAL SIGNAL PROCESSOR BASED IMPLEMENTATION

To the vast majority, the mobile wireless device like mobile phone is the ultimate communication tool, and now becomes more like multimedia communications device. It can be expected that the increasing need for function diversification will drive the programmable digital signal processor into an even more integrated role within the mobile devices of tomorrow. Figure 2.7 shows a common functional block diagram of a global system for mobile (GSM), where signal compression, error correction, encryption, modulation and equalization algorithms can be done on programmable digital signal processor. The early GSM phones were mostly application-specific integrated circuit (ASIC) designs, which may result in the low-power consumption and more efficient implementation than the programmable processor solutions, but the programmable processors have an advantage in their flexibility and shorter development periods. Today, wireless technology standards are still evolving, and the advantages of programmability become very important, as they enable the support for high performance and high flexibility solutions with a diversity of services.

Benefits over ASIC

Generally speaking, a programmable digital signal processor would have the below listed cost-saving advantages in the product development process [Gath 00]:

1. Digital signal processors scale better with process improvement. This is because a programmable device, when migrating to a higher clock rate, is capable of increased functionality. Many ASIC designs, on the other hand, do not gain functionality with increased clock speed.

2. Digital signal processors are multitasking devices. As process technology improves, two different functions which were performed on two digital signal processors, can now be performed on a single digital signal processor by merging the code. This is not possible with ASIC design. The development of real time operating system

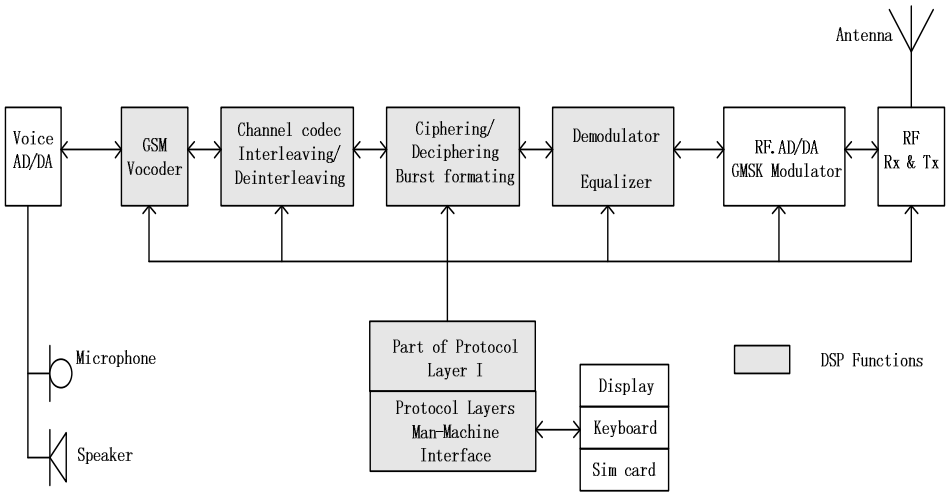

Fig. 2.7 Functional block diagram of a GSM phone.

for digital signal processors has also reduced the development costs of multitasking considerably.

3. Digital signal processors are a lower risk solution. Programmable digital signal processors can react to changes in algorithms and bug fixes much more rapidly, and with much lower development costs. They also tend to be used to develop platforms that support several handset designs, so that changes can be applied to all handset designs at once. Testing of digital signal processor solutions is also easier than ASIC solutions.

Code optimization

Programmable digital signal processor applications are becoming broad, but writing digital signal processing code in low-level assembly language would be very complex and would slow down the development. Digital signal processor vendors have developed a number of C compiler tools and allow signal processing programming on C language, which greatly improves the development time, ease of debugging, code browsing, and maintenance.

Today, signal processing algorithms written by C language can be easily adapted on the programmable digital signal processor. And their performance mainly relies on the code efficiency generated by the C compiler. One important part of code efficiency would be the loop intensive code, which repeats the same continuous operations, i.e., consecutive multiplication and accumulation, on large amounts of input samples. It is important for C compiler to figure out the parallel operations in the algorithm and schedule them together, to make maximal use of all the hardware resources in these important loops. For quick evaluation of signal processing algorithm performances on the programmable digital signal processors, the simulated codes mixed with C and assembly language would be a trade-off between performance and development time. In Publications [P6] and [P7], we

have employed common optimization techniques on Texas Instruments C64xx and C55xx digital signal processors.

It should be noted that since the executable code generated from C language commonly has a larger size, and it is less efficient than hand-optimized assembler, the achievable performances in Publications [P6] and [P7] would be improved when using hand-optimized assembler code. Moreover, using the latest processors with a higher clock rate would also give higher performance immediately.

Chapter 3

Channel Equalization

The difficulties of channel equalization in single-carrier broadband systems is regarded as a major obstacle to high data rate transmission over mobile radio channels. This chapter provides a general description of channel equalization techniques. Firstly, a brief description of the considered radio channel model is presented, followed by a number of commonly-used equalizer techniques. For severe wireless channels, frequency-domain equalization is preferred, as a low-complexity solution. The EMFBs described in the previous chapter are utilized for time-frequency transforms. The performance of EMFB based frequency-domain equalization is presented [P1][P2]. One important reason for using EMFB is that EMFB can be applied not only to combat channel distortion, but also to implement part of the channel filtering with much higher performance than using the FFT-FDE structures. In Publications [P1][P5], FB-FDE is shown to be an easily configurable structure for the final stage of the channel filtering chain, together with the channel equalization functionality.

3.1 A DISCRETE-TIME SYSTEM MODEL

A communication channel refers to a physical medium, wireline or wireless, for sending a signal from a transmitter to a receiver. In this thesis, we consider the wireless channel (illustrated in Figure 3.1), where the signals from the transmitter arrive at the receiver through multiple paths. The receiver signal is actually a superposition of several delayed and scaled signals which have traveled through different paths. There might not be a line-of-sign (LOS) component between the transmitter and receiver antennas. An important characteristic of such a multipath channel is the time delay spread T_m. When the symbol duration T is much larger than T_m, these multipath components would have little interference effect on subsequently transmitted symbols. While in broadband transmission case, T_m would be much larger than T, and these multipath components would interfere significantly with subsequently transmitted pulses. This would result in intersymbol interference and cause heavy signal distortion, which needs for compensation at the receiver side for correct detection.

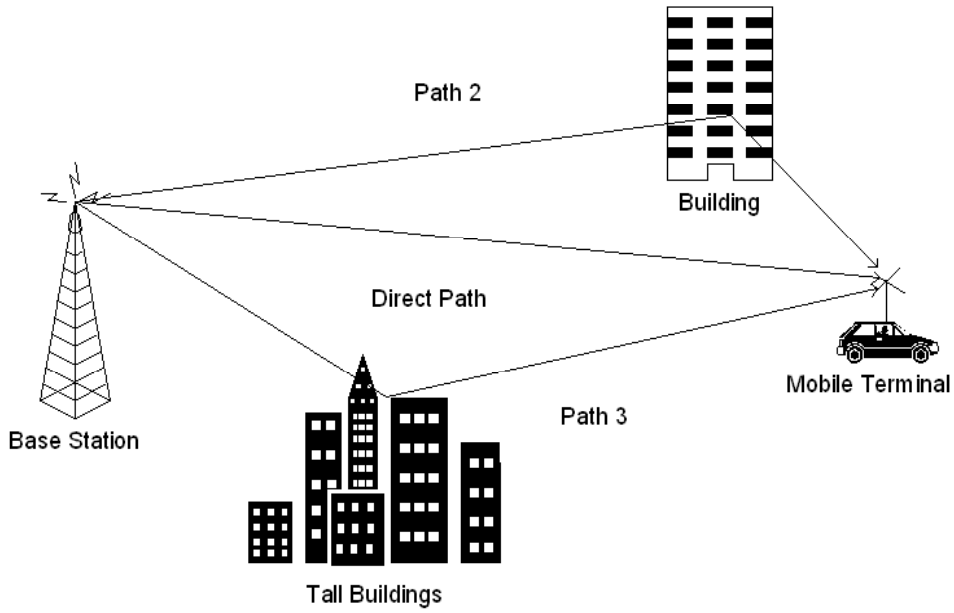

Fig. 3.1 Multipath environment in wireless channel.

The physical wireless channel can be modeled as a baseband equivalent discrete-time channel, illustrated in Figure 3.2. Ideally, the receive front-end comprises the receiver filter followed by a symbol-rate sampler. It intends to provide transition from continuous-time to T-spaced discrete-time without information-loss. It is well-known that a matched filter, whose impulse response is matched to the cascade of the transmitter filter and channel, $H_R(\omega) = H_T^*(\omega)H_C^*(\omega)$, can maximize the SNR at the sampler output, so as to provide sufficient estimation of the transmitted data sequence $\{x_m\}$ [Forn 72, Proa 01]. As depicted in Figure 3.2, $H_{eq}(z)$ represents the combined operations of transmit filtering, propagation over continuous-time channel, receiver filtering and symbol-spaced sampling, together with perfect coherent demodulation and timing synchronization.

Let $H_0(\omega)$ denote the frequency response of the overall continuous-time baseband equivalent channel,

$$H_0(\omega) = H_T(\omega)H_C(\omega)H_R(\omega). \tag{3.1}$$

The frequency response of the discrete-time channel is related to the frequency response of the continuous-time channel by

$$H_{eq}(e^{j\omega T}) = \frac{1}{T}\sum_m H_0(\omega - \frac{2m\pi}{T}), \quad |\omega| \le \frac{\pi}{T}, \tag{3.2}$$

which shows that $H_{eq}(\omega)$ is simply obtained as the folded-spectrum of $H_0(\omega)$ [Proa 01].

However, the noise is usually correlated at the output of the matched filter, and it is necessary to cascade the sampled matched filter with an appropriate discrete-time noise whitening filter in order to simplify the receiver analysis and design. This receiver front end is named as whitened matched filter (WMF) [Ande 73, Forn 72, Proa 01].

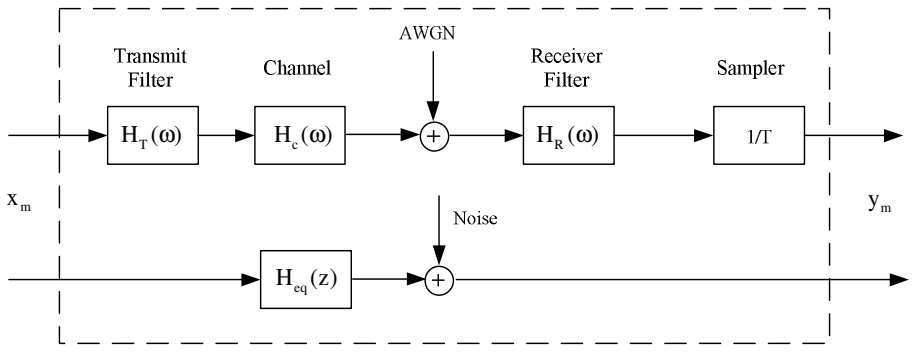

Fig. 3.2 Discrete-time baseband equivalent channel model.

One sub-optimal solution, which is commonly adopted in practical transmission systems, is to use a square-root raised cosine (RRC) filter [Proa 01] instead of the matched filter. Such a receiver filter is usually matched to the transmit pulse shape and provides uncorrelated noise at the sampler input. In [Gers 02], it is claimed that a fixed RRC filter with a carefully optimized roll-off factor may cause only a small degradation with respect to the optimum WMF.

The system model, including transmit filter, channel, receiver filter, and symbol-rate sampling, can be represented as a discrete finite impulse response (FIR) filter with additive Gaussian noise, as illustrated in Figure 3.3. It should be emphasized that the noise in this model is white only when the receiver filter is an RRC filter and the channel matched part of the receiver filter is ignored. The discrete-time filter model of Figure 3.3 will be used throughout the rest of this thesis. In addition, we assumed that the channel has unit energy, i.e.,

$$\sum_{l=0}^{L} |h_l|^2 = 1, \tag{3.3}$$

where $\{h_l\}$ denotes the weights of the equivalent baseband system impulse response and L is the channel delay spread. The data symbols $\{x_m\}$ are modeled as a sequence of independent, identically distributed complex random variables x_m, with zero mean and unity variance, $\sigma_x^2 = 1$. The data symbols are transmitted at the rate $R = 1/T$, where T is the symbol period. The additive Gaussian noise v_m has zero mean and variance N_0. Moreover, the noise sequence $\{v_m\}$ is uncorrelated with transmitted symbol sequence $\{x_m\}$. The output y_m can be represented by FIR filtering and additive noise, as follows:

$$y_m = \sum_{l=0}^{L-1} h_l x_{m-l} + v_m. \tag{3.4}$$

Here we consider the scenario of frequency-selective wireless channel, where the channel is considered as quasi-static, i.e., the channel response is constant during the transmission of each block.

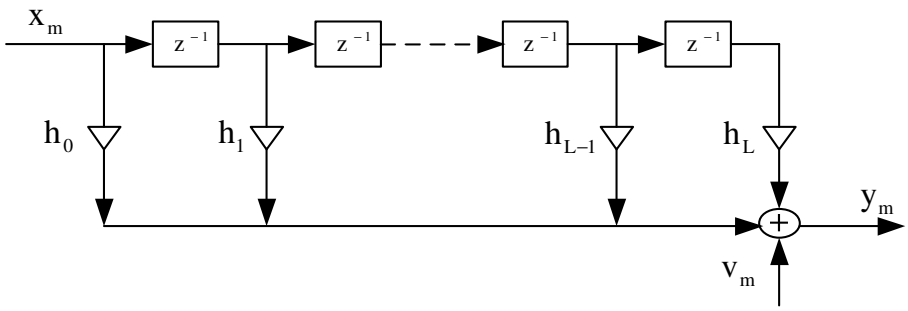

Fig. 3.3 An ISI channel modeled as an FIR filter with AWGN.

3.2 EQUALIZER DESIGN CRITERIA

Basically, there are two connected tasks involved in the equalization process: one is to mitigate the ISI effects, another is to prevent noise power in the received signal to be enhanced in the processing of ISI mitigation. These two tasks must be balanced in frequency-selective channel equalization. Figure 3.4 illustrates the basic idea of channel equalization. The input y_m of a linear equalizer can be represented in z-transform domain as

$$Y(z) = X(z)H_{eq}(z) + V(z), \tag{3.5}$$

where $V(z)$ has the power spectral density of $N_0 H_{eq}(e^{j\omega})$. The equalized signal $\bar{Y}(z)$ would be totally free of ISI effect when the zero forcing (ZF) criterion is applied. The ZF equalizer response $W(z)$ is defined as [Proa 01]:

$$W(z) = \frac{1}{H_{eq}(z)}. \tag{3.6}$$

The receiver signal $\bar{Y}(z)$, after passing through equalizer, can be represented as:

$$\begin{aligned} \bar{Y}(z) &= (X(z)H_{eq}(z) + V(z))W(z) \\ &= X(z) + \bar{V}(z). \end{aligned} \tag{3.7}$$

It is noted that $\bar{V}(z)$ is colored Gaussian noise with power spectral density $N_0/H_{eq}(e^{j\omega})$. Thus, if $H_{eq}(j\omega)$ has a spectral null at any frequency within the bandwidth, then the power of the noise $\bar{V}(z)$ becomes infinite. In this case, even though the ISI effects would be totally removed, the system will perform poorly due to its greatly reduced SNR at the decision device.

The ZF equalizer is designed based on full ISI mitigation, while another alternative method, MSE equalizer, is to minimize the error signal at the output of the decision device, so that it is capable to achieve better performance in the case of heavily frequency-selective wireless channels. In fact, the error at the output of a linear equalizer with MSE criterion would be a combination of residual ISI and noise signal, and its equalizer response is given

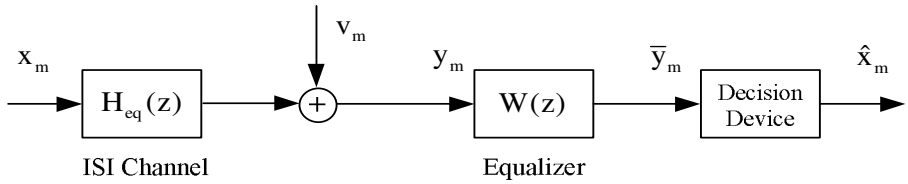

Fig. 3.4 System model with channel equalization.

by [Proa 01]

$$W(z) = \frac{1}{(H_{eq}(z) + N_0)}, \tag{3.8}$$

assuming that the signal energy is normalized to unity. It should be noted that MSE and ZF equalizers result in the same performance in the high SNR range.

Symbol-spaced equalizer and fractionally-spaced equalizer

For symbol-spaced equalizer (SSE), the tap delay spacings are set at the symbol interval T. Since the multipath components can arrive at arbitrary times depending on the nature of the propagation environment, the time resolution of the equalizer adjustments is not ideal and results in high sensitivity to the sampling time. This led to the development of fractionally-spaced equalizer (FSE) in which the tap delay spacing was less than T. As described in [Belf 79, Proa 01], the FSE equalizer can perform equally well as a SSE that is preceded by the ideal matched filter. Since the matched filter is hard to realize in continuous-time signal processing when the channel response is not known or varying, the FSE represents an attractive solution. The advantage of FSE over SSE can be seen in Publication [P1] as well.

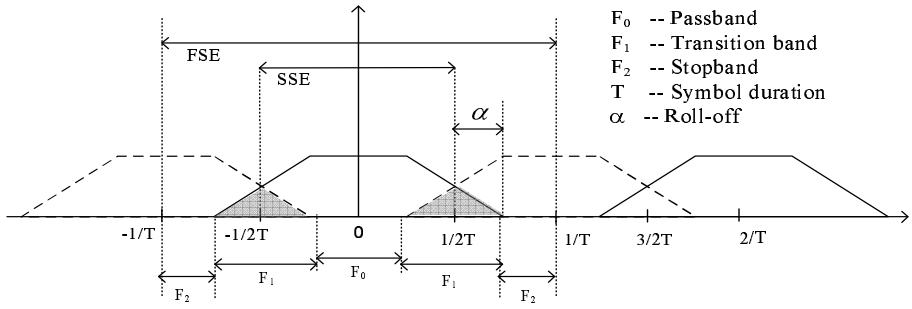

Fig. 3.5 Signal spectra in the cases of SSE and FSE.

Figure 3.5 illustrates the limitation of SSE, when the transmitted signal consists of a RRC spectrum with roll-off factor α. In SSE, since the symbol rate sampling $1/T$ is not two times larger than the whole baseband spectrum width of $(1 + \alpha)/2T$, the process of sampling a signal at rate of $1/T$ superimposes its spectral components. Hence, the input

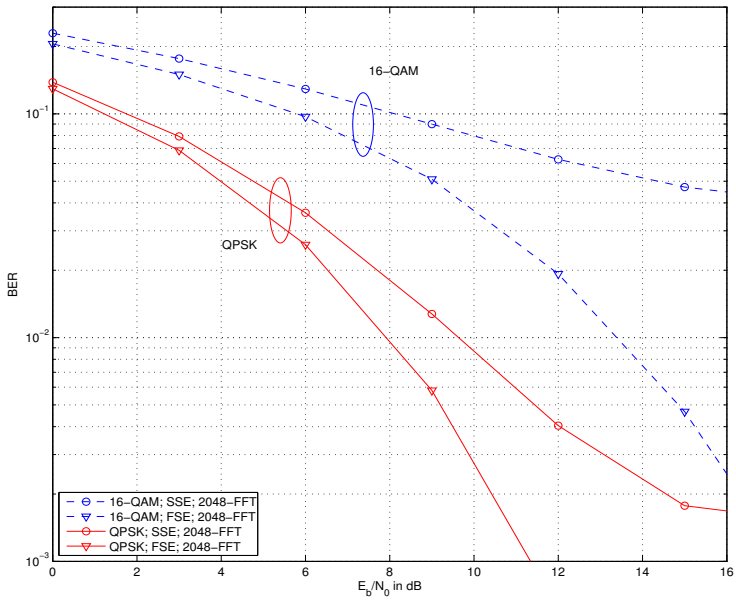

Fig. 3.6 Frequency-domain SSE and FSE performance comparison in the ITU-R Vechicular A channel model with 20 MHz bandwidth (uncoded cases).

signal to the SSE has already aliased components in the transition bands. The SSE cannot compensate optimally the channel distortion in the transition bands, which leads to some performance degradation. It is also clear that the SSE performance is very sensitive to the choice of sampling time [Proa 01].

FSE is often named as $T/2$-spaced equalizer [Trei 96, Proa 01], where the received signal is sampled at every $T/2$ interval. In Figure 3.5, the sampling rate becomes sufficiently large to accommodate the transmitted signal spectrum $(1 + \alpha)/2T$ without aliasing and hence $H_{eq}(e^{j\omega}) = H_0(f)$ for $-f_s \leq f \leq f_s$. The equalization task can be performed on the full frequency range $[-1/T,\ 1/T]$. This means that FSE can provide the optimum receive filter, thus avoiding the need for a separate matched filter to process the signal optimally before sampling. It should be noted that the signal at the output of the FSE is still sampled at the rate of $1/T$. But, since the input is sampled at the rate of $2/T$, the equalizer acts on the received signal before alias effects take place. In the case of FFT-FDE, the FSE performance gain over SSE is shown in Figure 3.6, where we applied the ITU-R Vechicular A channel model of 20 MHz bandwidth and the practical parameters, as discussed in [P1], in our simulations.

In summary, we can say that a SSE cannot perform matched filtering in practice, while FSE can incorporate the functions of a matched filter and an equalizer.

The equalization can be operated on passband or baseband. The following subsections will briefly address baseband equalization of two different main categories; time-domain equalizers and frequency-domain equalizers. In addition, time-domain equalizers can be

grouped into linear equalizers (LEs) and nonlinear equalizer. Nonlinear approaches are motivated by further mitigation of signal distortion and the noise variance at the output of the LE. It actually improves SNR at the input of the decision device and results in performance improvement over LE.

3.3 TIME-DOMAIN EQUALIZER

The conventional equalizers are implemented at baseband, using adaptive time-domain FIR filters. Due to the time variations of the wireless channel, the filter coefficients are computed from the channel estimates or, more commonly, by using adaptive algorithms which are used to minimize the MSE at the decision device. One of the most popular methods is to use training sequences, fixed-length known bit sequences, embedded in each transmitted frame. The equalizer at the receiver uses this known sequence to adjust its equalizer coefficients to match the channel response. Because a sufficient-length training sequence has to be embedded in each data packet, it wastes the transmitted information bandwidth and power. One alternative channel equalization method is blind equalization, where the training sequence is removed. The major advantage of blind equalization is the improved bandwidth efficiency for time-varying channels. However, compared to training sequence based methods, blind methods need high SNR to get similar performance and current blind algorithms have high computational complexity and slow convergence [Tugn 00]. Semi-blind channel estimation [Cirp 98] provides a tradeoff between bandwidth efficiency and calculation complexity.

Here perfect channel knowledge is assumed and the common equalizer structures used in various applications are present below.

3.3.1 Maximum likelihood equalizer

ML equalizer is a kind of nonlinear equalization techniques, which avoids the problem of noise enhancement since it doesn't try to invert the channel by using a filter structure. Instead, it estimates the sequence of transmitted symbols using the maximum likelihood principle [Forn 72, Li 95, Proa 01].

ML equalizer assumes that the noise at its input is white. In the ideal model, noise whitening filter is included after matched filtering and symbol rate sampling. The noise whitening filter is then also included in the system impulse response coefficients $\{h_l,\ l = 0, 1, ..., L\}$ in Figure 3.3. The ISI only affects a finite number of symbols, i.e., the channel output is constructed as the output of a discrete-time finite-state machine. When information symbols are M-ary, the channel has M^L states. Thus the channel can be represented by an M^L-state trellis, which are computed as

$$p\left(y_m|x_{m-L}, x_{m-L+1}, ..., x_m\right) = \frac{1}{\pi N_0} \exp\left[-\frac{1}{N_0}\left|y_m - \sum_{l=0}^{L} h_l x_{m-l}\right|^2\right]. \tag{3.9}$$

The maximum likelihood estimate of an information sequence is simply the most probable path through the trellis. The well-known Viterbi algorithm is an efficient means for

performing the trellis search. Assuming perfect knowledge of the channel, the ML equalizer provides good signal reconstruction and is considered to give superior performance in terms of BER, as shown in Figure 3.9 [Mars 01]. However, the biggest barrier with the ML equalizer comes from the computational complexity, since the Viterbi algorithm complexity grows exponentially with channel delay spread and the size of transmitted symbol alphabet. This would be unfavorable for high spectral efficiency transmission on wireless channels with long delay spreads.

In many channels of practical interest, such a large computational complexity makes ML approach impractical. This motivates to study the low-complexity equalization solutions. Some of them combat the complexity of Viterbi algorithm by reducing the number of searched paths in the trellis, employing truncation of channel impulse response combined with state partitioning techniques [Hash 87, Eyub 88, Auli 99]. Alternative approach is to consider filter-based approaches, LE, DFE and their variants. SSE or FSE structure can be used for both LE and DFE. The filter coefficients can be updated according to the selected performance criterion: ZF or MSE.

3.3.2 Linear equalizer

Compared to the ML equalizer, an LE is very simple to implement, and it is effective in channels where ISI is not severe. It can be implemented as a transversal or a lattice filter [Proa 01]. Commonly, a linear transversal filter is utilized and the corresponding equalizer output is presented as

$$\bar{y}_m = \sum_{l=-M}^{M} w_l y_{m-l}, \tag{3.10}$$

where $\{w_l, l = -M, ..., 0, ..., M\}$ are the tap weights of the equalizer. The complexity of the LE would be linear function of the equalizer order $2M$. In the case of MSE criterion, the filter coefficients $\{w_l\}$ can be designed by minimizing the MSE,

$$J_{MSE} = E\left\{|\bar{y}_m - x_m|^2\right\}. \tag{3.11}$$

In the theoretical case of infinite-length equalizer, the optimal linear equalizer coefficients satisfy the frequency-domain conditions represented in Section 3.2. For practical finite-length equalizers, the equalizer coefficients minimizing the MSE criterion can be calculated from the channel estimate, or they can be obtained adaptively using, e.g., LMS or RLS algorithms [Proa 01].

3.3.3 Decision-feedback equalizer

LEs have the drawback of enhancing noise, especially when the channel has severe amplitude distortion. This shortcoming led to the development of DFE, a nonlinear equalizer structure. A DFE uses previous detection decisions to eliminate the ISI on the symbol currently being detected. Figure 3.7 shows a block diagram of a DFE consisting of two filters: a feedforward filter and a feedback filter. The feedforward filter can be either SSE or FSE. The feedback filter is a transversal filter whose input is the set of previously detected

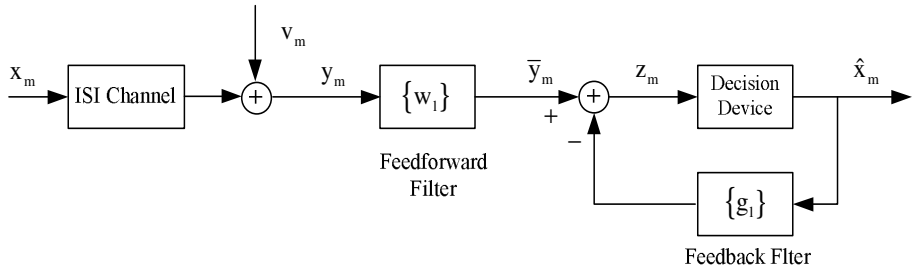

Fig. 3.7 Block diagram of decision-feedback equalizer.

symbols. The input z_m to decision device can be expressed as

$$z_m = \sum_{l_1=-M}^{M} w_{l_1} y_{m-l_1} - \sum_{l_2=1}^{B} g_{l_2} \hat{x}_{m-l_2}. \tag{3.12}$$

The feedback filter coefficients are denoted by $\{g_{l_2}, l_2 = 1, ..., B\}$, where B is the number of feedback taps. Again, these two sets of filters coefficients, $\{w_l\}$ and $\{g_l\}$, can be designed with the MSE criterion, by minimizing the error signal $E\left\{|z_m|^2\right\}$. One drawback with DFEs is the error propagation, which occurs because of the feedback of the decision error from one symbol to the following symbols. It will result in significant performance degradation.

Basically, there are two kinds of DFE structures: the conventional approach and the noise prediction (NP) approach [Belf 79, Proa 01]. Both structures would give equivalent performance when their filters lengths are infinite. The NP-DFE structure is suboptimum when the lengths of the two filters are finite. The reason for the optimality of the conventional DFE is that its tap coefficients in feedforward and feedback filters are adjusted jointly, yielding the minimum MSE. One important property of NP-DFE is that the feedforward filter is just a linear equalizer based on the MSE criterion and performance improvement can be adjusted by only changing the order of the noise prediction in the feedback. This is clearly more flexible scheme than the conventional method.

3.3.4 Interference cancelation equalizer

The concept of decision feedback of past symbols to cancel ISI can be extended to include future symbols as well. If all the past and future symbols are assumed to be known exactly on the receiver end, then all the ISI effect would be completely eliminated without noise enhancement. This kind of equalizer is named the interference cancelation (IC) equalizer [Proa 70], depicted in Figure 3.8.

Recall from equation (3.4) that the energy of transmitted symbol x_m would be spread into a number of output samples $\{y_m, y_{m+1}, ..., y_{m+L}\}$. Supposed the sample r_m defines a

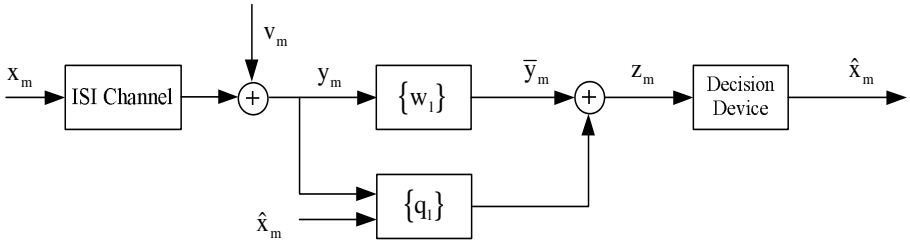

Fig. 3.8 Block diagram of the interference cancelation equalizer.

sample which absorbs all the energy of x_m from the received samples $\{y_m, y_{m+1}, ..., y_{m+L}\}$,

$$\begin{aligned} r_m &= \sum_{l_1=0}^{L} h_{l_1}^* y_{m+l_1} \\ &= \sum_{l_1=0}^{L} h_{l_1}^* \left[\sum_{l_2=0}^{L} h_{l_2} x_{m+l_1-l_2} + v_{m+l_1} \right]. \end{aligned} \tag{3.13}$$

When channel impulse response is unity: $\sum_{l=0}^{L} |h_l|^2 = 1$, we can obtain

$$r_m = x_m + \sum_{l=1}^{L} q_l x_{m-l} + \sum_{l=1}^{L} q_l^* x_{m+l} + \hat{v}_m, \tag{3.14}$$

where

$$q_l = \sum_{k=l}^{L} h_k h_{k-l}^* \quad \text{and} \quad \hat{v}_m = \sum_{l=0}^{L} h_l^* v_{m+l}. \tag{3.15}$$

The terms $\sum_{l=1}^{L} q_l x_{m-l}$ and $\sum_{l=1}^{L} q_l^* x_{m+l}$ are considered as the precursor and postcursor ISI effects of x_m. The idea of IC equalizer is to remove the whole ISI based on the past and future symbols $\{x_m, m = -L, ... - 1, \ 1, ..., L\}$. Then the output signal of IC can be given as

$$z_m = y_m - \sum_{l=1}^{L} q_l \hat{x}_{m-l} - \sum_{l=1}^{L} q_l^* \hat{x}_{m+l}. \tag{3.16}$$

where $\{\hat{x}_m\}$ are the estimates of the transmitted symbols. Such an IC equalizer performance would largely depend on the reliability of the estimated symbols $\hat{x}_m$. Turbo equalizer, which iterates the equalization/decoding process on one transmitted symbol block, would provide a good way for this IC scheme: In the beginning of iterations, a LE or even DFE could be applied and a reliable estimate of transmitter symbols can be ready after decoding, then these decisions will be fed back to perform ISI mitigation on the received and un-equalized samples $\{y_m\}$, using IC approach instead of LE or DFE.

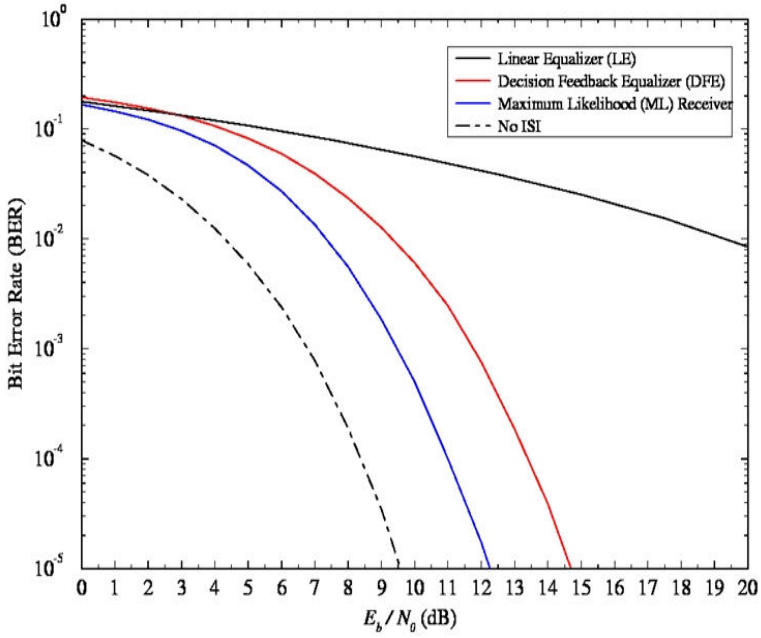

Fig. 3.9 Performance comparison among the traditional equalizers; Uncoded QPSK modulation in Proakis type B channel.

3.4 FREQUENCY-DOMAIN EQUALIZER

The main barrier of time-domain equalization techniques is that their complexity per detected symbol generally grows linearly with, or even as a square of, the number of dispersed symbols [Clar 98]. For example, consider 400 kb/s quaternary phase-shift keying (QPSK), i.e., with a symbol period of $T = 5\ \mu s$, over a typical area multipath channel, with up to 15 μs of dispersion. This corresponds to 3 symbols of dispersion, where a state-of-the-art time-domain equalizer, e.g.,, ML method, would be effective to combat ISI. If the rate was increased 20 times, to 8 Mb/s, we could have $L = 60$ symbols of dispersion. In terms of required operations per second, the complexity of a typical time-domain equalizer design would thus increase at least 400 times ($\propto L^2$) [Clar 98]. Coupled with others issues, such as performance and equalizer convergence speed, time-domain equalizers may not, therefore, be viable candidates for high-rate wireless data links. Instead, broadband channels need low-complexity solutions [Ariy 97].

Frequency-domain equalization (FDE) is a techniques that exhibits the property of relatively low complexity growth with increasing channel dispersion. Meanwhile, it shares some common elements with OFDM [Walz 73, Shyn 92, Sari 94, Sari 95], which is popular for broadband wireless systems and offers a similar performance and complexity. However, unlike OFDM, single-carrier FDE does not suffer from high peak-to-average power ratio, and it is less sensitive to frequency and phase offsets [Falc 02a]. It has been shown that SC-FDEs are more robust without heavy interleaving and error-correction coding and less sensitive to nonlinear distortion and carrier synchronization difficulties [Sari 95, Czyl 97].

SC-FDE has been accepted as an option in the uplink of wireless broadband standard IEEE 802.16 [Air 01].

3.4.1 FFT-FDE

At the transmitter, the time-domain vector $\{x_m, m = 0, 1, ..., M-1\}$ results from a direct mapping from original data block onto a selected signal constellation, for example, QAM symbols. The sample blocks are transmitted over frequency-selective channels with a dispersion of L symbols. It is noted that in each transmitted block, the vector $\{x_m\}$ is preceded by a L-length cyclic prefix (CP), which contains the last L samples of $\{x_m\}$, i.e., the whole block is formed as $\{x_{M-L+1}, ..., x_{M-1}, x_0, x_1, ..., x_{M-1}\}$. Again we assumed that $\{x_m\}$ is the independent, identically distributed random complex samples with zero mean and unity variance, $E(|x_m|^2) = 1$.

Basically CP insertion in block transmission has two goals: 1) The received signal can be obtained as a cyclic convolution of the transmitted signal and channel impulse response. Therefore, the channel frequency response is accurately modeled by a complex coefficient for each frequency bin [Oppe 75, Benv 02]; 2) FDE operates block-wise. If the length of CP is longer than channel delay spread L, then the interblock interference (IBI) can be avoided. At the receiver side, CP is discarded before equalization. This results in bandwidth efficiency reduction by the factor $M/(M + L)$. In general, for time-varying wireless environment, M is chosen in such a way that the channel impulse response can be considered to be static during each block transmission.

Assuming that the matched filter and optimal sampling phase are available at the front-end receiver, then the received data y_m can be represented in frequency-domain by

$$Y_k = H_k X_k + V_k, \quad k = 0, 1, ..., M-1, \tag{3.17}$$

where $\{H_k, n = 0, 1, ..., M-1\}$ is the equivalent channel frequency response, including the transmitter and receiver filters. The $\{V_k\}$ is the additive Gaussian noise with zero mean and variance equal to σ_n^2.

To minimize the combined effect of ISI and Gaussian noise, the set of FDE coefficient $\{W_k, k = 0, 1, ..., M-1\}$ can be optimized under the MSE criterion. The equalized time-domain sample block can be described as

$$\bar{y}_m = \frac{1}{M} \sum_{k=0}^{M-1} W_k (H_k X_k + V_k) e^{j\frac{2\pi}{M}km}, \quad m = 0, 1, ..., M. \tag{3.18}$$

Then the MSE error signal is given by

$$\begin{aligned} J_{MSE} &= E\left\{|\bar{y}_m - x_m|^2\right\} \\ &= \frac{1}{M} \sum_{k=0}^{M-1} |W_k|^2 \left(|H_k|^2 + \sigma_n^2\right) - \frac{2}{M} \sum_{k=0}^{M-1} W_k H_k + 1. \end{aligned} \tag{3.19}$$

The FDE coefficients $\{W_k\}$ based on MSE criterion can be derived by minimizing the error signal J_{MSE}, i.e., setting the derivatives of equation (3.19) with respect to W_k to zero. This

solution for optimum FDE coefficients can be represented as [Proa 01, Falc 02a]

$$W_k = \frac{H_k^*}{\sigma_n^2 + |H_k|^2}, \quad k = 0, 1, ..., M. \tag{3.20}$$

Finally, the minimum value of J_{MSE} after equalization can be then expressed as

$$\text{MSE} = \frac{1}{M} \sum_{k=0}^{M-1} \frac{\sigma_n^2}{\sigma_n^2 + |H_k|^2}. \tag{3.21}$$

3.4.2 Noise prediction DFE

The DFE structure, shown in Figure 3.10, consists of a feedforward filter operating in frequency-domain, and a feedback filter doing noise prediction in time-domain. The task of noise prediction is to estimate the ISI effect based on the previous symbol decisions.

The input signal $\{z_m\}$ to decision device can be expressed as

$$z_m = \frac{1}{M} \sum_{k=0}^{M-1} W_k Y_k e^{j\frac{2\pi}{M}km} - \sum_{l=1}^{B} g_l(\bar{y}_{m-l} - \hat{x}_{m-l}). \tag{3.22}$$

where $\{g_l, l = 1, 2, ..., B\}$ denotes feedback coefficients and B is the number of feedback taps.

When the past B symbols decisions are assumed to be correct, i.e., $\{\hat{x}_{m-l} = x_{m-l}, l = 1, 2, ..., B\}$, then the error signal which contains the ISI and noise terms is represented by

$$\begin{aligned} e_m &= x_m - z_m \\ &= \frac{1}{M} \sum_{k=0}^{M-1} X_k e^{j\frac{2\pi}{M}km} - \frac{1}{M} \sum_{k=0}^{M-1} W_k(H_k X_k + V_k) e^{j\frac{2\pi}{M}km} \\ &+ \frac{1}{M} \sum_{k=0}^{M-1} \sum_{l=1}^{B} g_l[W_k(H_k X_k + V_k) - X_k] e^{j\frac{2\pi}{M}k(m-l)}. \end{aligned} \tag{3.23}$$

Let

$$G_k = 1 - \sum_{l=1}^{B} g_l e^{j\frac{2\pi}{M}kl}, \tag{3.24}$$

then the MSE error signal is given by

$$\begin{aligned} J_{MSE} &= E\left\{|e_m|^2\right\} \\ &= E\left\{\left|\sum_{k=0}^{M-1} G_k[X_k - W_k(H_k X_k - V_k)] e^{j\frac{2\pi}{M}km}\right|^2\right\}. \end{aligned} \tag{3.25}$$

It is evident that the design of the FDE coefficients $\{W_k, k = 0, 1, ..., M-1\}$ and NP coefficients G_k, (i.e., any g_l, $l = 1, ..., B$), are independent. For any G_k, the minimum MSE

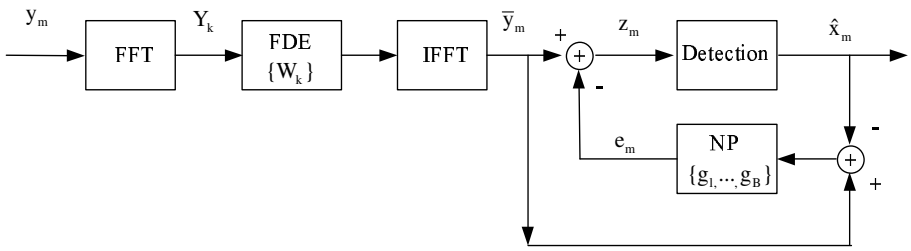

Fig. 3.10 FFT-FDE and noise prediction type DFE.

solution for W_k minimizes the $E\left[|e_m|^2\right]$. Then the MSE can be written as:

$$\begin{aligned} J_{MSE} &= \sum_{k=0}^{M-1} \frac{\sigma_n^2}{|H_k|^2 + \sigma_n^2} |G_k|^2 \\ &= \sum_{k=0}^{M-1} \frac{\sigma_n^2}{|H_k|^2 + \sigma_n^2} \left| 1 - \sum_{l=1}^{B} g_l e^{-j\frac{2\pi}{M}kl} \right|^2 . \end{aligned} \tag{3.26}$$

Minimizing equation (3.26) with respect to g_l for $l = 1, ..B$, we get a set of B equations from which the FBF coefficients g_l can be solved [Belf 79, Zhu 04, Benv 02].

$$\sum_{l=1}^{B} \sum_{k=0}^{M-1} g_l \frac{\sigma_n^2 e^{-j\frac{2\pi}{M}k(p-l)}}{|H_k|^2 + \sigma_n^2} = \sum_{k=0}^{M-1} \frac{\sigma_n^2 e^{-j\frac{2\pi}{M}kp}}{|H_k|^2 + \sigma_n^2}, \qquad \text{for} \quad p = 1, 2, ...B. \tag{3.27}$$

The advantage of this DFE structure is that we are able to adjust the order of NP without changing the FDE design. This advantage makes it easier to adjust the performance complexity trade-off and makes the FDE-NP scheme more flexible and adaptive to practical systems.

3.5 OUR STUDIES

In the case of the DFT banks, the subband frequency responses consist of a mainlobe partly overlapping with the adjacent channels and high sidelobes spreading over a wide frequency band, as shown in Figure 2.3. On the contrary, with frequency-selective filter banks, it is possible to design subband filters with arbitrarily high stopband attenuation. It has been widely recognized that frequency-selective filter banks can offer many advantages over the current DFT-based approaches in multicarrier transmission [Tzan 94, Sand 95, Sioh 02, Ihal 07]. The use of complex modulated filter bank based systems in the SC-FDE application is also interesting to explore.

FB-FDE

Since the filter bank basis functions are longer than a symbol block, the CP used in the DFT approach cannot be utilized. Thus the subbands cannot be considered to have flat fre-

quency responses. On the other hand, the absence of CPs would be a benefit because CPs add overhead and reduce the spectral efficiency.

A high performance single-carrier FB-FDE model without CP overhead was developed in Publication [P1], which applied EMFB introduced in Chapter 2 instead of the FFT transforms. It was found that FB-FDE with mildly frequency-selective subband processing and a modest number of subbands has performance advantage over the FFT-FDE under the most interesting coded frame error rate (FER) region. This is due to the absence of E_b/N_0 degradation related to CPs. Moreover, we examined also the receiver complexity between FB-FDE and FFT-FDE in terms of real multiplications per detected symbol in Publication [P1]. Although the FB-FDE introduces higher complexity than FFT-FDE structures, the same filter bank provides an easily configurable structure for the final stage of the channel filtering chain and a possibility for narrowband interference mitigation, together with the channel equalization functionality. Furthermore, FB-FDE is applicable to any single carrier system, whether CP is included or not. In Publication [P2], the FB-FDE study was extended to DFE case using the noise-prediction feedback filter model.

In these studies, the FB-FDEs equalizer coefficients are calculated at regular intervals based on the channel estimates. We considered ML-based channel estimation method (also known as the least-squares method) [Kay 93] using Gold-codes [Pete 72] as training sequences. The basic ML channel estimation algorithm has been modified to the fractionally-spaced case as explained in [P1]. In our approach, the estimated channel includes also the transmitter and receiver RRC filters.

The channel estimation based equalizer coefficient adaptation approach has various advantages in comparison to adaptive equalization algorithms:

- Fast convergence
- Easy to combine with the frequency-domain matched filter implementation in the FSE case.
- Narrowband interference (NBI) mitigation can be easily included.
- It can be easily adapted to different symbol rates and multi-user FDMA receiver cases.

Our main interest is in the FB-FSE because it has a clear performance advantage over SSE, and the receiver RRC filter can be implemented in frequency-domain with a minor additional complexity. Moreover, since no guard-interval is employed and the subbands are highly frequency-selective, frequency-domain RRC filtering can be implemented independently of the roll-off and other filtering requirements, as long as the stopband attenuation in the filter bank design is sufficient for the receiver filter. Thus FB-FSE structure provides a flexible solution for channel equalization and channel filtering.

Narrowband interference (NBI) mitigation

In certain wireless communication scenarios, strong narrowband interferences (NBI) are considered as a serious problem [Hara 96], and various methods have been developed for mitigating their effects. Frequency-domain NBI mitigation can be easily combined with both FFT-FDE and FB-FDE with minor additional complexity.

The basic scheme for FB-based NBI mitigation was developed in [Stit 04]. In Publication [P5], we proposed a narrowband interference mitigation scheme, where FB-FDE responses wihin subbands can be designed to cope with NBI power, attenuating the interfering frequency while maintaining the NBI-free components of subbands. This is in contrast with complete subband elimination, where the NBI-free frequency components in the subband would be also removed. Meanwhile, a new method to estimate the NBI power and its frequency location within a subband is also studied. The BER performance was estimated as a function of the signal to interference ratio in a channel following the ITU-R Vehicular A model, using 4.685 MHz system bandwidth for 32 subbands. For moderate NBI powers up to 0 dB signal to interference ratio, the proposed FB-FDE scheme yields better performance than complete suppression of the affected subbands. The mitigation method is especially suitable in FDMA multi-user cases where the signal bandwidth allocated to a single user fits in a low or moderate number of subbands. In such cases, the signal energy saved by the proposed approach becomes significant.

Chapter 4

On Combined Equalization and Decoding

For coded transmission, the optimal receiver should perform equalization and decoding jointly. However, this requires a huge calculation complexity and thus is impractical for realization [Tuch 02a, Koet 04]. Under these constraints, the conventional approach is to perform disjoint equalization and decoding at receiver side, i.e., to apply these two tasks sequentially. This disjoint strategy obviously results in a performance loss.

Turbo equalization has been proposed [Doui 95, Glav 97], in which the equalization and decoding procedures are done in iterative way and the result of each iteration is enhanced by the information gained from the previous iteration. Turbo equalizer would yield a tremendous BER performance. This chapter will deal with such an equalization/decoding scheme in the presence of long channel delay spreads. Two proposed equalization/decoding schemes utilizing the low-complexity filter bank based equalizer is presented in Publications [P3][P4].

4.1 INTRODUCTION

Basically, the receiver can request a retransmission of the data block that contained an error sequence that could not be corrected. This is known as automatic retransmission request (ARQ). Repeated transmissions reduce the link data throughput and also add the round-trip delay in the delivery of data, which may make ARQ unsuitable for real-time applications such as voice or video conversations. The ARQ mechanisms are important in today's and emerging broadband wireless communication systems, which utilize extensively internet protocols. However, effective feedforward error control techniques are also mandatory elements in order to utilize the capacity of the wireless transmission channel efficiently. For the sake of securing the reliable bandwidth-efficient data transmission over frequency-selective channels, there is a need for the combination of equalization and decoding functions at the receiver side.

Turbo equalization is a scheme where equalization and decoding are performed in an iterative manner, by exchanging soft information at all stages of the process. Such a system was first proposed in [Doui 95], building upon the principle of Turbo codes introduced by Berrou et al. in [Berr 93]. The conventional approach to turbo equalization [Doui 95, Bahl 74] uses a soft-input soft-output (SISO) MAP equalizer based on the forward-backward algorithm of Bahl, Cocke, Jelinek, and Raviv (BCJR) [Bahl 74]. The computational complexity of this algorithm increases exponentially as a function of the signal alphabet size and the length of discrete channel impulse response. This prevents its practical use in broadband wireless transmission systems, where multilevel signaling is usually required and where long delay spread ISI channels may be encountered. This barrier has motivated the development of reduced-complexity alternatives to the MAP equalizer. The reduced low-complexity solutions usually fall into two main categories, either relaying on reduced-states trellis-based algorithms [Bert 01, Cola 01, Frag 02] or filter based equalizers. In [Glav 97, Ariy 98, Dejo 02, Raph 02, Tuch 02a], a linear filter is used to equalize the received symbols instead of the MAP equalizer, and the equalizer filter parameters are updated using the MSE criterion.

In the following, we present two common structures for turbo equalization with different types of equalizers. One is MAP equalizer, another is MSE equalizer. Again, we assume that, as consistently with Chapter 3, a coherent symbol-spaced receiver front end with perfect knowledge of channel impulse response and symbol timing is assumed. The received waveform is passed through the receiver filter, which is matched to the transmit pulse shape and channel impulse response. Then we can use the symbol-rate baseband system model of equation (3.4).

4.2 TRANSMISSION SCHEME

Figure 4.1 shows a basic structure of the transmitter model in coded transmission. A blocks of data bits $\{b_i, i = 0, 1, ..., N_1 - 1\}$ is encoded to a block of coded bits $\{c_i, i = 0, 1, ..., N_2 - 1\}$. The coded output block length N_2 is $N_1/R_c + K_0$, where N_1 is the input block length, R_c is the code rate and K_0 is the overhead introduced by the encoder. Here, a fixed random bit-interleaver of length N_2 is employed and the corresponding de-interleaver in the receiver performs the inverse operation of the interleaver. The symbol mapper in the transmitter converts blocks of coded bits $\{c_i, i = 0, 1, ...N_2\}$ into blocks of symbols $\{x_m, m = 0, 1, ..., M\}$. For simplicity, here binary phase shift keying (BPSK) is assumed, i.e., $x_m \in \{+1, -1\}$. The relationship between c_i and x_m can be expressed as $x_m = 2c_i - 1$. Both sequences have the same length, $M = N_2$. However, the subscript i denotes the bit-wise index, and the subscript m represents the symbol-wise index.

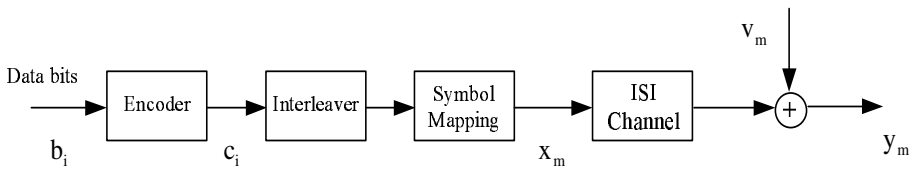

Fig. 4.1 Transmitter side in the coded modulation.

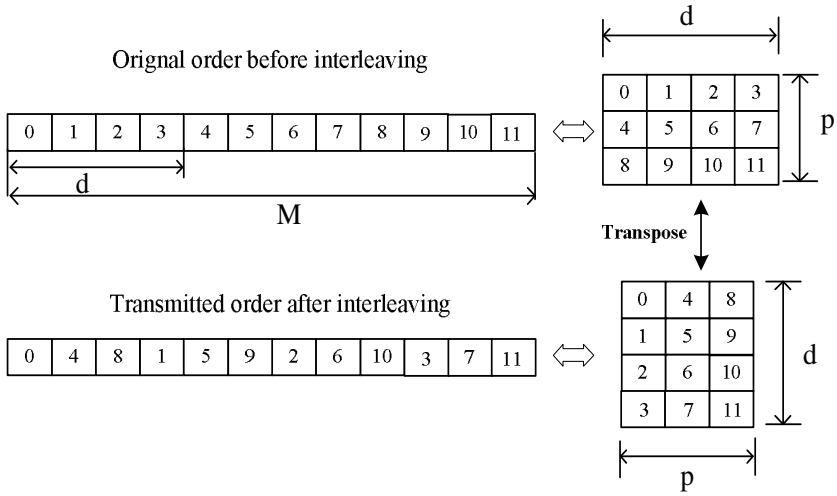

Fig. 4.2 An example of block interleaver with parameters (4,3).

Interleaving

For severe channels in which the errors are not uniformly distributed, but come in as bursts due to sudden deep fades, interleaving technique is combined with error control coding to make it effective in a burst noise environment. The interleaver spreads out adjacent symbols over multiple blocks of symbols. Any burst noise occurring will thus be reflected on the receive side decoder, after de-interleaving, as independent random symbol errors which are more manageable than burst errors.

Interleaving can be classified as either periodic or pseudo-random. The periodic interleaver rearranges the order of the symbols in a repeating sequence. Block interleaving, shown in Figure 4.2, is an example of periodic interleaving. These interleavers accept symbols in blocks and perform identical permutations over each block of data. This is accomplished by taking the input symbols and writing the symbols row-by-row into a matrix with p rows and d columns and then reading the symbols out of the matrix by columns. This is referred to as a $(p,\ d)$ block interleaver. Pseudo-random interleavers rearrange the data in a pseudo-random sequence. Periodic interleaving is more commonly invoked because it is more easily accomplished in hardware. In addition, interleaving can be grouped into two types, namely bit-wise and symbol-wise.

Today, interleaving operations are standard parts of most modern digital communication systems. They require no additional overhead bandwidth, but they do introduce delays since all the code words that populate an interleaving vector must be received before any of them can be extracted and sent on to the decoder.

4.3 TURBO EQUALIZATION

Figure 4.3 depicts the receiver structure of MAP turbo equalizer. In general, the superscripts E and D represent the equalizer and decoder, and the subscript e denotes extrinsic

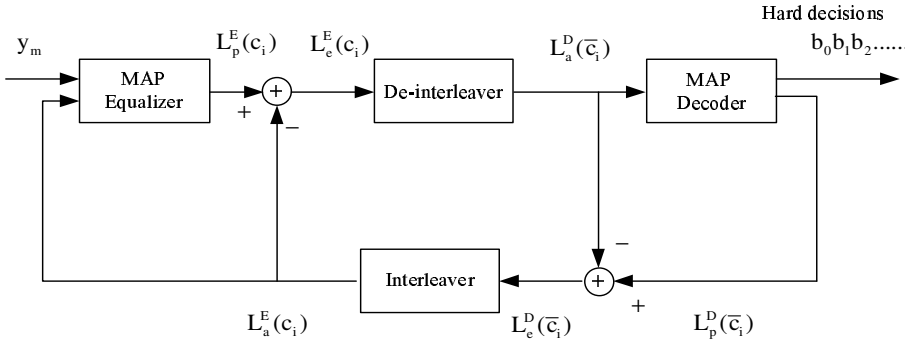

Fig. 4.3 A receiver diagram of turbo equalization using MAP equalizer.

information. The subscripts p and a denote a priori and a posteriori quantities, respectively. In the Figure 4.3, the SISO blocks (both equalizer and decoder) accept and deliver extrinsic information indicating the relative likelihood of each transmitted bit [Koet 04]. The important property of turbo equalizer is that extrinsic information provided by one of the SISO block becomes the a priori information for another SISO block, which increases detection reliability progressively, especially for a few iterations.

4.3.1 MAP equalizer

The MAP equalizer was shown to perform best in simulations among the trellis-based detection schemes [Bauc 98]. As shown in Figure 4.3, the MAP equalizer has two inputs. One is the received sample sequence $\{y_m, m = 0, 1, ..., M-1\}$, the other is the log prior ratio, commonly named as a priori bit log-likelihood ratio (LLR) $\{L_a^E(c_i), i = 0, 1, ..., M-1\}$, which is defined for BPSK modulation by:

$$\begin{aligned} L_a^E(c_i) &= \ln \frac{P_a(c_i = 1)}{P_a(c_i = 0)} \\ &= \ln \frac{P_a(x_m = +1)}{P_a(x_m = -1)}. \end{aligned} \tag{4.1}$$

It is equivalent to extrinsic information $L_e^D(c_i)$, which can be obtained by interleaving the extrinsic information sequence computed by the decoder at the preceding iteration. At the first iteration, no priori information is available, and this sequence reduces to a zero-valued sequence. After the initial stage, block-wise decoding and equalization operations are performed on the same set of received samples.

The MAP equalizer is to generate a posteriori bit LLR sequence of length M, corresponding to the received coded symbols sequence $\{y_m\}$. It can be defined as:

$$L_p^E(c_i) = \ln \frac{P(x_m = +1 | y_0, y_1, ..., y_{M-1})}{P(x_m = -1 | y_0, y_1, ..., y_{M-1})}. \tag{4.2}$$

And this can be expressed in two terms:

$$L_p^E(c_i) = L_a^E(c_i) + L_e^E(c_i). \tag{4.3}$$

The first term $L_a^E(c_i)$ is the priori information available about the coded symbols y_m at the MAP equalizer input. The second term $L_e^E(c_i)$ is the extrinsic information about the coded symbol x_m. Intuitively, it corresponds to the supply of soft information brought by the equalization process. It depends on the received sequence $\{y_m\}$ and on the a priori information available for the other symbols, i.e., $L_a^E(c_j)$ for $j = 0, 1, ...N_2$, with $j \neq i$.

In order to avoid undesired correlation, only the extrinsic part $L_e^E(c_i)$ of the posteriori LLR will be sent (after de-interleaving to preserve time coherence) to the SISO decoder, where it will be used as a priori information. From equation (4.3), this extrinsic information is easily obtained by subtracting the a priori information available at the input from the a posteriori LLR calculated by the SISO equalizer: $L_e^E(c_i) = L_p^E(c_i) - L_a^E(c_i)$.

4.3.2 MAP decoder

The MAP decoder uses the extrinsic information $L_e^E(c_i)$ from the MAP equalizer and computes a posteriori LLR

$$L_p^D(c_i) = \ln \frac{P\left(x_m = +1 | L_e^E(c_0), L_e^E(c_1), ..., L_e^E(c_{M-1})\right)}{P\left(x_m = -1 | L_e^E(c_0), L_e^E(c_1), ..., L_e^E(c_{M-1})\right)}. \tag{4.4}$$

Once again, this posteriori LLR can be expressed in two terms $L_a^D(c_i)$, $L_e^D(c_i)$. Only the extrinsic information $L_e^D(c_i)$ will be fed back to the MAP equalizer.

Meanwhile, the transmitted coded bit sequence can be estimated as:

$$c_i' \approx \underset{u \in \{0,1\}}{\operatorname{argmax}} P(c_i = u | L_p^E(c_0), L_p^E(c_1), ..., L_p^E(c_{M-1})). \tag{4.5}$$

In addition, both the equalizer and decoder can be implemented using the BCJR algorithm, which is optimal in the sense of minimizing the symbol error rate [Bahl 74].

4.3.3 Turbo equalization using MSE equalizer

Instead of using MAP equalizer, the MSE equalizer development leads to a low-complexity solution. The basic turbo equalization structure based on the MSE equalizer is depicted in Figure 4.4. The MSE equalizers, e.g., DFE and IC approaches, can be easily applied. On the basis of available LLR information, $L_e^D(c_i)$, a soft symbol mapper computes symbol estimates $\{\hat{x}_m\}$, which will be fed back to combat the ISI effect and produce more reliable symbols $\{\bar{y}_m\}$ within the MSE equalizer. After the equalizer, a symbol demapper is applied to calculate updated extrinsic LLRs of $\{c_i\}$. The algorithms performing the symbol mapping/demapping operations can be found from [Laot 01, Tuch 02b].

The procedure of such a turbo equalizer is as follows:

1. First the received sample sequence $\{y_m\}$ will be equalized using a MSE equalizer, without any priori information.

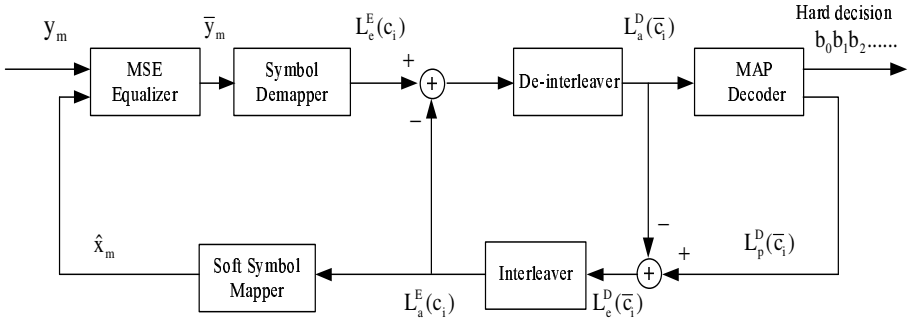

Fig. 4.4 A receiver diagram of turbo equalization using MSE filter equalizer.

2. The symbol demapper following the equalizer computes the updated extrinsic bit LLRs $L_e^E(c_i)$ on the equalized symbols $\bar{y}_m$.

$$L_e^E(c_i|\bar{y}) = \ln\frac{P(x_m = +1|\bar{y}_i)}{P(x_m = -1|\bar{y}_i)} - \ln\frac{P(x_m = +1)}{P(x_m = -1)}.$$

3. SISO decoder uses the extrinsic information $L_e^E(c_i)$ and generates the extrinsic information $L_e^D(\bar{c}_i)$, which will be interleaved, and then the symbol mapper operation is performed. The symbol mapper converts blocks of the extrinsic LLR information into the estimated symbol blocks $\{\hat{x}_m\}$. In the case of BPSK modulation, the mapping can be done in soft decision manner by

$$\hat{x}_m = \sum_{u\in\{+1,-1\}} x \cdot P(x_i = u) = \frac{e^{L_e^D(c_i)} - 1}{e^{L_e^D(c_i)} + 1}. \tag{4.6}$$

Or, on the other hand, $\{\hat{x}_m\}$ can be obtained in hard decision way, according to

$$\hat{x}_m = \begin{cases} 1, & L_e^D(c_i) > 0 \\ -1, & L_e^D(c_i) \le 0. \end{cases} \tag{4.7}$$

4. The reliable feedback samples $\{\hat{x}_m\}$ are applied to combat the ISI effect, based on minimizing the cost function $E(|x_m - \hat{x}_m|^2)$. The approaches discussed the Chapter 3.2 can be then easily adopted.

5. Repeat from step 2 until a suitable termination criterion is reached.

4.4 OUR STUDIES

The most popular combined equalization/decoding scheme is turbo equalization. Basically, turbo equalization systems can choose different structures for the equalization task. For example, MAP equalizers were used in [Bauc 98, Doui 95], while LEs and DFEs were applied in [Glav 97, Tuch 02a]. In the decoder, most of them use exclusively MAP techniques. The

major motivation for developing these different turbo equalization systems is to search for good tradeoff between computational complexity and performance.

The main contribution in this area is to integrate the filter bank based equalizer into equalization/decoding loop. We examined two new low-complexity equalization/decoding schemes with LDPC coded single-carrier modulation. Both MSE equalizer structures utilize the same filter bank based frequency-domain equalizer and noise prediction as feedforward and feedback filters, respectively. One is turbo equalization method in Publication [P3], another is named block DFE in Publication [P4], where a simple symbol-wise interleaver/de-interleaver pair is utilized to re-arrange the received symbols for decoding, in such a way that previous detected symbol blocks can be used to predict ISI effects in next blocks. In this latter case, a short code block is preferred so as to have more reliable detected feedback for noise prediction in the feedback loop. This is in contrast with turbo equalization, where the whole transmitted frame is first decoded completely and then the possible feedback taps can be selected freely. Moreover, for one iteration of turbo DFE, each block of symbols is decoded twice before the final decision is made. Block DFE is a kind of successive decoding scheme, where every symbol block is decoded only once, and the previous symbol blocks are used to combat the ISI effects in the current block. Then it naturally has lower complexity than the turbo DFE.

Various design considerations and performance assessment are presented in Publications [P3][P4]. Simulations show that the proposed combined equalization/decoding schemes with five feedback taps can achieve most of the performance gain over the linear equalizer in time dispersive multipath wireless channels (ITU-R Vehicular-A channel model assumed). Moreover, in Publication [P4], performance comparison between these two different schemes is addressed. It demonstrates that the block DFE with reference blocks can achieve a similar performance as the turbo DFE with one iteration, while it has clearly lower complexity than the turbo approach.

The drawback of the block DFE scheme of Publication [P4] is that only relatively short code block lengths are feasible. This is because, if the code block length is increased while keeping the interleaver block size fixed, the performance is degraded due to reduced average number of feedback taps. Also the overhead due to reference symbols grows with the code block length. On the other hand, the interleaver depth cannot be increased significantly in wireless communication systems with moderate or high mobility, since the channel is assumed to be constant over one transmitted frame.

Chapter 5

Summary of Publications

5.1 OVERVIEW OF STUDIES

This thesis includes seven publications [P1]-[P7]. They address different aspects of filter bank based signal processing in communications receivers. The studied methods are mainly intended for single carrier transmission utilizing linear digital modulation techniques (e.g., m-QAM), but they can be used for various other waveforms (like spread-spectrum) as well.

In Publication [P1], a novel filter bank based frequency-domain equalization technique was introduced and analyzed in detail. The basic idea had been earlier published in compact form in [Yang 05]. This method combines an analysis-synthesis filter bank system with low-complexity subband-wise equalizers. Two different subband-wise equalizer structures are studied: (i) a 3-tap FIR filter with complex coefficients, (ii) the cascade of an allpass filter as phase equalizer and a linear-phase FIR filter as amplitude equalizer. It was found that the BER/FER performance of FB-FDE exceeds the performance of FFT-FDE in LDPC coded transmission due to the absence of CP, while the number of subbands needed in the FB-FDE can be significantly lower than in the FFT based approach. In addition, the receiver complexity between FB-FDEs and FFT-FDEs in terms of real multiplications per detected symbol was examined. The complexity metric includes the FB/FFT transform and subband equalizers, as well as the baseband filtering. It was found that FSE may actually be less complex to implement than SSE because the baseband filtering can be implemented ideally in frequency-domain by FSE without additional complexity. Moreover, the complexity of FB-FDE depends heavily on the overlapping factor of the FB design. The type of subband equalizer has a minor effect on the overall complexity.

Publication [P2] established a hybrid frequency-time domain equalization structure in the case of uncoded single-carrier modulation. The structure includes a filter bank based fractionally-spaced linear equalizer and a noise predictor as decision feedback block. It was demonstrated that this hybrid equalizer has the capability of achieving significant performance gain over the linear equalizer if correct feedback decisions are assumed. The sensitivity of the performance on decision errors was also clearly demonstrated. This mo-

tivated us to study DFE configurations where the error control decoding is included in the feedback loop.

In Publications [P3] and [P4], we studied two different equalization/decoding schemes in coded single-carrier transmission, where the hybrid equalizer structure of Publication [P2] and a soft-input soft-output decoding block are applied. Publication [P3] combined a widely-studied turbo equalization approach to the hybrid DFE structure, while Publication [P4] examined an interleaving based block DFE scheme in coded transmission, which results in low-complexity solution compared to the turbo equalization approach. The BER/FER performance comparison between two schemes is also addressed.

Publication [P5] discussed the use of the developed FB-FDE structure in narrowband interference mitigation. It is known from earlier studies [Stit 04] that filter bank based narrowband interference mitigation has a clear benefit over FFT-based frequency-domain approaches. The Publication [P5] showed how to improve the selectivity of interference mitigation by tuning the subband equalizer coefficients in such a way that only the interference contaminated parts of each subband are suppressed. This gives a useful performance enhancement with very minor additional computational complexity, affecting only on the equalizer coefficient calculation but not on the equalizer operation. The method is especially suitable in FDMA-based multi-user cases where the signal bandwidth allocated to a single user fits in a low or moderate number of subbands. In such cases, the signal energy saved by the proposed approach becomes significant.

Publications [P6] and [P7] include two case studies where the implementability of the studied algorithms with programmable digital signal processors is examined. Publication [P6] explored the implementation of the key elements of a filter bank based multicarrier system, which are basically the same as in in the FB-FDE. The main difference is that the filter banks are used in the transmultiplexer (synthesis-analysis) configuration. The same structures can be used for subchannel equalization that are used in FB-FDE. Publications [P7] studied a multirate filter bank system with analysis-synthesis configuration. The subband signal processing was used to cancel narrowband interferences in a CDMA system. The memory and achievable sampling rate with the used digital signal processor are the main issues studied in both of these publications.

5.2 AUTHOR'S CONTRIBUTIONS TO THE PUBLICATIONS

The research work of this thesis was carried out at the the Institute of Communications Engineering at Tampere University of Technology as one member of an active research group, developing multirate filter bank solution for both MC and SC modulations. The whole research work has been supported and supervised by Prof. Markku Renfors. None of the above publications has been used as a part of any doctoral dissertation or any other academic thesis.

Naturally, all of the coauthors have contributed to the final appearance of each paper, but the author was the main contributor to all publications. The author's contribution in Publication [P1] is an efficient combination of analysis-synthesis filter bank system and low-complexity subband-wise equalizers, applied to frequency-domain equalization in single-carrier systems. The analysis and synthesis filter bank designs were provided by Ari Viholainen and Juuso Alhava. The general idea of subband-wise channel equalization was

due to Prof. Markku Renfors and it has been used earlier in the multicarrier context. The FB-FDE system implementation in the MATLAB environment and comparisons with FFT-FDE were done by the author. In Publication [P2], the author worked out the combination of FB-FDE as feedforward filter and noise predictor as feedback section, after considering possibilities to include the FB-FDE in different DFE configurations. The numerical results were also obtained by the author. In the Publication [P1], [P3] and [P4], a public-domain MATLAB script for LDPC was utilized. In [P3] and [P4], the author worked out the receiver structures where the error control decoding is included in the DFE feedback loop. In Publication [P5], Prof. Markku Renfors and Tobias Hidalgo Stitz proposed the general idea of interference mitigation within the subband. The author developed its realization in FB-FDE configuration and completed the performance analysis. In [P6] and [P7], all the code development and optimization and the numerical results were produced by the author, while the MATLAB scripts performing interference calculation in CDMA system and channel equalization in MC modulation were developed by Tobias Hidalgo Stitz and Tero Ihalainen, respectively. The work included the investigation of the feasibility of different complex-modulated filter bank structures in digital signal processor implementation.

Chapter 6

Conclusions and Future Work

Design techniques for filter banks reached a stage of maturity a decode or so back, and modern research trends in this direction have accordingly focused more on suitability of a filter bank design to the particular application. This work was motivated by the desire to explore the multirate filter bank applications in digital communication systems. One of the main technical challenges in advanced wireless communications stems from the characteristics of a wireless channel, i.e., fading multipath propagation. Channel equalization, together with error control coding, is essential for achieving reliable information transmission for practical wireless communication applications. Numerous channel equalization structures have been developed for different underlying channels and communication waveforms.

In this thesis, we presented a novel frequency-domain equalizer without CP in single-carrier transmission, using exponentially modulated filter bank transform. The subband channel response is not flat anymore, as in the FFT-based scheme, and two subband equalizer structures were examined. The one, referred to as CFIR-FBEQ, consists of a complex FIR filter, another one, referred to as AP-FBEQ, has separate filter sections for amplitude and phase equalization. It was shown how the equalizer coefficients can be calculated for each subband independently of the others, when using an oversampled analysis bank. The two subband equalizer structures have rather similar computational complexity in terms of the multiplication rate. CFIR-FBEQ has a simple structure, but AP-FBEQ has certain very useful advantages. First, narrowband interference mitigation can be easily combined with AP-FBEQ, where it affects only on the amplitude equalizer part. Second, AP-FBEQ is more robust to timing offsets. Due to multipath channel, different subband signals experience different group delays. The subband equalizers compensate those differences, as well as a possible common delay due to non-ideal timing synchronization in the input. The AP-FBEQ performance is clearly better with significant timing offsets, approaching half of the subband sample spacing. Third, AP-FBEQ is helpful in the design of the synthesis filter bank with reduced number of subbands, as needed in the efficient implementation of the fractionally-spaced FDE. In [Viho 06b], a filter bank system with a 2M-channel analysis bank and an M-channel synthesis bank is developed, and it is observed that tuning of the phase response in the subband equalizers is needed to achieve nearly perfect reconstruction characteristics with low distortion.

The FB-FDEs introduce, no doubt, higher calculation complexity than FFT-FDE structures. However, the filter bank can be used simultaneously to implement part of the channel filtering, with much higher performance than when using the FFT-FDE structures. FB-FDE provides an easily configurable structure for the final stage of the channel filtering chain and a possibility for narrowband interference mitigation, together with the channel equalization functionality.

For securing the reliable transmission using error control coding, we also have investigated combined equalization/decoding schemes which integrate FB-FDE as feedforward filter and time-domain noise prediction as feedback filter. Especially, it turned out that the DFE structure can provide significant performance gain if the error control decoding is carefully combined with the decision feedback structure. Two structures were studied; One of them belongs to the concept of turbo equalization, where equalization and decoding are performed in iterative way. The other approach is a kind of successive equalization/decoding structure, in which previous decoding blocks are applied to combat the ISI effect of the current block. The latter approach results in lower complexity, but it implies significant limitations on the coding block length in case of fading channels.

In our studies, using the time-domain noise prediction model, the feedback filter can only cancel the postcursor ISI. It would result in better performance if the precursor could also be eliminated, in the same way as in the time-domain interference cancelation method stated in Chapter 3. In [Ng 07, Benv 05], frequency-domain interference cancelation in the feedback loop is proposed, where DFT transform is applied in a block iterative equalizer. Both precursor and postcursor ISI can be eliminated and it is shown to deliver performance very close to the matched filter bound with relatively low complexity, compared to the time-domain counterpart.

The exploration of using frequency-domain feedback filter in filter bank configuration would be an interesting future work. Then it would be important to find how feedforward and feedback filters are jointly optimized in each iteration to mitigate error propagation in the decision feedback process. It would also be worthy to investigate whether the filter bank based equalizers offer sensibly different extrinsic information transfer functions compared to conventional time-domain equalizers and DFT based frequency-domain equalizers, and whether this has an impact on convergence time and the critical signal-to-noise ratio beyond which the turbo effect is observed to trigger. These would contribute a better understanding to the performance issues of frequency-domain equalizers in iterative receiver design.

References

[3GPP] "3GPP". http://www.3gpp.org/Highlights/LTE/LTE.htm.

[Air 01] "Air Interface for Fixed Broadband Wireless Access Systems Part A: Systems between 2 and 11 GHz". IEEE Std. 802.16ab-01/01, 2001.

[Alha 01] J. Alhava and M. Renfors. "Adaptive sine-modulated/cosine-modulated filter bank equalizer for transmultiplexers". In: *Proc. European Conference on Circuit Theory and Design*, pp. 337–340, Espoo, Finland, Aug. 2001.

[Ande 73] I. N. Andersen. "Sample-whitened match filters". *IEEE Transactions on Information Theory*, Vol. IT-19, pp. 653–650, Sep. 1973.

[Ariy 97] S. Ariyavisitakul and L. J. Greenstein. "Reduced-complexity equalization techniques for broadband wireless channels". *IEEE Journal on Selected Areas in Communications*, Vol. 15, pp. 5–15, Jan. 1997.

[Ariy 98] S. Ariyavisitakul and Y. Li. "Joint coding and decision feedback equalization for broadband wireless channels". *IEEE Journal on Selected Areas in Communications*, Vol. 16, pp. 96–102, Dec. 1998.

[Auli 99] T. M. Aulin. "Breadth-first maximum likelihood sequence detection: Basics". *IEEE Transactions on Communications*, Vol. 47, pp. 208–216, Feb. 1999.

[Baha 99] A. R. S. Bahai and B. R. Saltzberg. *Multi-carrier digital communications: Theory and applications*. Kluwer Academic Publishers, Norwell, MA, 1999.

[Bahl 74] L. R. Bahl, J. Cocke, F. Jelinek, and J. Raviv. "Optimal decoding of linear codes for minimizing symbol error rate". *IEEE Transactions on Information Theory*, Vol. IT-20, pp. 284–287, March 1974.

[Bauc 98] G. Bauch and V. Franz. "A comparison of soft-in/soft-out algorithms for turbo detection". In: *Proc. International Conference on Telecommunications*, pp. 259–263, 1998.

[Belf 79] C. A. Belfiore and J. H. Park. "Decision feedback equalization". *Proc. IEEE*, Vol. 67, pp. 1143–1156, Aug. 1979.

[Bell 74] M. G. Bellanger and J. L. Gaguet. "TDM-FDM transmultiplexer: Digital polyphase and FFT". *IEEE Transactions on Communications*, Vol. 22, pp. 1199–1204, 1974.

[Benv 02] N. Benvenuto and S. Tomasin. "On the comparison between OFDM and single carrier with a DFE using a frequency domain feedforward filter". *IEEE Transactions on Communications*, Vol. 50, pp. 947–955, June 2002.

[Benv 05] N. Benvenuto and S. Tomasin. "Iterative design and detection of a DFE in the frequency domain". *IEEE Transactions on Communications*, Vol. 53, pp. 1867–1875, nov 2005.

[Berr 93] C. Berrou, A. Glavieux, and P. Thitimajshima. "Near shannon limit error-correcting coding and decoding: Turbo codes". In: *Proc. IEEE International Conference on Communications*, pp. 1064–1070, Geneva, Switzerland, May 1993.

[Bert 01] A. O. Berthet, B. S. Ünal, and R. Visoz. "Iterative decoding of convolutionally encoded signals over multipath Rayleigh fading channels". *IEEE Journal on Selected Areas in Communications*, Vol. 19, pp. 1729–1743, Sep. 2001.

[Bing 90] J. A. C. Bingham. "Multicarrier modulation: An idea whose time has come". *IEEE Communications Magazine*, Vol. 28, pp. 5–14, May 1990.

[Bolc 97] H. Bolcskei and F. Hlawatsch. "Oversampled filter banks: Optimal noise shaping, design freedom, and noise analysis". In: *Proc. IEEE International Conference on Acoustics, Speech, and Signal processing*, pp. 2453–2456, Apr. 1997.

[Bolc 98] H. Bolcskei and F. Hlawatsch. "Oversampled cosine modulated filter banks with perfect reconstruction". *IEEE Transactions on Circuits and Systems II*, Vol. 45, pp. 1057–1071, Aug. 1998.

[Chen 05] S. Cheng and Z. Xiong. "Audio coding and image denoising based on the nonuniform modulated complex lapped transform". *IEEE Transactions on Multimedia*, Vol. 7, pp. 817–827, Oct. 2005.

[Cirp 98] H. A. Cirpan and M. K. Tsatsanis. "Stochastic maximum likelihood methods for semi-blind channel estimation". *IEEE Signal Processing Letters*, Vol. 5, pp. 21–24, Jan. 1998.

[Clar 98] M. V. Clark. "Adaptive frequency-domain equalization and diversity combining for broadband wireless communications". *IEEE Journal on Selected Areas in Communications*, Vol. 16, No. 8, pp. 1385–1395, Oct. 1998.

[Cola 01] G. Colavolpe, G. Ferrari, and R. Raheli. "Reduced-state BCJR-type algorithms". *IEEE Journal on Selected Areas in Communications*, Vol. 19, pp. 848–859, May 2001.

[Croc 83] R. E. Crochiere and L. R. Rabiner. *Multirate digital signal processing*. Prentice Hall, 1983.

[Cvet 03] Z. Cvetkovic and J. D. Johnston. "Nonuniform oversampled filter banks for audio signal processing". *IEEE Transactions on Acoustics, Speech, and Signal Processing*, Vol. 11, pp. 393–399, Sep. 2003.

[Czyl 97] A. Czyliwk. "Comparison between adaptive OFDM and single carrier modulation with frequency domain equalization". In: *Proc. IEEE Vehicular Technology Conference*, pp. 865–869, Phoenix, May 1997.

[Dejo 02] A. Dejonghe and L. Vanderdorpe. "Turbo equalization for multilevel modulation: An efficient low-complexity scheme". In: *Proc. IEEE International Conference on Communications*, pp. 1863–1867, 2002.

[Doui 95] C. Douillard, M. Jezequel, and C. Berrou. "Iterative correction of intersymbol interference: Turbo–equalization". *European Transactions on Telecommunications*, Vol. 6, pp. 507–511, Sep. 1995.

[Eyub 88] M. V. Eyuboglu and S. U. H. Qureshiu. "Reduced-state sequence estimation with set partitioning and decision-feedback". *IEEE Transactions on Communications*, Vol. 36, pp. 13–20, Jan. 1988.

[Falc 02a] D. Falconer, S. L. Ariyavisitakul, A. Benyamin-Seeyar, and B. Eidson. "Frequency domain equalization for single-carrier broadband wireless systems". *IEEE Communications Magazine*, Vol. 40, No. 4, pp. 58–66, Apr. 2002.

[Falc 02b] D. Falconer and S. Ariyavisitakul. "Broadband wireless using single carrier and frequency domain equalization". In: *Proc. 5th International Symposium Wireless Personal Multimedia Communications*, pp. 27–36, Oct. 2002.

[Faze 03] K. Fazel and S. Kaiser. *Multi-carrier and spread spectrum systems*. John Wiley & Sons, Inc., NY, USA, 2003.

[Forn 72] G. Forney. "Maximum-likelihood estimation of digital sequences in the presence of intersymbol interference". *IEEE Transactions on Information Theory*, Vol. 18, pp. 363–378, May 1972.

[Frag 02] C. Fragouli, N. Al-Dhahir, S. N. Diggavi, and W. Turin. "Prefiltered space-time M-BCJR equalizer for frequency-selective channels". *IEEE Transactions on Communications*, Vol. 50, pp. 742–753, May 2002.

[Gath 00] A. Gatherer, T. Stetzler, M. McMahan, and et al. "DSP-based architectures for mobile communications: Past, present and future". *IEEE Communications Magazine*, Vol. 38, pp. 84–90, Jan. 2000.

[Gers 02] W. Gerstacker and R. Schober. "Equalization concepts for EDGE". *IEEE Transactions on Wireless Communications*, Vol. 1, pp. 190–199, Jan. 2002.

[Gian 97] G. B. Giannakis. "Filter banks for blind channel identification and equalization". *IEEE Signal Processing Letters*, Vol. 4, pp. 184–187, June 1997.

[Glav 97] A. Glavieux, C. Laot, and J. Labat. "Turbo equalization over a frequency selective channel". In: *Proc. International Symposium Turbo Codes & Related Topics*, pp. 96–102, Brest, France, Sep. 1997.

[Gold 05] A. Goldsmith. *Wireless communications*. Cambridge University Press, NY, USA, 2005.

[Gusm 03] A. Gusmao, R. Dinis, and N. Esteves. "On frequency domain equalization and diversity combining for broadband wireless communications". *IEEE Transactions on Communications*, Vol. 51, pp. 1029–1043, jul 2003.

[Hara 96] S. Hara, T. Matsuda, K. Ishikura, and N. Morinaga. "Co-existence problem of TDMA and DS-CDMA systems-application of complex multirate filter bank". In: *Proc. IEEE Global Communications Conference*, pp. 1281–1285, London, UK, Nov. 1996.

[Hash 87] T. Hashimoto. "A list-type reduced-constraint generalization of the Viterbi algorithm". *IEEE Transactions on Information Theory*, Vol. IT-33, pp. 866–876, Nov. 1987.

[Hell 99] P. N. Heller, T. Karp, and T. Q. Nguyen. "A general formulation of modulated filter banks". *IEEE Transactions on Signal Processing*, Vol. 47, pp. 986–1002, Apr. 1999.

[Hiro 80] B. Hirosaki. "An analysis of automatic equalizers for orthogonally multiplexed QAM systems". *IEEE Transactions on Communications*, Vol. 15, No. 1, pp. 73–83, 1980.

[Ihal 05] T. Ihalainen, T. H. Stitz, and M. Renfors. "Efficient per-carrier channel equalizer for filter bank based multicarrier systems". In: *Proc. IEEE International Symposium on Circuits and Systems*, Japan, May 2005.

[Ihal 07] T. Ihalainen, T. Hidalgo Stitz, M. Rinne, and M. Renfors. "Channel equalization in filter bank based multicarrier modulation for wireless communications". *EURASIP Journal on Advances in Signal Processing*, Vol. 2007, pp. Article ID 49389, 18 pages, 2007. doi:10.1155/2007/49389.

[Kade 97] G. Kadel. "Diversity and equalization in frequency domain - A robust and flexible receiver technology for broadband mobile communication systems". In: *Proc. IEEE Vehicular Technology Conference*, pp. 894–898, Phoenix, May 1997.

[Karp 99] T. Karp and N. J. Fliege. "Modified DFT filter banks with perfect reconstruction". *IEEE Transactions on Circuits and Systems II*, Vol. 46, pp. 1404–1414, Nov. 1999.

[Kay 93] S. M. Kay. *Fundamentals of statistical signal processing: estimation theory*. Prentice-Hall, Inc., Upper Saddle River, NJ, USA, 1993.

[Koet 04] R. Koetter, A. C. Singer, and M. Tuchler. "Turbo equalization". *IEEE Signal Processing Magazine*, Vol. 21, pp. 67–80, Jan. 2004.

[Koil 92] R. D. Koilpillai and P. P. Vaidyanathan. "Cosine-modulated FIR filter banks satisfying perfect reconstruction". *IEEE Transactions on Signal Processing*, Vol. 40, pp. 770–783, Apr. 1992.

[Laot 01] C. Laot, A. Glavieux, and J. Labat. "Turbo equalization: adaptive equalization and channel decoding jointly optimized". *IEEE Journal on Selected Areas in Communications*, Vol. 19, pp. 1744–1752, Sep. 2001.

[Li 95] Y. Li, B. Vucetic, and Y. Sato. "Optimum soft-output detection for channels with intersymbol interference". *IEEE Transactions on Information Theory*, Vol. 41, pp. 704–713, May 1995.

[Malv 92a] H. S. Malvar. "Extended lapped transforms: Properties, applications and fast algorithm". *IEEE Transactions on Signal Processing*, Vol. 40, pp. 2703–2714, Nov. 1992.

[Malv 92b] H. S. Malvar. *Signal processing with lapped transforms*. Artech House, 1992.

[Mars 01] I. Marsland. "An introduction to Turbo equalization". Seminar presentation, http://www.sce.carleton.ca/bcws/, March 2001.

[Mart 03] I. Martoyo, T. Weiss, F. Capar, and F. Jondral. "Low complexity CDMA downlink receiver based on frequency domain equalization". In: *Proc. IEEE Vehicular Technology Conference*, pp. 987–991, Oct. 2003.

[Medl 97] M. J. Medley, G. J. Saulnier, and P. K. Das. "Narrow-band interference excision in spread spectrum systems using lapped transforms". *IEEE Transactions on Communications*, Vol. 45, pp. 1444–1455, Nov. 1997.

[Ng 07] B. Ng, C.-T. Lam, and D. Falconer. "Turbo frequency domain equalization for single-carrier broadband wireless systems". *IEEE Transactions on Communications*, Vol. 6, pp. 759–767, Feb. 2007.

[Oppe 75] A. V. Oppenheim and R. W. Schafer. *Digital signal processing*. Prentice-Hall, NJ, 1975.

[Pete 72] W. W. Peterson and E. J. W. Jr. *Error-correcting codes, 2nd ed.* Cambridge, MIT Press, 1972.

[Petr 00] M. Petraglia, R. Alves, and P. Diniz. "New structures for adaptive filtering in subbands with critical sampling". *IEEE Transactions on Acoustics, Speech, and Signal Processing*, Vol. 48, pp. 3316–3327, Dec. 2000.

[Proa 01] J. G. Proakis. *Digital Communications (4th Edition)*. McGraw-Hill, NY, USA, 2001.

[Proa 70] J. G. Proakis. "Adaptive nonlinear filtering techniques for data transmission". In: *Proc. IEEE Symposium on Adaptive Processes, Decision and Control*, pp. XV.2.1–XV.2.5, 1970.

[Raph 02] D. Raphaeli and A. Saguy. "Reduced complexity APP for turbo equalization". In: *Proc. IEEE International Conference on Communications*, pp. 1940–1943, 2002.

[Sand 95] S. D. Sandberg and M. A. Tzannes. "Overlapped discrete multitone modulation for high speed copper wire communications". *IEEE Journal on Selected Areas in Communications*, Vol. 13, No. 9, pp. 1571–1585, 1995.

[Sara 92] T. Saramaki. "Designing prototype filters for perfect-reconstruction cosine-modulated filter banks". In: *Proc. IEEE International Symposium on Circuits and Systems*, pp. 1605–1608, San Diego, USA, May 1992.

[Sari 94] H. Sari, G. Karam, and I. Jeanclaude. "An analysis of orthogonal frequency-division multiplexing for mobile radio applications". In: *Proc. IEEE Vehicular Technology Conference*, pp. 1635–1639, Stolkholm, Sweden, June 1994.

[Sari 95] H. Sari, G. Karam, and I. Jeanclaude. "Frequency-domain equalization of digital terrestrial TV broadcasting". *IEEE Communications Magazine*, Vol. 33, pp. 100–109, Feb. 1995.

[Schn 04] P. Schniter and H. Liu. "Iterative frequency-domain equalization for single-carrier systems in doubly-dispersive channels". In: *Proc. 38th Asilomar Conference on Signals, Systems and Computers*, pp. 667–671, Asilomar, CA, USA, Nov. 2004.

[Shyn 92] J. J. Shynk. "Frequency-domain and multirate adaptive filtering". *IEEE Signal Processing Magazine*, Vol. 9, pp. 14–35, Jan. 1992.

[Sioh 02] P. Siohan, C. Siclet, and N. Lacaille. "Analysis and design of OFDM/OQAM systems based on filterbank theory". *IEEE Transactions on Signal Processing*, Vol. 50, pp. 1170–1183, 2002.

[Star 99] T. Starr, J. M. Cioffi, and P. J. Silverman. *Understanding digital subscriber line technology*. Prentice Hall, 1999.

[Stit 04] T. H. Stitz and M. Renfors. "Filter bank based narrowband interference detection and suppression in spread spectrum systems". *EURASIP Journal on Applied Signal Processing*, Vol. 2004, No. 8, pp. 1163–1176, 2004. doi:10.1155/S1110865704312102.

[Stra 96] G. Strang and T. Nguyen. *Wavelets and Filter Banks*. Wellesley-Cambridge, MA, 1996.

[Trei 96] J. Treichler, I. Fijalkow, and J. C.R. Johnson. "Fractionally spaced equalizers: How long should they really be". *IEEE Signal Processing Magazine*, Vol. 13, pp. 65–81, Nov. 1996.

[Tuch 02a] M. Tuchler, R. Koetter, and A. Singer. "Turbo equalization: Principles and new results". *IEEE Transactions on Communications*, Vol. 50, pp. 754–767, May 2002.

[Tuch 02b] M. Tuchler, A. Singer, and R. Koetter. "Minimum mean square error equalization using a Priori information". *IEEE Transactions on Signal Processing*, Vol. 50, No. 3, pp. 673–683, March 2002.

[Tugn 00] J. K. Tugnait, L. Tong, and Z. Ding. "Single-user channel estimation and equalization". *IEEE Signal Processing Magazine*, Vol. 17, pp. 16–28, May 2000.

[Turi 80] G. L. Turin. "Introduction to spread-spectrum anti-multipath techniques and their application to urban digital radio". In: *Proc. IEEE*, pp. 328–353, March 1980.

[Tzan 94] M. A. Tzannes, M. C. Tzannes, J. Proakis, and P. N. Heller. "DMT systems, DWMT systems and digital filter banks". In: *Proc. IEEE International Conference on Communications*, pp. 311–315, May 1994.

[Vaid 00] P. P. Vaidyanathan, Y. P. Lin, S. Akkarakaran, and S. M. Phoong. "Optimalilty of principal component filter banks for discrete multitone communication systems". In: *Proc. IEEE International Symposium on Circuits and Systems*, Geneva, May 2000.

[Vaid 01] P. P. Vaidyanathan. "Filter banks in digital communications". *IEEE Circuits and Systems Magazine*, Vol. 1, pp. 4–25, 2001.

[Vaid 93] P. P. Vaidyanathan. *Mutlirate System and Filter Banks*. Prentice-Hall, NJ, 1993.

[Viho 02] A. Viholainen, T. H. Stitz, J. Alhava, T. Ihalainen, and M. Renfors. "Complex modulated critically sampled filter banks based on cosine and sine modulation". In: *Proc. IEEE International Symposium on Circuits and Systems*, pp. 833–836, Scottsdale, USA, May 2002.

[Viho 04] A. Viholainen. *Modulated filter bank design for communications signal processing*. PhD thesis, Tampere University of Technology, Nov., 2004.

[Viho 06a] A. Viholainen, J. Alhava, and M. Renfors. "Efficient implementation of 2x oversampled exponentially modulated filter banks". *IEEE Transactions on Circuits and Systems II*, Vol. 53, pp. 1138–1142, Oct. 2006.

[Viho 06b] A. Viholainen, T. Ihalainen, T. H. Stitz, Y. Yang, and M. Renfors. "Flexible filter bank dimensioning for multicarrier modulation and frequency domain equalization". In: *Proc. 2006 IEEE Asia Pacific Conference on Circuits and Systems*, pp. 451–454, Singapore, Dec. 2006.

[Walz 73] T. Walzman and M. Schwartz. "Automatic equalization using the discrete frequency domain". *IEEE Transactions on Information Theory*, Vol. IT-19, pp. 59–68, Jan. 1973.

[Wang 84] Z. Wang. "On computing the discrete Fourier and cosine transform". *IEEE Transactions on Acoustics, Speech, and Signal Processing*, Vol. 32, pp. 803–816, Aug. 1984.

[Wein 71] S. B. Weinstein and P. M. Ebert. "Data transmission by frequency-division multiplexing using the discrete Fourier transform". *IEEE Transactions on Communications*, Vol. COM-19, No. 5, pp. 628–634, Oct. 1971.

[Yang 05] Y. Yang, T. Ihalainen, and M. Renfors. “Filter bank based frequency-domain equalizer in single-carrier modulation”. In: *Proc. 14th IST Mobile and Wireless Communications Summit*, Dresden, Germany, June 2005.

[Zhu 04] Y. Zhu and K. B. Letaief. “Single carrier frequency domain equalization with noise prediction for broadband wireless systems”. In: *Proc. IEEE Global Communications Conference*, pp. 3098–3102, Dallas, Texas, USA, Dec. 2004.

Publications

Publication P1

Y. Yang, T. Ihalainen, M. Rinne, and M. Renfors, "Frequency-domain equalization in single-carrier transmission: Filter bank approach," *EURASIP Journal on Advances in Signal Processing*, vol. 2007, Article ID 10438, 16 pages, 2007.

Hindawi Publishing Corporation
EURASIP Journal on Advances in Signal Processing
Volume 2007, Article ID 10438, 16 pages
doi:10.1155/2007/10438

Research Article

Frequency-Domain Equalization in Single-Carrier Transmission: Filter Bank Approach

Yuan Yang,[1] Tero Ihalainen,[1] Mika Rinne,[2] and Markku Renfors[1]

[1] *Institute of Communications Engineering, Tampere University of Technology, P.O. Box 553, 33101 Tampere, Finland*
[2] *Nokia Research Center, P. O. Box 407, Helsinki 00045, Finland*

Received 12 January 2006; Revised 24 August 2006; Accepted 14 October 2006

Recommended by Yuan-Pei Lin

This paper investigates the use of complex-modulated oversampled filter banks (FBs) for frequency-domain equalization (FDE) in single-carrier systems. The key aspect is mildly frequency-selective subband processing instead of a simple complex gain factor per subband. Two alternative low-complexity linear equalizer structures with MSE criterion are considered for subband-wise equalization: a complex FIR filter structure and a cascade of a linear-phase FIR filter and an allpass filter. The simulation results indicate that in a broadband wireless channel the performance of the studied FB-FDE structures, with modest number of subbands, reaches or exceeds the performance of the widely used FFT-FDE system with cyclic prefix. Furthermore, FB-FDE can perform a significant part of the baseband channel selection filtering. It is thus observed that fractionally spaced processing provides significant performance benefit, with a similar complexity to the symbol-rate system, when the baseband filtering is included. In addition, FB-FDE effectively suppresses narrowband interference present in the signal band.

1. INTRODUCTION

Future wireless communications must provide ever increasing data transmission rates to satisfy the growing demands of wireless networking. As symbol-rates increase, the intersymbol interference, caused by the bandlimited time-dispersive channel, distorts the transmitted signal even more. The difficulty of channel equalization in single-carrier broadband systems is thus regarded as a major challenge to high-rate transmission over mobile radio channels. Single-carrier time-domain equalization has become impractical because of the high computational complexity of needed transversal filters with a high number of taps to cover the maximum delay spread of the channel [1]. This has lead to extensive research on spread spectrum techniques and multicarrier modulation. On the other hand, single-carrier transmission has the benefit, especially for uplink, of a very simple transmitter architecture, which avoids, to a large extent, the peak-to-average power ratio problems of multicarrier and CDMA techniques. In recent years, the idea of single-carrier transmission in broadband wireless communications has been revived through the application of frequency-domain equalizers, which have clearly lower implementation complexity than time-domain equalizers [1–3]. Both linear and decision feedback structures have been considered. In [2, 4–6], it has been demonstrated that the single-carrier frequency-domain equalization may have a performance advantage and that it is less sensitive to nonlinear distortion and carrier synchronization inaccuracies compared to multicarrier modulation.

The most common approach for FDE is based on FFT/IFFT transforms between the time and frequency domains. Usually, a cyclic prefix (CP) is employed for the transmission blocks. Such a system can be derived, for example, from OFDM by moving the IFFT from the transmitter to the receiver [4]. FFT-FDEs with CP are characterized by a flat-fading model of the subband responses, which means that one complex coefficient per subband is sufficient for ideal linear equalization. This approach has overhead in data transmission due to the guard interval between symbol blocks. Another approach is to use overlapped processing of FFT blocks [7–9] which allows equalization without CP. This results in a highly flexible FDE concept that can basically be used for any single-carrier system, including also CDMA [8].

This paper develops high performance single-carrier FDE techniques without CP by the use of highly frequency-selective filter banks in the analysis-synthesis configuration, instead of the FFT and IFFT transforms. We examine the use of subband equalization for mildly frequency-selective

subbands, which helps to reduce the number of subbands required to achieve close-to-ideal performance. This is facilitated by utilizing a proper complex, partially oversampled filter bank structure [10–13].

One central choice in the FDE design is between symbol-spaced equalizers (SSE) and fractionally spaced equalizers (FSE) [3, 14]. An ideal receiver includes a matched filter with the channel matched part, in addition to the root raised cosine (RRC) filter, before the symbol-rate sampling. SSE ignores the channel matched part, leading to performance degradation, whereas FSEs are, in principle, able to achieve ideal linear equalizer performance. However, symbol-rate sampling is often used due to its simplicity. In frequency-domain equalization, FSE can be done by doubling the number of subbands and the sampling rate at the filter bank input [1, 3, 6]. This paper examines also the performance and complexity tradeoffs of the SSE and FSE structures.

The main contribution of this paper is an efficient combination of analysis-synthesis filter bank system and low-complexity subband-wise equalizers, applied to frequency-domain equalization. The filter bank has a complex I/Q input and output signals suitable for processing baseband communication signals as such, so no additional single sideband filtering is needed in the receiver (real analysis-synthesis systems cannot be easily adapted to this application). The filter bank also has oversampled subband signals to facilitate subband-wise equalization. We consider two low-complexity equalizer structures operating subband-wise: (i) a 3-tap complex-valued FIR filter (CFIR-FBEQ), and (ii) the cascade of a low-order allpass filter as the phase equalizer and a linear-phase FIR filter as the amplitude equalizer (AP-FBEQ). In the latter structure, the amplitude and phase equalizer stages can be adjusted independently of each other, which turns out to have several benefits. Simple channel estimation based approaches for calculation of the equalizer coefficients both in SSE and FSE configurations and for both equalizer structures are developed. Further, the benefits of FB-FSEs in contributing significantly to the receiver selectivity will be addressed.

In a companion paper [15], a similar subband equalizer structure is utilized in filter bank based multicarrier (FBMC) modulation, and its performance is compared to a reference OFDM modulation in a doubly dispersive broadband wireless communication channel. In this paper, we continue with the comparisons of OFDM, FBMC, single-carrier FFT-FDE, and FB-FDE systems. The key idea of our equalizer concept has been presented in the earlier work [16] together with two of the simplest cases of the subband equalizer.

The content of this paper is organized as follows: Section 2 gives an overview of FFT-SSE and FFT-FSE. In addition, the mean-squared error (MSE) criterion based subband equalizer coefficients are derived. Section 3 addresses the exponentially modulated oversampled filter banks and the subband equalization structures, CFIR-FBEQ and AP-FBEQ. The particular low-complexity cases of these structures are presented, together with the formulas for calculating the equalizer coefficients from the channel estimates. Also, the channel estimation principle is briefly described. Section 4 gives numerical results, including simulation results to illustrate the effects of filter bank and equalizer parameters on the system performance. Then detailed comparisons of the studied FB-SSE and FB-FSE structures with the reference systems are given.

2. FFT BASED FREQUENCY-DOMAIN EQUALIZATION IN A SINGLE-CARRIER TRANSMISSION

Throughout this paper, we consider single-carrier block transmission over a linear bandlimited channel with additive white Gaussian noise. We assume that the channel has time-invariant impulse response during each block transmission. For each block, a CP is inserted in front of the block, as shown in Figure 1. In this case, the received signal is obtained as a cyclic convolution of the transmitted signal and channel impulse response. Therefore, the channel frequency response is accurately modeled by a complex coefficient for each frequency bin [17]. The length of the CP extension is $P \geq L$, where L is the maximum length of the channel impulse response. The CP includes a copy of information symbols from the tail of the block. This results in bandwidth efficiency reduction by the factor $M/(M+P)$, where M is the length of the information symbol block. In general, for time-varying wireless environment, M is chosen in such a way that the channel impulse response can be considered to be static during each block transmission.

The block diagram of a communication link with FFT-SSE and FFT-FSE is shown in Figure 1. The operations of the equalization include the forward transform from time to frequency domain, channel inversion, and the reverse transform from frequency to time domain. The CP is inserted after the symbol mapping in the transmitter and discarded before equalization in the receiver. At the transmitter side, a block of M symbols $x(m)$, $m = 0, 1, \ldots, M-1$, is oversampled and transmitted with the average power σ_x^2. The received oversampled signal $r(n)$ can be written as

$$\begin{aligned} r(n) &= x(n) \otimes c(n) + v(n), \\ c(n) &= g_T(n) \otimes h_{\mathrm{ch}}(n) \otimes g_R(n). \end{aligned} \tag{1}$$

Here $v(n)$ is additive white Gaussian noise with variance σ_n^2. The symbol $\otimes$ represents convolution, $h_{\mathrm{ch}}(n)$ is the channel impulse response, and $g_T(n)$ and $g_R(n)$ are the transmit and receive filters, respectively. They are both RRC filters with the roll-off factor $\alpha \leq 1$ and the total signal bandwidth $B = (1+\alpha)/T$, with T denoting the symbol duration.

Generally in the paper, the lowercase letters will be used for time-domain notations and the uppercase letters for frequency-domain notations. The letter n is used for time-domain $2\times$ symbol-rate data sequences and m for symbol-rate sequences, while the script k represents the index of frequency-domain subband signals. For example, in Figure 1, R_k is the received signal of kth subband, and W_k and $\widehat{W}_k$ represent the kth subband equalizer coefficients of SSE and FSE, respectively.

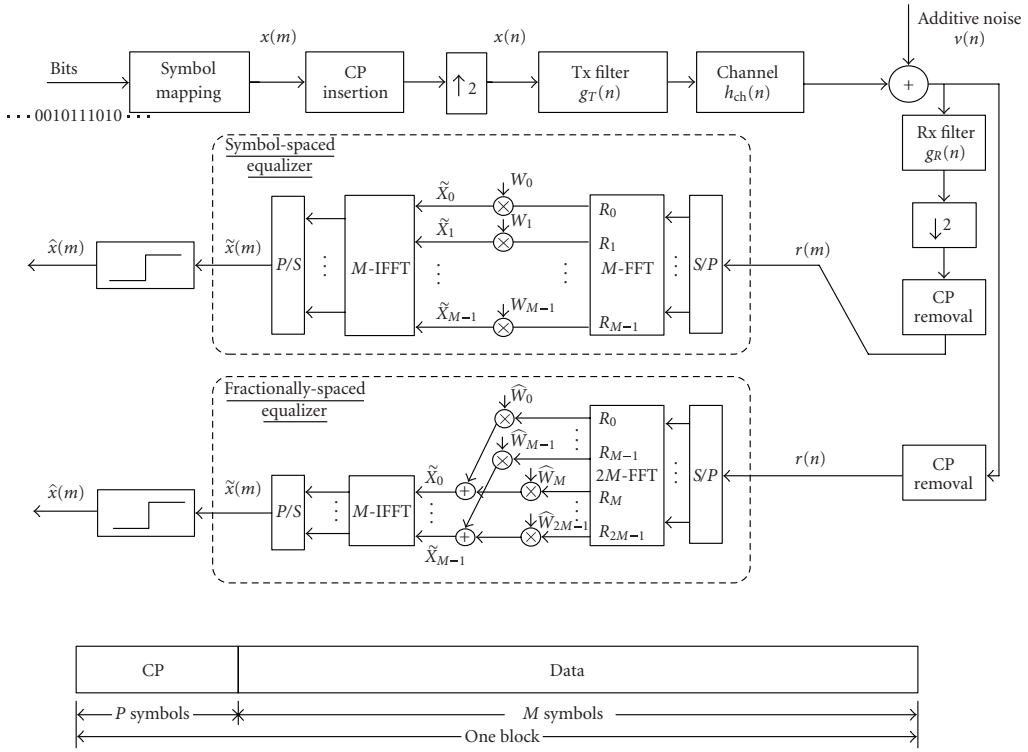

Figure 1: General model of FFT-SSE and FFT-FSE for single-carrier frequency-domain equalization.

2.1. Symbol-spaced equalizer

Suppose that $c^{\mathrm{SSE}}(m)$ is the symbol-rate impulse response of the cascade of transmit filter $g_T(n)$, channel $h_{\mathrm{ch}}(n)$, and receiver filter $g_R(n)$, and C_k^{SSE} is the kth bin of its DFT transform, the DFT length being equal to the symbol block length M. Assuming that the length of the CP is sufficient, that is, longer than the delay spread of $c^{\mathrm{SSE}}(n)$, we can express the kth subband sample as

$$R_k = C_k^{\mathrm{SSE}} X_k + N_k, \quad k = 0, 1, \ldots, M-1, \tag{2}$$

where X_k is the ideal noise- and distortion-free sample and N_k is zero mean Gaussian noise. The equalized frequency-domain samples are $\widetilde{X}_k = W_k R_k, k = 0, 1, \ldots, M-1$. After the IFFT, the equalized time-domain signal $\tilde{x}(m)$ is processed by a slicer to get the detected symbols $\hat{x}(m)$. The error sequence at the slicer is $e(m) = x(m) - \tilde{x}(m)$ and MSE is defined as $E[|e(m)|^2]$.

The subband equalizer optimization criterion could be zero forcing (ZF) or MSE. In this paper, we are focusing on wideband single-carrier transmission, with heavily frequency-selective channels. In such cases, the ZF equalizers suffer from severe noise enhancement [14] and MSE provides clearly better performance. We consider here only the MSE criterion.

To minimize MSE, considering the residual intersymbol interference and additive noise, the frequency response of the optimum linear equalizer is given by [14]

$$W_k = \frac{(C_k^{\mathrm{SSE}})^*}{|C_k^{\mathrm{SSE}}|^2 + \sigma_n^2/\sigma_x^2}, \tag{3}$$

where $k = 0, 1, \ldots, M-1$ and $(\cdot)^*$ represents complex conjugate.

2.2. Fractionally-spaced equalizer

The FFT-FSE, shown in Figure 1, operates at 2× symbol-rate, $2/T$. In some papers, it is also named as $T/2$-spaced equalizer [14, 18]. For each transmitted block, the received samples are processed using a $2M$-point FFT. The RRC filter block at the receiver is absent since it can be realized together with the equalizer in the frequency domain [1].

In the case of SSE, the folding is carried out before equalization, where the folding frequency is $1/2T$. It is evident in Figure 2 that uncontrolled aliasing over the transition band F_1 takes place. This means that SSE can only compensate for the channel distortion in the aliased received signal, which results in performance loss. On the other hand, FSE compensates for the channel distortion in received signal before the aliasing takes place. After equalization, the aliasing takes

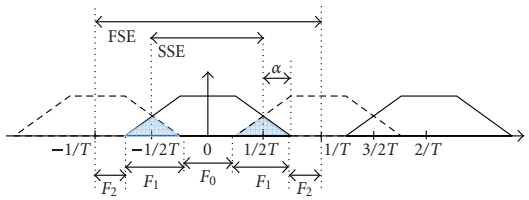

F_0 Passband
F_1 Transition band
F_2 Stopband
T Symbol duration
α Roll-off

Figure 2: Signal spectra in the cases of SSE and FSE.

place in an optimal manner. The performance is expected to approach the performance of an ideal linear equalizer.

Let H_k^{ch}, $k = 0, 1, \ldots, 2M-1$, denote the $2M$-point DFT of the $T/2$-spaced channel impulse response, and G_k denote the RRC filter in the transmitter or in the receiver side. Assuming zero-phase model for the RRC filters, G_k is always real-valued. The optimum linear equalizer model includes now the following elements: transmitter RRC filter, channel $h_{\text{ch}}(n)$, matched filter including receiver RRC filter and channel matched filter $h_{\text{ch}}^*(-n)$, resampling at the symbol-rate, and MSE linear equalizer at symbol-rate. The 2×-oversampled system frequency response can be written as

$$Q_k = G_k H_k^{\text{ch}} (H_k^{\text{ch}})^* G_k = \frac{|C_k^{\text{FSE}}|^2}{(G_k)^2}, \qquad C_k^{\text{FSE}} = H_k^{\text{ch}} {G_k}^2. \tag{4}$$

Here C_k^{FSE} is the kth bin of DFT transform of the $T/2$-spaced impulse response of the cascade of the channel and the two RRC filters. The channel estimator described in Section 3.4 provides estimates for C_k^{FSE}. Now the frequency bins k and $M+k$ carry redundant information about the same subband data, just weighted differently by the RRC filters and the channel. The folding takes place in the sampling rate reduction, adding up these pairs of frequency bins. Before the addition, it is important to compensate the channel phase response so that the two bins are combined coherently, and also to weight the amplitudes in such a way that the SNR is maximized. The maximum ratio combining idea [1] and the sampled matched filter model [14] lead to the same result. Combining this front-end model with the MSE linear equalizer leads to the following expression for the optimal subband equalizer coefficients:

$$\widehat{W}_k = \frac{(C_k^{\text{FSE}})^* / G_k}{|Q_k| + |Q_{(M+k)_{\text{mod}(2M)}}| + \sigma_n^2/\sigma_x^2}. \tag{5}$$

The frequency index $k = 0, 1, \ldots, 2M-1$ covers the entire spectrum $[0, 2\pi]$ as $\omega_k = 2\pi k/2M$, that is, $k = 0$ corresponds to DC and $k = M$ corresponds to the symbol-rate $1/T$. It should be noted that here the equalizer coefficients implement the whole matched filter together with the MSE equalizer. The whole spectrum, where the equalization takes place, that is, the FFT frequency bins, can be grouped into three frequency regions with different equalizer actions.

(i) *Passbands* F_0: $k \in [0, (1-\alpha)M/2] \cup [(3+\alpha)M/2, 2M-1]$.
There is no aliasing in these two regions, so the equalizer coefficients can be written in simplified form as

$$\widehat{W}_k = \frac{(C_k^{\text{FSE}})^* / G_k}{|Q_k| + \sigma_n^2/\sigma_x^2}. \tag{6}$$

(ii) *Transition bands* F_1: $k \in [(1-\alpha)M/2, (1+\alpha)M/2] \cup [(3-\alpha)M/2, (3+\alpha)M/2]$.
Aliasing takes place when the received signal is folded, and (5) should be used.

(iii) *Stopbands* F_2: $k \in [(1+\alpha)M/2, (3-\alpha)M/2]$.
Only noise and interference components are included and all subband signals can be set to zero, $\widehat{W}_k = 0$.

The use of oversampling provides robustness to the sampling phase. Basically the frequency-domain equalizer implements also symbol-timing adjustment. Furthermore, compared with the SSE system, the receiver filter of the FSE system can be implemented efficiently in the frequency domain. This means that the pulse shaping filtering will not introduce additional computational complexity, even if it has very sharp transition bands.

2.3. Computational complexity of SSE and FSE

In the following example, we will count the real multiplications at the receiver side. The complexity mainly comes from RRC filtering, FFT and IFFT, and equalization.

(i) Suppose that $M = 512$ symbols are transmitted in a block. The number of the received samples is $2M = 1024$ because of the oversampling by 2.
(ii) Each subband equalizer has only one complex weight, resulting in 4 real multiplications per subband.
(iii) The pulse shaping filter is an RRC filter with the roll-off factor of $\alpha = 0.22$ and the length of $N_{\text{RRC}} = 31$. Because of symmetry, only $(N_{\text{RRC}}+1)/2 = 16$ multipliers are needed for the RRC filtering in the SSE. In an efficient decimation structure, $(N_{\text{RRC}}+1)/2$ multiplications per symbol are needed, both for the real and imaginary parts of the received signal.
(iv) The split-radix algorithm [19] is applied to the FFT. For an M-point FFT, $M(\log_2 M - 3) + 4$ real multiplications are needed.
(v) In the case of SSE, the total number of real multiplications per symbol is about $(N_{\text{RRC}}+1)+2\log_2 M - 2 \approx 48$.
(vi) In the case of FSE, the number of subbands used is $M(1+\alpha)$. The total number of real multiplications per symbol is about $3\log_2 M - 3 + 4\alpha \approx 25$.

From the above discussion, we can easily conclude that FFT-FSE has lower rate of real multiplications than FFT-SSE. This is mainly due to the reason that much of the complexity is saved when the RRC filter is realized in frequency domain.

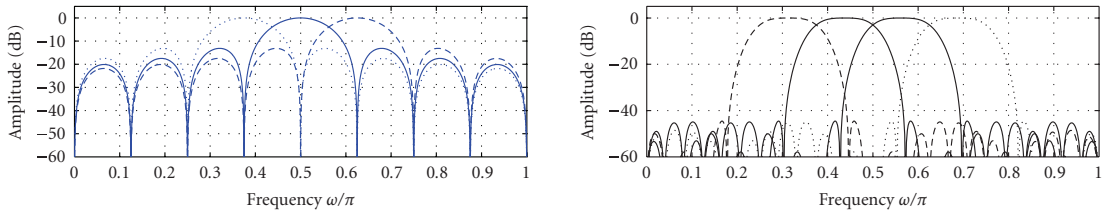

(a) DFT bank (b) EMFB

Figure 3: Comparison of the subband frequency responses of DFT and EMFB.

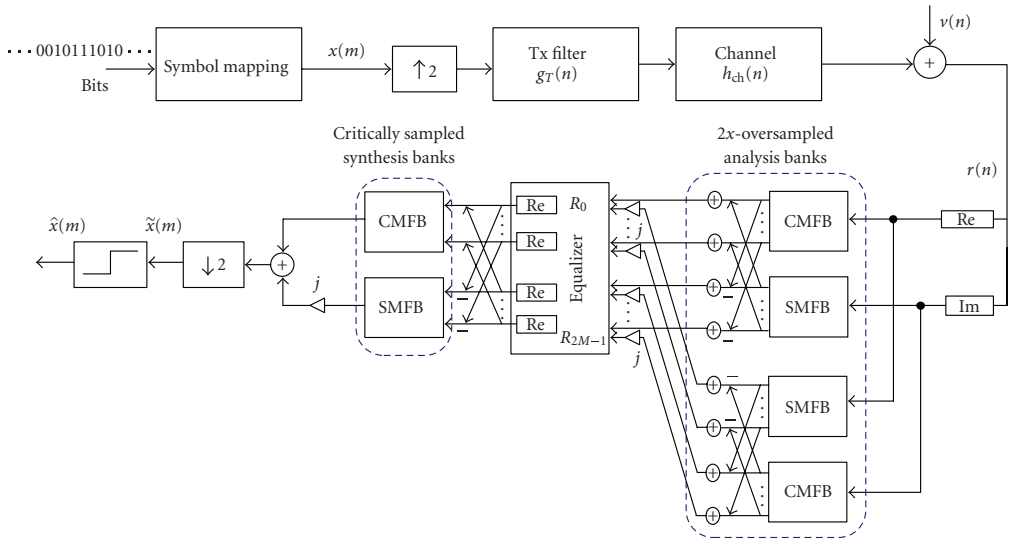

Figure 4: Generic FB-FDE system model in the FSE case.

3. EXPONENTIALLY MODULATED FILTER BANK BASED FDE

Filter banks provide an alternative way to perform the signal transforms between time and frequency domains, instead of FFT. As shown in Figure 3, exponentially modulated FBs (EMFBs) achieve better frequency selectivity than DFT banks, but they have the drawback that, since the basis functions are overlapping and longer than a symbol block, the CP cannot be utilized. Consequently, the subbands cannot be considered to have flat frequency responses. However, the lack of CPs can be considered a benefit, since CPs add overhead and reduce the spectral efficiency. Furthermore, in the FSE case, frequency-domain filtering with a filter bank is quite effective in suppressing strong interfering spectral components in the stopband regions of the RRC filter.

Figure 4 shows the FB-FSE model including a complex exponentially modulated analysis-synthesis filter bank structure as the core of frequency-domain processing. The filter bank structure has complex baseband I/Q signals as its input and output, as required for spectrally efficient radio communications. The sampling rate conversion factor in the analysis and synthesis banks is M, and there are $2M$ low-rate subbands equally spaced between $[0, 2\pi]$. In the critically sampled case, this FB has a real format for the low-rate subband signals [12].

3.1. *Exponentially modulated filter bank*

EMFB belongs to a class of filter banks in which the subfilters are formed by modulating an exponential sequence with the lowpass prototype impulse response $h_p(n)$ [11, 12]. Exponential modulation translates $H_p(e^{j\omega})$ (lowpass frequency response of the prototype filter) to a new center frequency determined by the subband index k. The prototype filter $h_p(n)$ can be optimized in such a manner that the filter bank satisfies the perfect reconstruction condition, that is,

the output signal is purely a delayed version of the input signal. In the general form, the EMFB synthesis filters $f_k^e(n)$ and analysis filters $g_k^e(n)$ can be written as

$$f_k^e(n) = \sqrt{\frac{2}{M}} h_p(n) \exp\left(j\left(n + \frac{M+1}{2}\right)\left(k + \frac{1}{2}\right)\frac{\pi}{M}\right),$$
$$g_k^e(n) = \sqrt{\frac{2}{M}} h_p(n) \exp\left(-j\left(N_B - n + \frac{M+1}{2}\right)\left(k + \frac{1}{2}\right)\frac{\pi}{M}\right), \tag{7}$$

where $n = 0, 1, \ldots, N_B$ and subband index $k = 0, 1, \ldots, 2M - 1$. Furthermore, it is assumed that the subband filter order is $N_B = 2KM - 1$. The overlapping factor K can be used as a design parameter because it affects how much stopband attenuation can be achieved. Another essential design parameter is the stopband edge of the prototype filter $\omega_s = (1 + \rho)\pi/2M$, where the roll-off parameter ρ determines how much adjacent subbands overlap. Typically, $\rho = 1.0$ is used, in which case only the neighboring subbands are overlapping with each other, and the overall subband bandwidth is twice the subband spacing.

The amplitude responses of the analysis and synthesis filters divide the whole frequency range $[0, 2\pi]$ into equally wide passbands. EMFB has odd channel stacking, that is, kth subband is centered at the frequency $(k + 1/2)\pi/M$. After decimation, the even-indexed subbands have their passbands centered at $\pi/2$ and the odd-indexed at $-\pi/2$. This unsymmetry has some implications in the later formulations of the subband equalizer design.

In our approach, EMFB is implemented using cosine- and sine-modulated filter bank (CMFB/SMFB) blocks [11, 12], as can be seen in Figure 4. The extended lapped transform is an efficient method for implementing perfect reconstruction CMFBs [20] and SMFBs [21]. The relations between the $2M$-channel EMFB and the corresponding M-channel CMFB and SMFB with the same real prototype are

$$f_k^e(n) = \begin{cases} f_k^c(n) + j f_k^s(n), & k \in [0, M-1], \\ -\left(f_{2M-1-k}^c(n) - j f_{2M-1-k}^s(n)\right), & k \in [M, 2M-1], \end{cases}$$

$$g_k^e(n) = \begin{cases} g_k^c(n) - j g_k^s(n), & k \in [0, M-1], \\ -\left(g_{2M-1-k}^c(n) + j g_{2M-1-k}^s(n)\right), & k \in [M, 2M-1], \end{cases} \tag{8}$$

where $g_k^c(n)$ and $g_k^s(n)$ are the analysis CMFB/SMFB subfilter impulse responses, $f_k^c(n)$ and $f_k^s(n)$ are the synthesis bank subfilter responses (the superscript denotes the type of modulation). They can be generated according to (7).

One additional feature of the structure in Figure 4 is that, while the synthesis filter bank is critically sampled, the subband output signals of the analysis bank are oversampled by the factor of two. This is achieved by using the complex I/Q subband signals, instead of the real ones which would be sufficient for reconstructing the analysis bank input signal in the synthesis bank when no subband processing is used [10, 13] (in a critically sampled implementation, the two lower most blocks of the analysis bank of Figure 4 would be omitted). For a block of M complex input samples, $2M$ real subband samples are generated in the critically sampled case and $2M$ complex subband samples are generated in the oversampled case.

The advantage of using 2×-oversampled analysis filter bank is that the channel equalization can be done within each subband independently of the other subbands. Assuming roll-off $\rho = 1.0$ or less in the filter bank design, the complex subband signals of the analysis bank are essentially alias-free. This is because the aliasing signal components are attenuated by the stopband attenuation of the subband responses. Subband-wise equalization compensates the channel frequency response over the whole subband bandwidth, including the passband and transition bands. The imaginary parts of the subband signals are needed only for equalization. The real parts of the subband equalizer outputs are sufficient for synthesizing the time-domain equalized signal, using a critically sampled synthesis filter bank.

It should be mentioned that an alternative to oversampled subband processing is to use a critically sampled analysis bank together with subband processing algorithms that have cross-connections between the adjacent subbands [22]. However, we believe that the oversampled model results in simplified subband processing algorithms and competitive complexity.

After the synthesis bank, the time-domain symbol-rate signal is fed to the detection device. In the FSE model of Figure 4, the synthesis bank output signal is downsampled to the symbol-rate. In the case of FSE with frequency-domain folding, an M-channel synthesis bank would be sufficient, instead of the $2M$-channel bank. The design of such a filter bank system in the nearly perfect reconstruction sense is discussed in [23].

We consider here the use of EMFB which has odd channel stacking, that is, the center-most pair of subbands is symmetrically located around the zero frequency at the baseband. We could equally well use a modified EMFB structure [13] with even channel stacking, that is, center-most subband is located symmetrically around the zero frequency, which has a slightly more efficient implementation structure based on DFT processing. Also modified DFT filter banks [24] could be utilized with some modifications in the baseband processing. However, the following analysis is based on EMFBs since they result in the most straightforward system model.

Further, the discussion is based on the use of perfect reconstruction filter banks, but also nearly perfect reconstruction (NPR) designs could be utilized, which usually result in shorter prototype filter length. In the critically sampled case, the implementation benefits of NPR are limited, because the efficient extended lapped transform structures cannot be utilized [12]. However, in the 2×-oversampled case, having parallel CMFB and SMFB blocks, the implementation benefit of the NPR designs could be significant.

3.2. Channel equalizer structures and designs

In the filter bank, the number of subbands is selected in such a way that the channel is mildly frequency selective within

each individual subband. We consider here several low-complexity subband equalizers which are designed to equalize the channel optimally at a small number of selected frequency points within each subband. Figure 5 shows one example, where the subband equalizer is determined by the channel response of three selected frequency points, one at the center frequency, the other two at the subband edges. In this example, the ZF criterion is used for equalization, that is, the channel frequency response is exactly compensated at those selected frequency points.

3.2.1. CFIR-FBEQ

A very basic approach is to use a complex FIR filter as a subband equalizer. A 3-tap FIR filter,[1] $E^{\mathrm{CFIR}}(z) = c_0 z + c_1 + c_2 z^{-1}$, has the required degrees of freedom to equalize the channel frequency response within each subband.

It should be noted that the subband equalizer response depends on the number of frequency points considered within each subband. Regarding the choice of the specific frequency points, the design can be greatly simplified when the choice is among the normalized frequencies $\omega = 0, \pm\pi/2$, and $\pm\pi$. At the selected frequency points, the equalizer is designed to take the target values given by (5) in the FSE case and by (3) in the SSE case. Below we focus on the MSE based FSE.

When three subband frequency points are selected in the subband equalizer design, there are a total of $4M$ frequency points for $2M$ subbands, that is, we consider the MSE equalizer response $\widehat{W}_\kappa$ at equally spaced frequency points $\kappa\pi/(2M)$, $\kappa = 0, 1, \ldots, 4M-1$. For notational convenience, we define the target frequency responses in terms of subband index $k = 0, 1, \ldots, 2M-1$, instead of frequency point index κ. The kth subband target response value is denoted as η_{ik}, which is defined as

$$\eta_{ik} = \widehat{W}_{2k+i}, \quad i = 0, 1, 2. \tag{9}$$

At the low rate after decimation, these frequency points $\{\eta_{0k}, \eta_{1k}, \eta_{2k}\}$ are located for the even subbands at the normalized frequencies $\omega = \{0, \pi/2, \pi\}$, and for the odd subbands at the frequencies $\omega = \{-\pi, -\pi/2, 0\}$. Combining (5) and (9), we can get the following equations for the subband equalizer response $E^{\mathrm{CFIR}}(e^{j\omega})$ at these target frequencies.

Even subbands:

$$E_k^{\mathrm{CFIR}}(e^{j\omega}) = \begin{cases} c_{0k} + c_{1k} + c_{2k} = \eta_{0k}, & (\omega = 0), \\ jc_{0k} + c_{1k} - jc_{2k} = \eta_{1k}, & \left(\omega = \dfrac{\pi}{2}\right), \\ -c_{0k} + c_{1k} - c_{2k} = \eta_{2k}, & (\omega = \pi). \end{cases} \tag{10}$$

[1] In practice, the filter is realized in the causal form $z^{-1}E^{\mathrm{CFIR}}(z)$.

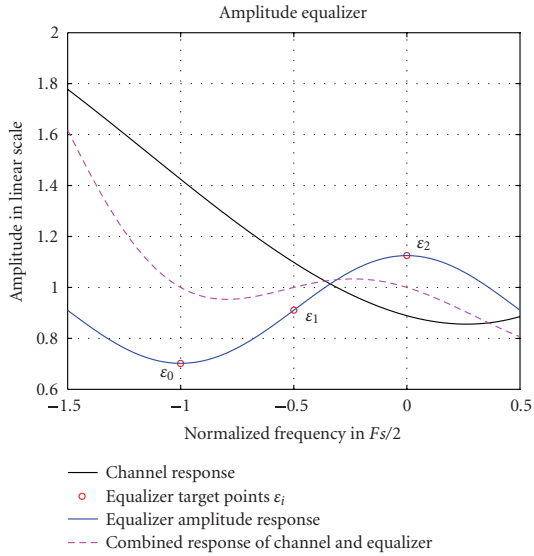

(a) Amplitude compensation

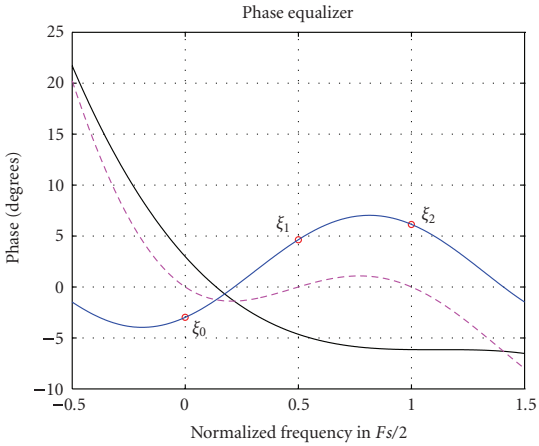

(b) Phase compensation

Figure 5: An example of AP-FBEQ subband equalizer responses.

Odd subbands:

$$E_k^{\mathrm{CFIR}}(e^{j\omega}) = \begin{cases} -c_{0k} + c_{1k} - c_{2k} = \eta_{0k}, & (\omega = -\pi), \\ -jc_{0k} + c_{1k} + jc_{2k} = \eta_{1k}, & \left(\omega = \dfrac{-\pi}{2}\right), \\ c_{0k} + c_{1k} + c_{2k} = \eta_{2k}, & (\omega = 0). \end{cases} \tag{11}$$

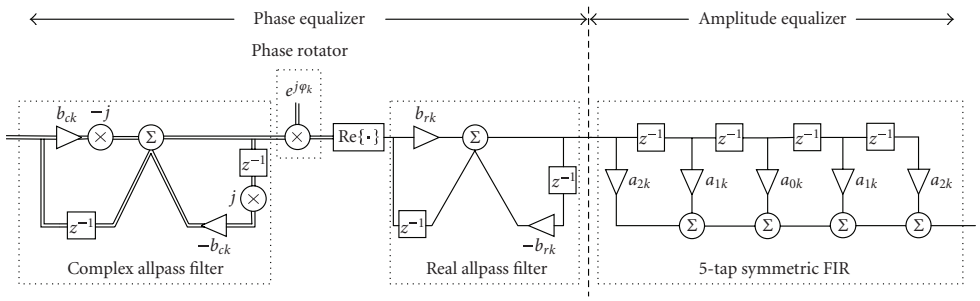

Figure 6: An example of the AP-FBEQ subband equalizer structure.

The 3-tap complex FIR coefficients $\{c_{0k}, c_{1k}, c_{2k}\}$ of the kth subband equalizer can be obtained as follows (+ signs stand for even subbands and − signs for odd subbands, resp.):

$$\begin{aligned} c_{0k} &= \pm\frac{1}{2}\left(\frac{\eta_{0k}-\eta_{2k}}{2} - j\left(\eta_{1k} - \frac{\eta_{0k}+\eta_{2k}}{2}\right)\right), \\ c_{1k} &= \frac{\eta_{0k}+\eta_{2k}}{2}, \\ c_{2k} &= \pm\frac{1}{2}\left(\frac{\eta_{0k}-\eta_{2k}}{2} + j\left(\eta_{1k} - \frac{\eta_{0k}+\eta_{2k}}{2}\right)\right). \end{aligned} \tag{12}$$

3.2.2. AP-FBEQ

The idea of AP-FBEQ approach is to compensate channel amplitude and phase distortion separately. In other words, at those selected frequency points, the amplitude response of the equalizer is proportional to the inverse of the channel amplitude response, and the phase response of the equalizer is the negative of the channel phase response.

The subband equalizer structure, shown in Figure 6, is a cascade of a phase equalization section, consisting of allpass filter stages and a phase rotator, and an amplitude equalization section, consisting of a linear-phase FIR filter. This particular structure makes it possible to design the amplitude equalization and phase equalization independently, leading to simple formulas for channel estimation based solutions, or simplified and fast adaptive algorithms for adaptive subband equalizers. In this paper, we refer to this frequency-domain equalization approach as the amplitude-phase filter bank equalizer, AP-FBEQ.

The real parts of the equalized subband signals are sufficient for constructing the sample sequence for detection, and the imaginary parts are irrelevant after the subband equalizers. In the basic form of the AP-FBEQ subband equalizer, the operation of taking the real part would be after all the filters of the subband equalizer. But since the real filters (real allpass and magnitude equalizer) act independently on the real (I) and imaginary (Q) branch signals, the results of the Q-branch computations after the phase rotator would never be utilized. Therefore, it is possible to move the real part operation and combine it with the phase rotator, that is, only the real part of the phase rotator output needs to be calculated, and the real filters are implemented only for the I-branch. The structure of Figure 6 is completely equivalent with the original one, but it is computationally much more efficient. With the same kind of reasoning, it is easy to see that in the CFIR-FBEQ case, only two real multipliers are needed to implement each of the taps.

The orders of the equalizer sections, as well as the number of specific frequency points used in the subband equalizer design, offer a degree of freedom and are chosen to obtain a low-complexity solution. Firstly, we consider the subband equalizer structure shown in Figure 6. The transfer functions of the complex and real first-order allpass filters $A_k^c(z)$ and $A_k^r(z)$ can be given by[2]

$$\begin{aligned} A_k^c(z) &= \frac{1 - jb_{ck}z}{1 + jb_{ck}z^{-1}}, \\ A_k^r(z) &= \frac{1 + b_{rk}z}{1 + b_{rk}z^{-1}}, \end{aligned} \tag{13}$$

respectively. The phase response of the equalizer for the kth subband can be described as

$$\begin{aligned} \arg\left[E_k^{\mathrm{AP}}(e^{j\omega})\right] &= \arg\left(e^{j\varphi_k} \cdot A_k^c(e^{j\omega}) \cdot A_k^r(e^{j\omega})\right) \\ &= \varphi_k + 2\arctan\left(\frac{-b_{ck}\cos\omega}{1 + b_{ck}\sin\omega}\right) \\ &\quad + 2\arctan\left(\frac{b_{rk}\cos\omega}{1 + b_{rk}\sin\omega}\right). \end{aligned} \tag{14}$$

The equalizer magnitude response for the kth subband can be written as

$$\left|E_k^{\mathrm{AP}}(e^{j\omega})\right| = \left|a_{0k} + 2a_{1k}\cos\omega + 2a_{2k}\cos 2\omega\right|. \tag{15}$$

The AP-FBEQ idea can be applied to both SSE and FSE in similar manner as CFIR-FBEQ. Here, we focus on the FSE case. Three subband frequency points at normalized frequencies $\omega=\{0, \pi/2, \pi\}$ for the even subbands and $\omega=\{-\pi, -\pi/2, 0\}$ for the odd subbands are selected in the subband equalizer design. Here, we define the target amplitude

[2] The allpass filters can be realized in the causal form $z^{-1}A_k(z)$.

and phase response values for subband k as ϵ_{ik} and ζ_{ik}, respectively:

$$\begin{aligned} \epsilon_{ik} &= |\widehat{W}_{2k+i}|, \\ \zeta_{ik} &= \arg(\widehat{W}_{2k+i}), \quad i = 0, 1, 2. \end{aligned} \tag{16}$$

Then, combining (5), (14), (15), and (16) at these target frequencies, we can derive two allpass filter coefficients $\{b_{ck}, b_{rk}\}$ and a phase rotator φ_k for phase compensation section and the FIR coefficients $\{a_{0k}, a_{1k}, a_{2k}\}$ for amplitude compensation.

In this paper, the following three different low-complexity designs of the AP-FBEQ structure are considered. (+ signs stand for the even subbands and − signs for the odd ones.)

Case 1. One frequency point is selected in the subband. This model of subband equalizer consists only of the phase rotator $e^{j\varphi_k}$ for phase compensation and a real coefficient a_{0k} for amplitude compensation. In fact, it behaves like one complex equalizer coefficient for each subband in the FFT-FDE system. The subband center frequency point is selected to determine the equalizer response

$$\varphi_k = \zeta_{1k}, \qquad a_{0k} = \epsilon_{1k}. \tag{17}$$

Case 2. Two frequency points are selected at the subband edges at the frequency points $\omega = 0$ and $\pm\pi$ to determine the equalizer coefficients. The subband equalizer structure consists of a cascade of a first-order complex allpass filter followed by a phase rotator and an operation of taking the real part of the signal. Finally, a symmetric linear-phase 3-tap FIR filter is applied for amplitude compensation. In this case, the equalizer coefficients can be calculated as

$$\begin{aligned} \varphi_k &= \frac{\zeta_{0k} + \zeta_{2k}}{2}, & a_{0k} &= \frac{1}{2}(\epsilon_{0k} + \epsilon_{2k}), \\ b_{ck} &= \pm\tan\left(\frac{\zeta_{2k} - \zeta_{0k}}{4}\right), & a_{2k} &= \pm\frac{1}{4}(\epsilon_{0k} - \epsilon_{2k}). \end{aligned} \tag{18}$$

Case 3. Three frequency points are used in each subband, as we have discussed above, one at the subband center and two at the passband edges. The equalizer structure contains two allpass filters, a phase rotation stage and a symmetric linear-phase 5-tap FIR filter. Their coefficients are calculated as below:

$$\begin{aligned} \varphi_k &= \frac{\zeta_{0k} + \zeta_{2k}}{2}, & a_{0k} &= \frac{\epsilon_{0k} + 2\epsilon_{1k} + \epsilon_{2k}}{4}, \\ b_{ck} &= \pm\tan\left(\frac{\zeta_{2k} - \zeta_{0k}}{4}\right), & a_{1k} &= \pm\left(\frac{\epsilon_{0k} - \epsilon_{2k}}{4}\right), \\ b_{rk} &= \pm\tan\left(\frac{\zeta_{1k} - \varphi_k}{2}\right), & a_{2k} &= \pm\left(\frac{\epsilon_{0k} - 2\epsilon_{1k} + \epsilon_{2k}}{8}\right). \end{aligned} \tag{19}$$

The subband equalizer structure is not necessarily fixed in advance but can be determined individually for each subband based on the frequency-domain channel estimates. This enables the structure of each subband equalizer to be controlled such that each subband response is equalized optimally at the minimum number of frequency points which can be expected to result in sufficient performance.

The performances of these three different subband equalizer designs, together with the 3-tap CFIR-FBEQ, will be examined in the next section.

3.3. FSE and SSE

Also in the SSE version of CFIR-FBEQ and AP-FBEQ, the decimating RRC filtering needs to be carried out before equalization, and uncontrolled aliasing results in similar performance loss as in the FFT-SSE.

In the FSE, the receiver RRC filter can again be implemented in the frequency domain together with the equalizer, with low complexity. Since no guard interval is employed and the subbands are highly frequency selective, frequency-domain filtering can be implemented independently of the roll-off and other filtering requirements, as long as the stopband attenuation in the filter bank design is sufficient for the receiver filter from the RF point of view. It can be noted that the FB-FSE structure provides a flexible solution for channel equalization and channel filtering, since the receiver filter bandwidth and roll-off can be controlled by adjusting the RRC-filtering part of the equalizer coefficient calculations.

In advanced receiver designs, a high initial sampling rate is often utilized, followed by a multistage decimation filter chain which is highly optimized for low-implementation complexity [25]. The first stages of the decimation chain often utilize multiplier-free structures, like the cascaded integrator comb, and the major part of the implementation complexity is at the last stage. In such designs, FB-FSE provides a flexible generic solution for the last stage of a channel filtering chain.

3.4. Channel estimation

FB-FDEs, as well as FFT-FDEs, can be implemented by using adaptive channel equalization algorithms to adjust the equalizer coefficients. However, we focus here on channel estimation based approach, where the equalizer coefficients are calculated at regular intervals based on the channel estimates and knowledge of the desired receiver filter frequency response, according to (3) or (5). In the performance studies, we have utilized a basic, maximum likelihood (ML) channel estimation method (also known as the least-squares method) using training sequences [26]. Here, Gold codes [27] of different lengths are used as training sequences.

In SSE, a training sequence is transmitted, and the symbol-rate channel impulse response (including transmitter and receiver RRC filters) is estimated based on the received training sequence at the decimating RRC filter output. This channel estimate is used for calculating the equalizer coefficients using (3).

In FSE, we have chosen to estimate $T/2$-spaced impulse responses (including the two RRC filters). Including the receiver RRC filter in the estimated response minimizes the noise and interference coming into the channel estimator. Now, the channel estimator utilizes the receiver RRC filter output at two times the symbol-rate. It must be noted that this approach requires a time-domain RRC filter for the training sequences in the receiver, even if frequency-domain filtering is applied to the data symbols.

4. NUMERICAL RESULTS

4.1. Basic simulations and numerical comparisons

The considered models of FFT-FDE and FB-FDE were introduced in Figures 1 and 4, respectively. The pulse shaping filters both in the transmitter and receiver are real-valued RRC filters with $\alpha = 0.22$. In the FSE case, the receiver RRC filter is realized by the equalizer. The filter bank designs in the simulations used roll-off $\rho = 1.0$, different numbers of subbands $2M = \{128, 256\}$ and overlapping factors $K = \{2, 3, 5\}$, resulting in about 30 dB, 38 dB, and 50 dB stopband attenuations, respectively.

The performances were tested using the extended vehicular-A channel model of ITU-R with the maximum excess delay of about 2.5 μs [28]. The symbol-rate was $1/T = 15.36$ MHz. The channel fading was modelled quasistatic, that is, the channel frequency response was time invariant during each frame transmission. 4000 independent channel instances were simulated to obtain the average performance. The MSE criterion was applied to solve the equalizer coefficients. The bit-error-rate (BER) performance was simulated with QPSK, 16-QAM, and 64-QAM modulations, with gray coding, and was compared to the performance of FFT-FDE. In all FFT-FDE simulations, the CP is included and assumed to be longer than the delay spread. Also the performance of the ideal MSE linear equalizer is included for reference. This analytic performance reference was obtained by applying the MSE formula for the infinite-length linear MSE equalizer from [14] and then using the well-known formulas of the Q-function and gray-coding assumption for estimating the BER. The BER measure is averaged over 5000 independent channel instances. Ideal channel estimation was assumed in Figures 7, 8, and 9, but in Figures 10, 11, and 12, the channel estimator described in Section 3.4 was utilized. The BER and frame-error-rate (FER) performance with low density parity check (LDPC) [29] error correction coding are presented in Figures 11 and 12.

Raw BER performance of FB-FSE

Figure 7 presents the uncoded BER performance of the CFIR-FBEQ and AP-FBEQ compared to the analytic performance with QPSK, 16-QAM, and 64-QAM modulations. The three different designs of AP-FBEQ and a 3-tap CFIR-FBEQ were examined. It can be seen that the CFIR-FBEQ and AP-FBEQ Case 3 performances are rather similar, however, with a minor but consistent benefit for AP-FBEQ. With a low number of subbands and with high-order modulation, the differences are more visible. In the following comparisons, AP-FBEQ performance is considered. It is clearly visible that AP-FBEQ Cases 2 and 3 equalizers improve the performance significantly compared to Case 1. When the modulation order becomes higher, the performance gaps between different equalizer structures increase. As the most interesting uncoded BER region is between 1% and 10%, it is seen that 256 subbands with Case 3 are sufficient to achieve good performance even with high-order modulation. The resulting performance is rather close to the analytic BER bound; however, it is clear that the gray-coding assumption is not very accurate at low E_b/N_0, and the analytic performance curve is somewhat optimistic. With this specific channel model, 128 subbands are sufficient for QPSK and 16-QAM modulations when AP-FBEQ Case 3 equalizer is used.

The FB design parameter, overlapping factor K, controls the level of stopband attenuation. Increasing K improves the stopband attenuation, with the cost of increased implementation complexity. Figure 8 presents the BER performance of Case 3 equalizer with 256 subbands and the different K-factors. For QPSK modulation, it can be seen that the K-factor has relatively small effect on the performance, and even $K = 2$ may provide sufficient performance. In the case of higher order modulations, $K = 3$ can achieve sufficient performance.

SSE versus FSE performance and FFT-FDE versus FB-FDE comparisons

Figure 9 presents the results for SSE and FSE in the FFT-FDE and FB-FDE receivers. It is clearly seen that FSE provides significant performance gain over SSE in the considered case. The performance differences between AP-FBEQ and the conventional FFT-FDE methods are relatively small. However, it should be noted that in Figure 9 the guard-interval overhead is not taken into account in the E_b/N_0-axis scaling, even though sufficiently long CP (200 samples) is utilized. In practice, the CP length effects in the BER plots only on the E_b/N_0-axis scaling.

Guard-interval considerations

For example, 10% or 25% guard-interval length would mean about 0.4 dB or 1 dB degradation on the E_b/N_0-axis, respectively. The delay spread of the channel model corresponds to about 39 symbol-rate samples or 77 samples at twice the symbol-rate. Then the minimum FFT size to reach 10% guard-interval overhead is about 350 for SSE and 700 for FSE. However, the RRC pulse shaping and baseband channel filtering extend the delay spread, possibly by a factor 2, so the CP length should be in the order of 5 μs in this example. Then the practical FFT length could be 512 or 1024 for SSE and 1024 or 2048 for FSE. The conclusion is that considerably higher number of subbands is needed in the FFT case to reach realistic CP overhead.

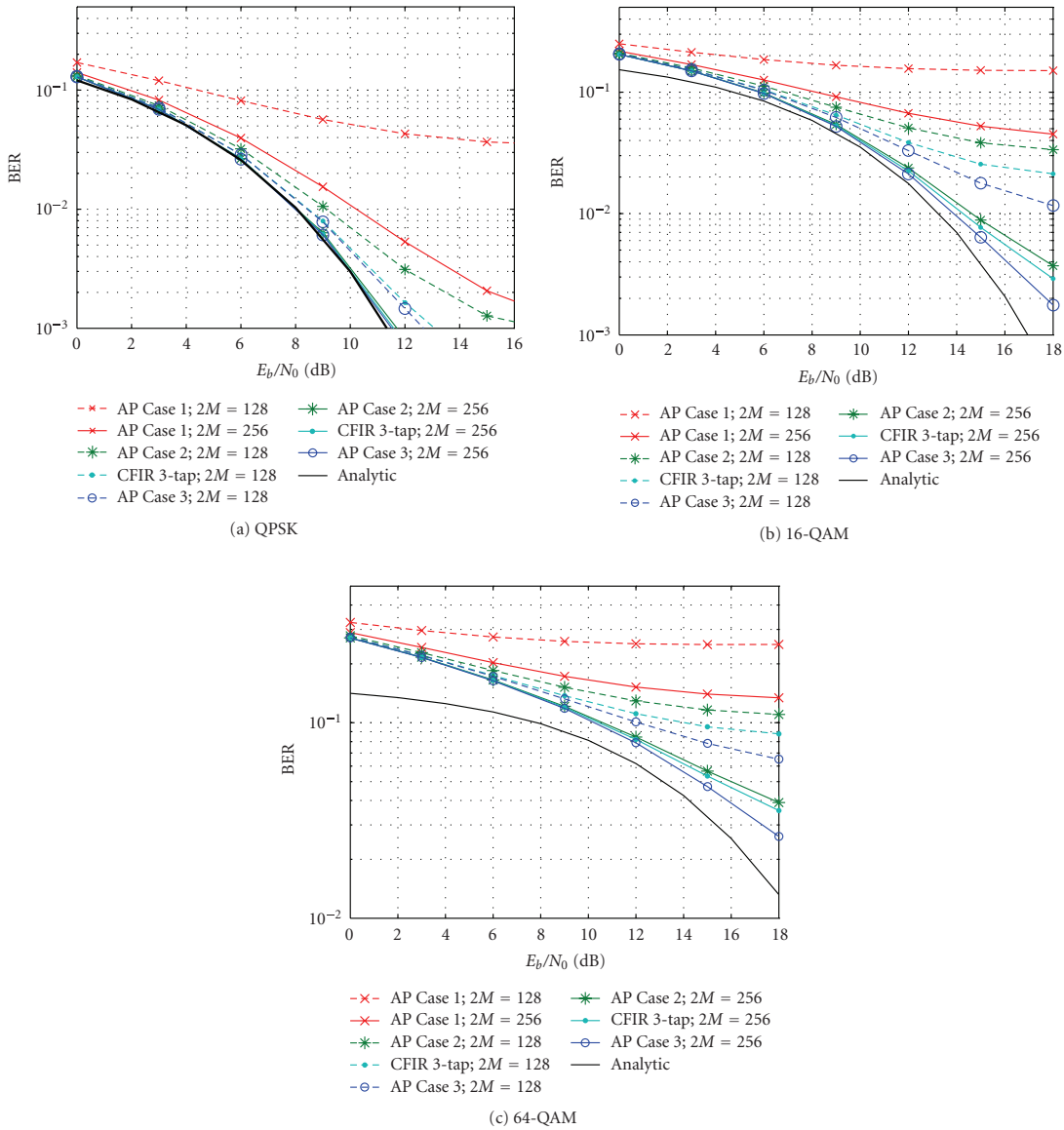

(a) QPSK

(b) 16-QAM

(c) 64-QAM

FIGURE 7: Uncoded BER performance of FB-FSE (CFIR-FBEQ 3-tap and AP-FBEQ Cases 1, 2, 3) with overlapping factor $K = 5$ and $2M = \{128, 256\}$ subbands.

Performance with channel estimation

In Figure 10, the uncoded BER performance of AP-FBEQ is simulated with a practical channel estimator. The channel estimator described in Section 3.4 is utilized, using Gold codes of different lengths as a training sequence. It is observed that the training sequence length of 384 symbols is quite sufficient.

4.2. *Performance comparison with practical parameters and error-correction coding*

Here, we include LDPC forward error correction (FEC) coding and the channel estimator in the simulation model. The main parameters are indicated in Table 1. With the chosen parameters, the training symbol overhead is 10% and the two systems with different LDPC code-rates transmit

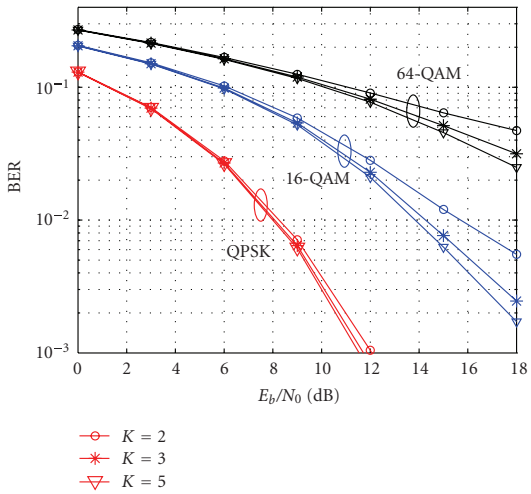

Figure 8: Uncoded BER performance for FB-FSE (AP-FBEQ Case 3 equalizer) with $2M = 256$ subbands and different K-factors.

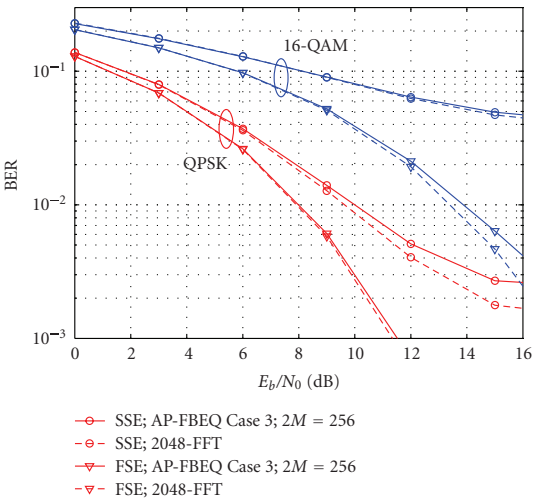

Figure 9: Uncoded BER performance comparison between SSE and FSE-type FB-FDE and FFT-FDE with QPSK and 16-QAM modulations. AP-FBEQ Case 3 equalizer with $2M = 256$ subbands and overlapping factor $K = 5$ was used.

exactly the same number of source bits per frame. Higher code-rate is needed in the FFT-FDE system to accommodate the CP overhead. Meanwhile, the CP length which is 1/8 of the useful symbol duration introduces E_b/N_0 degradation of $10\log_{10}(9/8)$ dB. The comparison of Figure 11 shows that FB-FDE has about 1 dB performance advantage over the FFT-FDE under the most interesting coded FER region 1%–10%. This is the joint results of using lower code-rate and the absence of CP E_b/N_0 degradation. Moreover, we can see that AP-FBEQ and CFIR-FBEQ have very similar performance.

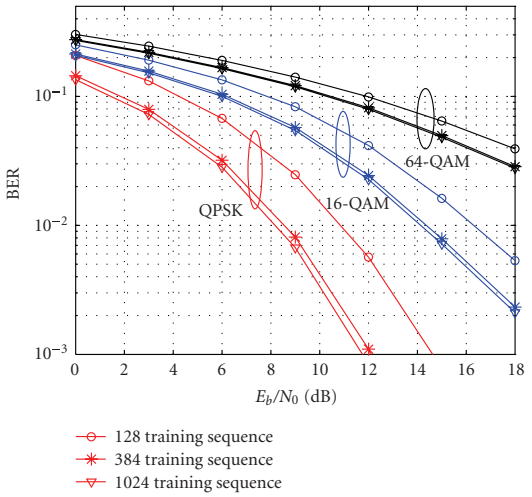

Figure 10: Uncoded BER performance for FB-FSE with ML based channel estimation using different training sequence lengths with QPSK, 16-QAM, and 64-QAM modulations. AP-FBEQ Case 3 equalizer with $2M = 256$ subbands and overlapping factor $K = 5$ was used.

The AP-FBEQ and CFIR-FBEQ systems are also compared in Figure 12 with the FBMC and OFDM systems of [15]. The parameters of FB-FDE are the same as in Table 1, except that code-rate 3/4 is used to reach similar bits rate with the other systems. The parameters are consistent with the ones considered in [15], with similar overhead for training sequences/pilots, signal bandwidth, and bit rates. The same type of LDPC code is used, however with higher code-rate 3/4 in OFDM and FB-FDE, and code-rate 2/3 in the FBMC system. Higher code-rate is needed in OFDM to accomodate the CP-overhead and FB-FDE to accommodate the overhead due to the excess band. With QPSK modulation, the number of source bits in one 250 μs frame are 5022, 5184, and 5320 for OFDM, FB-FDE, and FBMC, respectively.

Figure 12 displays that with QPSK modulation, FB-FDE has clear performance benefit over FBMC and CP-OFDM; whereas with 16-QAM modulation, FB-FDE and CP-OFDM are rather similar and clearly worse than that of FBMC.

4.3. Complexity comparison between FFT-FDEs and FB-FDEs

Here we evaluate the receiver complexity of FFT-FDEs and FB-FDEs in terms of real multiplications per detected symbol. The complexity metric includes the FB or FFT transform, subband equalizers, as well as the baseband filtering in the SSE case. The time-domain RRC filter is assumed to be of length $N_{\text{RRC}} = 31$. The receiver RRC filtering and decimation are realized in the frequency domain in both FSE systems, using half-sized IFFT or FB on the synthesis side. The split-radix algorithm [19] is applied for FFT/IFFT, critically sampled filter banks are implemented with the fast extended

Table 1: FFT-FDE and FB-FDE system parameters.

	FB-FSE			FFT-FSE		
Sampling rate	30.72 MHz			30.72 MHz		
symbol-rate	15.36 MHz			15.36 MHz		
RRC roll-off	0.22			0.22		
Signal bandwidth	18.74 MHz			18.74 MHz		
No. of subbands	256			1024		
Data symbols per frame	3456			3072		
Cyclic prefix (symbols)	0			64		
Training symbols	384			384		
Total symbols	3840			3840		
Frame duration	250 μs			250 μs		
FEC	LDPC code-rate 2/3			LDPC code-rate 3/4		
Modulation	QPSK	16-QAM	64-QAM	QPSK	16-QAM	64-QAM
Transmit bits (coded)	6912	13824	20736	6144	12288	18432
Source bits	4608	9216	13824	4608	9216	13824

Table 2: Receiver complexity comparison between the FB-FDE and FFT-FDE receivers: number of real multiplications per symbol.

FFT-FDE		$M = 1024$	$M = 2048$
SSE	$2\log_2 M - 4 + (N_{\text{RRC}} + 1)$	48	50
FSE	$3\log_2 M - 6 + 4\alpha$	24	27
FSE with time-domain RRC	$3\log_2 M - 6 + 4\alpha + 2(N_{\text{RRC}} + 1)$	88	91
FB-FDE		$M = 128; K = 2$	$M = 256; K = 5$
(1) *AP-FBEQ*			
SSE, Case 1	$6K + 3\log_2 M - 1 + N_{\text{RRC}}$	63	84
SSE, Case 2	$6K + 3\log_2 M + 2 + N_{\text{RRC}}$	66	87
SSE, Case 3	$6K + 3\log_2 M + 4 + N_{\text{RRC}}$	68	89
FSE, Case 1	$10K + 5\log_2 M - 4 + 2\alpha$	51	86
FSE, Case 2	$10K + 5\log_2 M - 1 + 5\alpha$	55	90
FSE, Case 3	$10K + 5\log_2 M + 1 + 7\alpha$	57	92
(2) *CFIR-FBEQ*			
FSE, 3-taps	$10K + 5\log_2 M + 6\alpha$	56	91

lapped transform algorithm [12], and the oversampled analysis banks are implemented using the optimized FFT based structure of [13]. The needed number of real multiplications for a block of M high-rate samples is $M(\log_2 M - 3) + 4$ for the FFT or IFFT, $M(2K + \log_2 M + 2)$ for the critically sampled synthesis bank, and $2M(2K + \log_2 M - 2)$ for an oversampled analysis bank. For FB-FDE, we have seen that 128 or 256 subbands are sufficient, whereas 1 k or 2 k FFT lengths are required. For FB-FDE, 2 real multipliers are needed for each tap of the CFIR, 2 for the first-order complex allpass and 1 for the real allpass (the two multipliers in the allpass structures of Figure 6 can be combined), two for phase rotation, and 2 for amplitude equalizer (we can scale $a_0 = 1$, and do the overall signal scaling in the phase rotator). The overall complexity figures are shown in Table 2, considering two extreme cases of filter bank complexity.

The comparison between SSE and FSE depends very much on the needed baseband RRC and channel filter complexity, but it is evident that, also in the FB-FDE case, FSE may actually be less complex to implement than SSE. The complexity of FB-FDE depends heavily on the K factor of the FB design. The subband equalizer choice has a minor effect on the overall complexity.

In a CP based system, the capability of the frequency-domain filter to suppress strong adjacent channels or other interferences in the stopbands are limited due to FFT blocking effects. Assume that there is a strong interference signal in the stopband of the RRC filter. Removing the CPs would cause transients in the interference waveforms, and these would cause relatively strong error transients at the ends of the time-domain symbol blocks even after filtering. Thus it seems that a baseband filter before the FFT is needed in CP based single-carrier FDE. FB-FSE may actually be very competitive compared to FFT-FSE, if additional baseband filtering is needed in the latter structure. With oversampled equalizer processing, the implementation of the baseband filter is not as efficient as in the SSE case. In the example setup, if the RRC filter is implemented in time-domain at 2× symbol-rate, the FFT-FSE multiplication rates are increased by 64 multiplications per symbol.

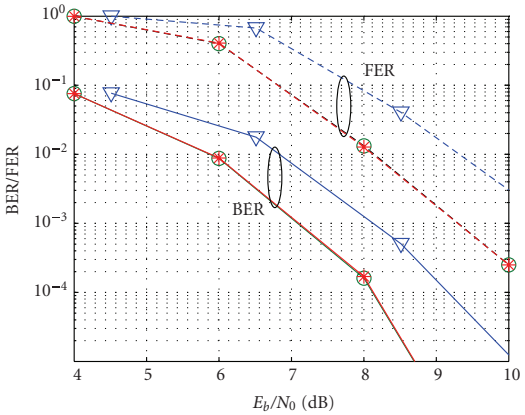

(a) QPSK modulation

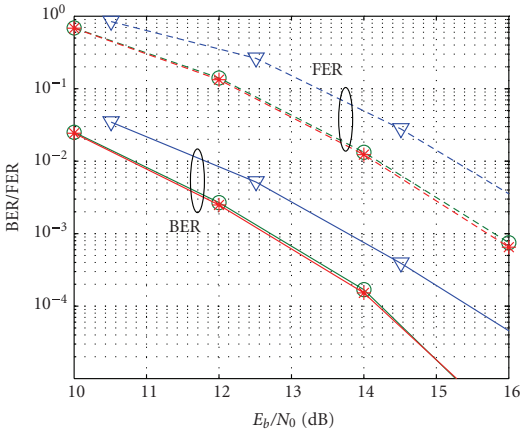

(b) 16-QAM modulation

Figure 11: Coded BER and FER performance comparison between FFT-FSE and FB-FSE with practical system parameters and LDPC coding. Both 3-tap CFIR and AP Case 3 subband equalizers are included in FB-FSE models.

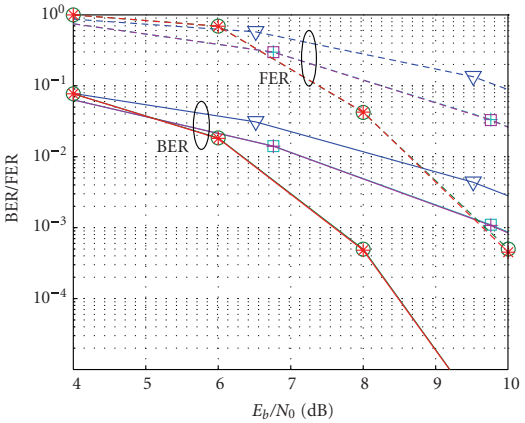

(a) QPSK modulation

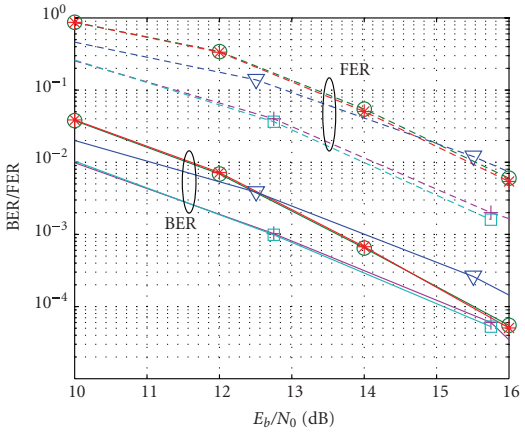

(b) 16-QAM modulation

Figure 12: Coded BER and FER performance comparison between CP-OFDM, FBMC, and FB-FSE with practical system parameters and LDPC coding. Both 3-tap CFIR and AP Case 3 subband equalizers are included in FBMC and FB-FSE models.

5. CONCLUSION

We have presented a filter bank based frequency-domain equalizer with mildly frequency-selective subband processing and a modest number of subbands. The performance is better than that of the FFT-FDE. Furthermore, FB-FDE is applicable to any single carrier system, whether CP is included or not.

In certain wireless communication scenarios, strong narrowband interferences (NBI) are considered as a serious problem [30], and various methods have been developed for mitigating their effects. Frequency-domain NBI mitigation can be easily combined with both FFT-FDE and FB-FDE with minor additional complexity. It has been observed that FFT based frequency-domain filtering has limitations as NBI mitigation method due to the FFT leakage, while filter bank based approaches provide clearly better performance [30–32].

Regarding the choice between CFIR-FBEQ and AP-FBEQ, it was seen that the latter gives consistently slightly better performance with the cost of slightly higher multiplication rate. Furthermore, in AP-FBEQ, the amplitude and phase responses can be adjusted independently of each other, which is a very useful feature in many respects. For example, in [33] the equalizer amplitude response is tuned to enhance narrowband interference suppression. In [23], a filter bank system with a $2M$-channel analysis bank and an M-channel synthesis bank is developed, and it is observed that tuning of the phase response in the subband equalizers is needed to achieve nearly perfect reconstruction characteristics with low distortion.

The overlapped-FFT algorithms also avoid the use of CPs. This structure can be seen as a kind of a simple filter bank with basis functions overlapping in time [7–9]. It can be seen that there is a continuum of filter bank design cases between the overlapped FFT based approach and the FB based designs with high K values. If the frequency selectivity of the filter bank design is not important, then relatively low-complexity designs probably provide the best tradeoff. As we have seen, the performance difference between $K = 3$ and $K = 5$ is relatively small.

The complexity of FB-FDEs is no doubt higher than that of FFT-FDE structures. However, we believe that the same filter bank can be used to implement part of the channel filtering, with much higher performance than when using the FFT-FDE structures. FB-FDE provides an easily configurable structure for the final stage of the channel filtering chain, together with the channel equalization functionality.

REFERENCES

[1] M. V. Clark, "Adaptive frequency-domain equalization and diversity combining for broadband wireless communications," *IEEE Journal on Selected Areas in Communications*, vol. 16, no. 8, pp. 1385–1395, 1998.

[2] G. Kadel, "Diversity and equalization in frequency domain - a robust and flexible receiver technology for broadband mobile communication systems," in *Proceedings of IEEE 47th Vehicular Technology Conference (VTC '97)*, vol. 2, pp. 894–898, Phoenix, Ariz, USA, May 1997.

[3] D. Falconer, S. L. Ariyavisitakul, A. Benyamin-Seeyar, and B. Eidson, "Frequency domain equalization for single-carrier broadband wireless systems," *IEEE Communications Magazine*, vol. 40, no. 4, pp. 58–66, 2002.

[4] H. Sari, G. Karam, and I. Jeanclaude, "Transmission techniques for digital terrestrial TV broadcasting," *IEEE Communications Magazine*, vol. 33, no. 2, pp. 100–109, 1995.

[5] A. Czylwik, "Comparison between adaptive OFDM and single carrier modulation with frequency domain equalization," in *Proceedings of IEEE 47th Vehicular Technology Conference (VTC '97)*, vol. 2, pp. 865–869, Phoenix, Ariz, USA, May 1997.

[6] A. Gusmão, R. Dinis, and N. Esteves, "On frequency-domain equalization and diversity combining for broadband wireless communications," *IEEE Transactions on Communications*, vol. 51, no. 7, pp. 1029–1033, 2003.

[7] D. D. Falconer and S. L. Ariyavisitakul, "Broadband wireless using single carrier and frequency domain equalization," in *Proceedings of the 5th International Symposium on Wireless Personal Multimedia Communications (WPMC '02)*, vol. 1, pp. 27–36, Honolulu, Hawaii, USA, October 2002.

[8] L. Martoyo, T. Weiss, F. Capar, and F. K. Jondral, "Low complexity CDMA downlink receiver based on frequency domain equalization," in *Proceedings of IEEE 58th Vehicular Technology Conference (VTC '03)*, vol. 2, pp. 987–991, Orlando, Fla, USA, October 2003.

[9] P. Schniter and H. Liu, "Iterative frequency-domain equalization for single-carrier systems in doubly-dispersive channels," in *Proceedings of the 38th Asilomar Conference on Signals, Systems, and Computers*, vol. 1, pp. 667–671, Pacific Grove, Calif, USA, November 2004.

[10] J. Alhava and M. Renfors, "Adaptive sine-modulated/cosine-modulated filter bank equalizer for transmultiplexers," in *Proceedings of the European Conference on Circuit Theory and Design (ECCTD '01)*, pp. 337–340, Espoo, Finland, August 2001.

[11] J. Alhava, A. Viholainen, and M. Renfors, "Efficient implementation of complex exponentially-modulated filter banks," in *Proceedings of IEEE International Symposium on Circuits and Systems*, vol. 4, pp. 157–160, Bangkok, Thailand, May 2003.

[12] A. Viholainen, J. Alhava, and M. Renfors, "Efficient implementation of complex modulated filter banks using cosine and sine modulated filter banks," *EURASIP Journal on Applied Signal Processing*, vol. 2006, Article ID 58 564, 10 pages, 2006.

[13] A. Viholainen, J. Alhava, and M. Renfors, "Efficient implementation of 2x oversampled exponentially modulated filter banks," *IEEE Transactions on Circuits and Systems II*, vol. 53, pp. 1138–1142, 2006.

[14] J. G. Proakis, *Digital Communications*, McGraw-Hill, New York, NY, USA, 4th edition, 2001.

[15] T. Ihalainen, T. Hidalgo Stitz, M. Rinne, and M. Renfors, "Channel equalization in filter bank based multicarrier modulation for wireless communications," to appear in EURASIP Journal of Applied Signal Processing.

[16] Y. Yang, T. Ihalainen, and M. Renfors, "Filter bank based frequency domain equalizer in single carrier modulation," in *Proceedings of the 14th IST Mobile and Wireless Communications Summit*, Dresden, Germany, June 2005.

[17] N. Benvenuto and S. Tomasin, "On the comparison between OFDM and single carrier modulation with a DFE using a frequency-domain feedforward filter," *IEEE Transactions on Communications*, vol. 50, no. 6, pp. 947–955, 2002.

[18] J. R. Treichler, I. Fijalkow, and C. R. Johnson Jr., "Fractionally spaced equalizers: how long should they really be?" *IEEE Signal Processing Magazine*, vol. 13, no. 3, pp. 65–81, 1996.

[19] P. Duhamel, "Implementation of split-radix FFT algorithms for complex, real, and real-symmetric data," *IEEE Transactions on Acoustics, Speech, and Signal Processing*, vol. 34, no. 2, pp. 285–295, 1986.

[20] H. S. Malvar, *Signal Processing with Lapped Transforms*, Artech House, Norwood, Mass, USA, 1992.

[21] A. Viholainen, T. Hidalgo Stitz, J. Alhava, T. Ihalainen, and M. Renfors, "Complex modulated critically sampled filter banks based on cosine and sine modulation," in *Proceedings of IEEE International Symposium on Circuits and Systems*, vol. 1, pp. 833–836, Scottsdale, Ariz, USA, May 2002.

[22] M. R. Petraglia, R. G. Alves, and P. S. R. Diniz, "New structures for adaptive filtering in subbands with critical sampling," *IEEE Transactions on Signal Processing*, vol. 48, no. 12, pp. 3316–3327, 2000.

[23] A. Viholainen, T. Ihalainen, T. Hidalgo Stitz, Y. Yang, and M. Renfors, "Flexible filter bank dimensioning for multicarrier modulation and frequency domain equalization,"

in *Proceedings of IEEE Asia Pacific Conference on Circuits and Systems*, pp. 451–454, Singapore, December 2006.
[24] T. Karp and N. J. Fliege, "Modified DFT filter banks with perfect reconstruction," *IEEE Transactions on Circuits and Systems II*, vol. 46, no. 11, pp. 1404–1414, 1999.
[25] T. Hentschel and G. Fettweis, *Software Radio Receivers*, Kluwer Academic, Boston, Mass, USA, 1999.
[26] S. Kay, *Fundamentals of Statistical Signal Processing: Estimation Theory*, Prentice-Hall, Englewood Cliffs, NJ, USA, 1993.
[27] W. W. Peterson and E. J. Weldon Jr., *Error-Correcting Codes*, MIT Press, Cambridge, Mass, USA, 2nd edition, 1972.
[28] T. B. Sorensen, P. E. Mogensen, and F. Frederiksen, "Extension of the ITU channel models for wideband OFDM systems," in *Proceedings of IEEE 62nd Vehicular Technology Conference (VTC '05)*, vol. 1, pp. 392–396, Dallas, Tex, USA, September 2005.
[29] R. G. Gallager, *Low-Density Parity-Check Codes*, MIT Press, Cambridge, Mass, USA, 1963.
[30] S. Hara, T. Matsuda, K. Ishikura, and N. Morinaga, "Co-existence problem of TDMA and DS-CDMA systems-application of complex multirate filter bank," in *Proceedings of IEEE Global Telecommunications Conference (GLOBECOM '96)*, vol. 2, pp. 1281–1285, London, UK, November 1996.
[31] M. J. Medley, G. J. Saulnier, and P. K. Das, "Narrow-band interference excision in spread spectrum systems using lapped transforms," *IEEE Transactions on Communications*, vol. 45, no. 11, pp. 1444–1455, 1997.
[32] T. Hidalgo Stitz and M. Renfors, "Filter-bank-based narrowband interference detection and suppression in spread spectrum systems," *EURASIP Journal on Applied Signal Processing*, vol. 2004, no. 8, pp. 1163–1176, 2004.
[33] Y. Yang, T. Hidalgo Stitz, M. Rinne, and M. Renfors, "Mitigation of narrowband interference in single carrier transmission with filter bank equalization," in *Proceedings of IEEE Asia Pacific Conference on Circuits and Systems*, pp. 749–752, Singapore, December 2006.

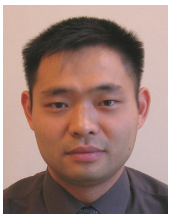

Yuan Yang received his B.S. degree in electrical engineering from HoHai University, Nanjing, China, in 1996, and his M.S. degree in information technology from Tampere University of Technology (TUT), Tampere, Finland, in 2001, respectively. Currently, he is a researcher and a postgraduate student at the Institute of Communications Engineering at TUT, working towards the doctoral degree. His research interests are in the field of broadband wireless communications, with emphasis in the topics of frequency-domain equalizers and multirate filter banks applications.

Tero Ihalainen received his M.S. degree in electrical engineering from Tampere University of Technology (TUT), Finland, in 2005. Currently, he is a researcher and a postgraduate student at the Institute of Communications Engineering at TUT, pursuing towards the doctoral degree. His main research interests are digital signal processing algorithms for multicarrier and frequency domain equalized single-carrier modulation based wireless communications, especially applications of multirate filter banks.

Mika Rinne received his M.S. degree from Tampere University of Technology (TUT) in signal processing and computer science, in 1989. He acts as Principal Scientist in the Radio Technologies laboratory of Nokia Research Center. His background is in research of multiple-access methods, radio resource management and implementation of packet decoders for radio communication systems. Currently, his interests are in research of protocols and algorithms for wireless communications including WCDMA, long-term evolution of 3G and beyond 3G systems.

Markku Renfors was born in Suoniemi, Finland, on January 21, 1953. He received the Diploma Engineer, Licentiate of Technology, and Doctor of Technology degrees from the Tampere University of Technology (TUT), Tampere, Finland, in 1978, 1981, and 1982, respectively. From 1976 to 1988, he held various research and teaching positions at TUT. From 1988 to 1991, he was a Design Manager at the Nokia Research Center and Nokia Consumer Electronics, Tampere, Finland, where he focused on video signal processing. Since 1992, he has been a Professor and Head of the Institute of Communications Engineering at TUT. His main research areas are multicarrier systems and signal processing algorithms for flexible radio receivers and transmitters.

Publication P2

Y. Yang, M. Rinne and M. Renfors, "Filter bank based frequency-domain equalization with noise prediction," in *Proc. 17th Annual IEEE International Symposium on Personal, Indoor and Mobile Radio Communications*, PIMRC'06, Helsinki, Finland, 2006

The 17th Annual IEEE International Symposium on Personal, Indoor and Mobile Radio Communications (PIMRC'06)

FILTER BANK BASED FREQUENCY-DOMAIN EQUALIZATION WITH NOISE PREDICTION

Yuan Yang
Institute of Communications Eng.
Tampere University of Technology, Finland
yang.yuan@tut.fi

Mika Rinne
Nokia Research Center
Helsinki, Finland
mika.p.rinne@nokia.com

Markku Renfors
Institute of Communications Eng.
Tampere University of Technology, Finland
markku.renfors@tut.fi

ABSTRACT

Complex modulated filter bank (FB) based frequency-domain equalization (FDE) provides an attractive single-carrier scheme for broadband wireless communications. With mildly frequency selective subband processing and modest number of subbands, it is able to provide better performance than the conventional FDE with FFT due to the lack of guard-interval overhead. Another significant benefit of this approach is that the same filter bank can be utilized to implement significant part of the receiver channel selectivity in a flexible way. This paper studies a hybrid frequency-time domain equalizer, which utilizes FB based equalizer for the feedforward part and a noise predictor (NP) for the feedback. The motivation is that the feedforward and feedback filter can be designed separately, in contrast to a conventional decision-feedback equalizer (DFE). The performance can be adjusted by the order of the NP. A significant advantage of NP based equalizer, over the traditional DFE, is that it is easier to include error control decoding in the equalizer feedback loop. This is able to provide significant performance enhancement over the DFE structure where the decoding is after the feedback loop.

I. INTRODUCTION

In wireless communication channels, the received signal is impaired by intersymbol interference and additive noise. Equalization is a process which helps to obtain more reliable estimates of the transmitted symbols. In recent years, the idea of single-carrier transmission in broadband wireless communications has been revived through the application of the FDE principle. In wideband channels, FDEs have clearly lower implementation complexity than time-domain equalizers with similar performance [1, 2]. Single-carrier transmission with FDE may have performance advantage and is less sensitive to nonlinear distortion and carrier synchronization accuracy compared to multicarrier techniques [3, 4]. The basic linear FDE scheme is based on the use of FFT and IFFT transforms and cyclic prefix as guard-interval between symbol blocks. The linear FDE can be realized with symbol-rate sampling or as fractionally-spaced equalizer with 2x symbol-rate sampling, the latter approach providing clear performance benefit over the former one.

In recent work [5, 6], we presented a novel linear FDE structure based on filter banks instead of FFT. In this so-called AP-FBEQ scheme, a low-order linear phase FIR filter and allpass filters are applied in subband-wise compensation of channel amplitude and phase distortions separately. Complex exponentially modulated analysis-synthesis FBs are used as the core of the frequency-domain processing. The performance of AP-FBEQ can exceed the performance of FFT-based systems, while the number of subbands needed in AP-FBEQ can be significantly lower than what is practical with the FFT-based FDE with cyclic prefix. The implementation complexity of AP-FBEQ is, no doubt, higher than that of a basic FFT-based FDE. However, in the fractionally-spaced realization of AP-FBEQ, the same filter bank that is used for equalization can be used also for implementing significant part of the channel selectivity, thus reducing the complexity of the baseband filtering part [6]. Furthermore, due to good frequency selectivity, the AP-FBEQ approach allows effective cancellation of narrowband interferences in the signal band.

Linear equalizers do not perform well with frequency selective channels which have deep spectral nulls in the passband. In an attempt to compensate the distortion, a linear equalizer places too much gain in the vicinity of the spectral null, thereby enhancing the noise present in those frequencies. DFE gives better performance for frequency selective wireless channels than the linear equalizer does. The hybrid frequency-time domain DFE was introduced in [1, 7]. On the other hand, time-domain NP based DFE structure was introduced in [8], and later discussed in [9] and [10]. An important property of NP type DFE is that the feedforward filter and the feedback filter coefficients are designed independently, while it achieves the same performance as the conventional DFE, if the feedforward filter length is sufficiently high. The hybrid time-frequency domain DFE with NP-based feedback part was introduced in [11] using the FFT-based scheme with cyclic prefix. It has been emphasized that in the NP structure it is easier to include the error control decoding in the feedback loop than in the traditional DFE structure.

This paper extends our earlier work on filter bank based FDE by investigating the performance improvement through a DFE scheme using AP-FBEQ as the feedforward filter and the noise predictor as a time-domain feedback filter. Further, we use fractionally-spaced feedforward filter to enhance the performance, instead of the symbol-rate approach considered in [11].

The contents of this paper is organized as follows: Section II briefly introduces analysis-synthesis FB and its use in frequency-domain equalization in the AP-FBEQ scheme. Section III examines the DFE scheme with a NP. The optimum NP coefficients in the case of fractionally-spaced equalizer are presented. The simulation results and conclusions will be given in Sections IV and V, respectively.

The notation in the paper uses lower case letters for time-domain and capital letters for frequency-domain functions. The

1-4244-0330-8/06/$20.00

script m is used for time-domain symbol rate sampled data sequences and the script n for oversampled sequences. The script k represents index of frequency-domain subband signals.

II. FREQUENCY-DOMAIN EQUALIZATION WITH EXPONENTIALLY MODULATED FILTER BANK

A. *Exponentially Modulated Filter Bank (EMFB)*

In this paper, EMFB is considered as an alternative way to do signal transforms, instead of FFT/IFFT. The filter bank basis functions are longer than a symbol block, and the guard-interval approach, commonly adopted to FFT-based FDE, cannot be used to obtain flat-fading subband signals. Therefore, we consider mildly frequency selective models for the subbands. On the other hand, the lack of guard-interval overhead results in better spectral efficiency.

EMFBs belong to a class of filter banks in which the subfilters are formed by modulating the lowpass prototype $h_p(n)$ with exponential sequences [12, 13]. The impulse response of the prototype can be optimized in such a manner that the filter bank satisfies the perfect reconstruction condition, i.e., the output signal is a delayed version of the input signal. There are two important design parameters of $h_p(n)$: the overlapping factor K determines the prototype filter length, as well as the achievable stopband attenuation; the roll-off ρ determines how much adjacent subbands are overlapping. In our studies we use $K = 5$, which results in about 50 dB stopband attenuation. We use a roll-off factor of $\rho = 1.0$, which means that only the neighboring subbands are overlapping with each other, and the overall subband bandwidth is twice the subband spacing.

EMFB can be implemented using cosine modulated FB (CMFB) and sine modulated FB (SMFB) blocks [12], as shown in Figure 1. There P^T denotes the real transform matrix of the analysis CMFB, and Q^T denotes the real transform matrix of the analysis SMFB. Then P and Q represent the corresponding transform matrices of the synthesis FB, respectively. The equalizer input and output are complex baseband I/Q signals, which are needed for spectrally efficient radio communications. The sampling rate conversion factor in the analysis and synthesis CMFB/SMFB is M, and there are totally $2M$ equally spaced low-rate subbands between $[-1/T,\ \ 1/T]$, where T is the symbol duration. The oversampled analysis bank includes two CMFBs and two SMFBs. Oversampling by 2 is achieved here by using complex subband signals instead of real ones that are sufficient in a basic perfect reconstruction analysis-synthesis system, and it allows frequency-domain equalization subbandwise. After equalization, only the real parts of the subband signals are needed for further processing. The synthesis bank is realized in the critically sampled form, consisting only of one CMFB and one SMFB block [5, 14].

B. *Linear equalizer with mean square error (MSE) criterion*

The key idea of AP-FBEQ equalization is to compensate amplitude and phase distortion separately within each subband, as demonstrated in papers [5,6]. The subband equalizer responses at the selected frequency points are obtained in the same way as for the FFT-based linear equalizer. In the case of ZF criterion,

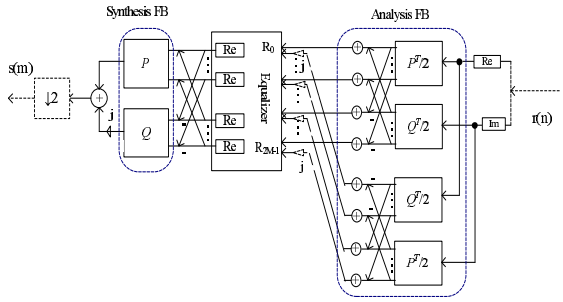

Figure 1: AP-FBEQ frequency-domain equalizer

for those selected frequency points, the amplitude response of the equalizer would be the inverse of the channel amplitude response, and the phase response of the equalizer would be the negative of the channel phase response.

MSE criterion is considered here since we are focusing on wideband single-carrier transmission with heavily frequency selective channels. In such systems, zero forcing criterion equalizer would suffer from severe noise enhancement [10] while MSE criterion provides clearly better performance. In addition, due to the FDE working on $2\times$ symbol rate, the root raise cosine (RRC) filter can be realized efficiently at the receiver together with the subband equalizer. The frequency response of optimum linear equalizer (including RRC) can be written as [1, 2, 6]

$$W_k = \frac{\sigma_x^2 C_k^*}{|\hat{C}_k|^2 \sigma_x^2 + \sigma_n^2} \qquad k = 0, 1, ..., 2M-1. \tag{1}$$

where we defined $|\hat{C}_k|^2 = |C_k|^2 + |C_{(M+k)_{mod(2M)}}|^2$, with $C_k = H_k^{ch} H_k^{RRC}$. Here H_k^{ch} and H_k^{RRC} are the channel and RRC filter frequency responses, and σ_x^2 and σ_n^2 are the signal and noise power, respectively. The symbol $*$ denotes complex conjugate. The frequency index k is defined in such a way that $k = 0$ corresponds to DC and $k = M$ corresponds to the symbol rate $1/T$. In the fractionally-spaced equalizer, the sampling rate is reduced to symbol rate after the feedforward filter. In frequency-domain, this can be implemented as a folding operation, after which the synthesis transform size is half of the analysis transform. Practical design of the needed FB based system with $2M$-channel analysis bank and M-channel synthesis bank is discussed in [15].

In AP-FBEQ, the subband equalizer structure is a cascade of a phase equalization section, consisting of allpass filter stages and a phase rotator, and amplitude equalization section, consisting of a linear phase FIR filter. This particular structure makes it possible to design independently the amplitude equalization and phase equalization. We have considered low-complexity cases where the allpass filter consists of one or two first-order allpass sections and the symmetric FIR filter is of length 3 or 5. In practice, the subband equalizer structure is not necessarily fixed in advance and it can be determined for

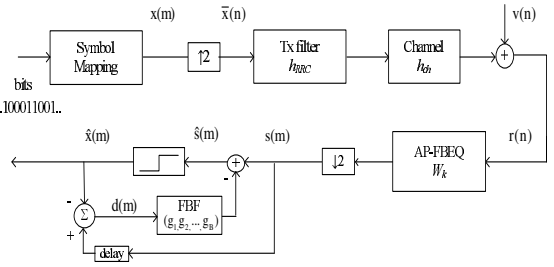

Figure 2: Basic model of frequency-time domain equalization

each subband based on frequency-domain channel estimation. The subband equalizer coefficients are calculated based on the channel amplitude and phase responses at two or three frequency points within each subband [5, 6].

III. System model for fractionally-spaced frequency-domain equalizer with a noise predictor

In this paper, we consider single-carrier block data transmission over a linear band-limited channel with additive white noise. The channel is assumed to have a time-invariant impulse response during each block transmission. The block diagram of the basic system model is shown in Figure 2. The equalization blocks include AP-FBEQ as feedforward filter in frequency-domain, operating at $2\times$ symbol rate, and a time-domain noise predictor operating at the symbol rate.

At the transmitter, the QAM sequences $x(m)$, $m = 0, 1, ..., P-1$, are transmitted in one block with unit symbol energy $\sigma_x^2 = 1$. The oversampled received signal $r(n)$ can be written as

$$\begin{aligned} r(n) &= \bar{x}(n) \otimes c(n) + v(n) \\ c(n) &= h_{RRC}(n) \otimes h_{ch}(n). \end{aligned} \tag{2}$$

Here $v(n)$ is additive white Gaussian noise with variance σ_n^2. The symbol $\otimes$ represents convolution. The received signal $r(n)$ can also be written in frequency-domain as $R_k = C_k X_k + V_k$. The symbol rate signal $\hat{s}(m)$ before the slicer can be represented by

$$\begin{aligned} \hat{s}(m) &= s(m) - \sum_{l=1}^{B} g(l) d(m-l) \\ &= s(m) - \sum_{l=1}^{B} g(l)(s(m-l) - \hat{x}(m-l)), \end{aligned} \tag{3}$$

where $g(l)$, $l = 1, 2, ..., B$, are the coefficients of the feedback filter. If the past B symbol decisions are assumed to be correct, i.e., $x(m) = \hat{x}(m)$, the error signal which contains the intersymbol interference and noise term is represented by $e(m) = d(m) - \sum_{l=1}^{B} g(l) d(m-l)$ [8]. Defining $\hat{g}(0)$=1 and $\hat{g}(l) = -g(l)$, the error signal can be written in a simple form as

$$e(m) = \sum_{l=0}^{B} \hat{g}(l) d(m-l). \tag{4}$$

It was shown in [8] that the optimum feedforward filter coefficients, minimizing $E[|e(m)|^2]$, are given by the linear equalizer with MSE criterion. In the fractionally-spaced structure we can directly use equation (1). Therefore, the feedforward filter can be implemented exactly as the MSE linear equalizer based on the AP-FBEQ idea [5, 6]. The feedback filter coefficients $\hat{g}(l)$ are obtained as the solutions of the following set of equations [8, 11]:

$$\begin{gathered} \sum_{m=1}^{B} \sum_{k=0}^{M-1} \hat{g}(m) e^{j\frac{2\pi}{M}k(l-m)} D_k = \sum_{k=0}^{M-1} e^{j\frac{2\pi}{M}kl} D_k \\ l = 1, 2, ...B, \end{gathered} \tag{5}$$

where D_k is the power spectrum of the total noise and intersymbol interference at the feedforward filter output. For the fractionally-spaced structure, we can write

$$D_k = \frac{\sigma_n^2}{|\hat{C}_k|^2 \sigma_x^2 + \sigma_n^2}. \tag{6}$$

It is now evident that the feedforward filter coefficients W_k and the feedback filter coefficients $g(l)$ can be designed independently. The advantage of this property is that performance tradeoff can be done through adjusting only the order of the feedback filter, without affecting the feedforward filter design. This is clearly more flexible scheme than the conventional method where the feedforward filter and feedback filter have to be designed jointly. The performance of such a SC-DFE system with different orders of the feedback filter is presented in the next section.

IV. Simulation Results

The system model is shown in Figure 2. The RRC filter has the roll-off $\alpha = 0.22$. The FB designs in the model use roll-off $\rho = 1.0$, overlapping factor of $K = 5$, and $2M = 256$ subbands. The performance was tested using the extended Vehicular A channel model of ITU-R with the maximum excess delay of about 2.5μs [16]. The symbol rate is 15.36 MHz. 1000 random channel instances were run to obtain the average performance. MSE criterion was applied to get the feedforward filter and feedback filter coefficients through equations (1) and (5). To ease the performance evaluation, the absence of feedback decision errors is assumed in all simulations below. The bit error rate (BER) performance was estimated for QPSK, 16-QAM, and 64-QAM modulations with Gray-coding.

Figure 3 shows the uncoded BER performance for different NP orders when perfect channel knowledge is assumed. Linear equalizer ($B = 0$) and ideal analytic DFE performance are given as references in the figures. Ideal analytic BER of DFE is obtained by applying the MSE DFE formula from [10] in the case of an infinite-length feedforward filter and feedback

filter. It is clear from the figures that DFE has much better performance than the linear equalizer. In the most interesting uncoded BER region $1\%...10\%$, it is seen that the performance of $B = 20$ taps is near to the analytic DFE bound in the case of QPSK and 16-QAM modulations. Furthermore, it is notable that the BER improvement when $B > 5$ is limited, which is due to the fact that major part of the channel power spread is within 5 taps. It was also noted that when the slicer output is used in the feedback, the performance in the interesting uncoded BER region is severely degraded and only marginally better than that of a linear equalizer. Therefore, it is important to include the error control decoder in the DFE feedback loop to obtain significant performance gains.

Figure 4 demonstrates the coded BER performance in terms of source bit E_b/N_0 -ratio for different NP orders when a maximum likelihood based channel estimator and LDPC-coding are included in the model. The channel estimator uses a Gold code of length 384 as the training sequence, and the binary training sequence is boosted in such a way that its peak power is equal to the peak power of data. The LDPC code has block length of 3840 and code rate of 3/4. It is seen that significant BER improvement can be achieved already with $B = 5$ taps, and the performance improves further with $B = 20$ taps.

It must be emphasized that Figure 4 gives idealized performance for the NP-based DFE. Here the results are obtained by implementing the LDPC decoder after the DFE and assuming that there are no decision errors in the feedback loop. In the future work, ways to include the error control decoder in the DFE feedback loop will be investigated. There are two basic alternatives. The interleaving based structure [9] is likely to lead to rather short code block length, and thus reduced performance, or to excessive transmission block length and latency. The other possible approach is to iterate the equalizer feedback loop and the decoding.

V. CONCLUSION

This paper has examined hybrid frequency-time domain equalization structure in single-carrier modulation which includes a filter bank based fractionally-spaced equalizer and a noise predictor. The results indicate that NP type DFE has the potential of achieving significantly improved performance over the linear equalizer. It was seen that it is important to include the error control decoder inside the DFE feedback loop, in order to capitalize the performance gain. It remains as a future topic to explore the performance gains with practical solutions for such a decoding structure.

ACKNOWLEDGMENT

This research work was supported by Nokia and the Academy of Finland.

REFERENCES

[1] D. Falconer, S. L. Ariyavisitakul, A. Benyamin-Seeyar, and B. Eidson, "Frequency domain equalization for single-carrier broadband wireless systems," *IEEE Communications Magazine*, vol. 40, no. 4, pp. 58–66, Apr. 2002.

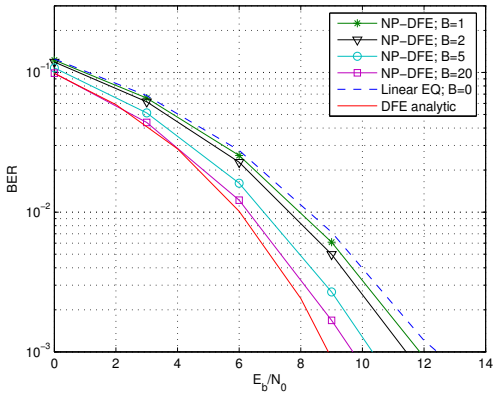

(a) QPSK modulation

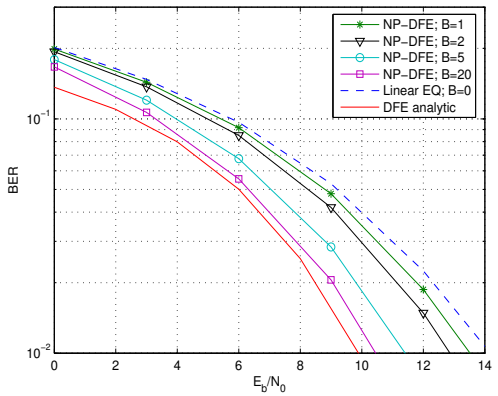

(b) 16-QAM modulation

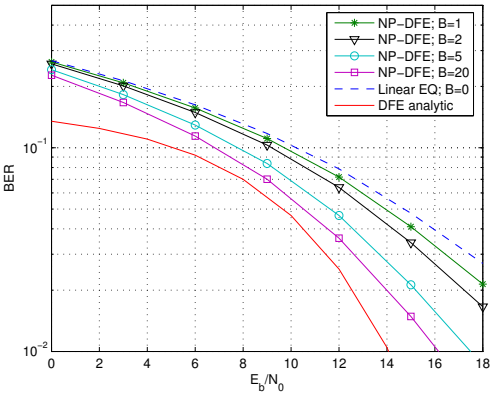

(c) 64-QAM modulation

Figure 3: Uncoded BER performance for different number of feedback taps, B =1, 2, 5, 20, with perfect channel knowledge

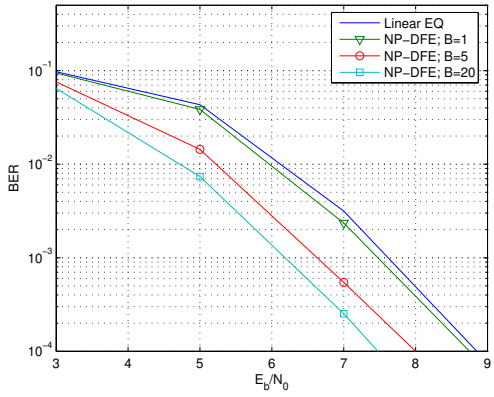

(a) QPSK modulation

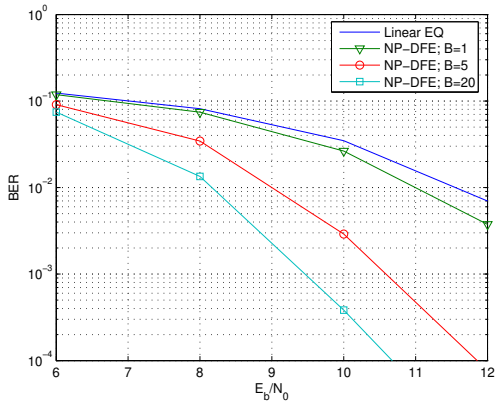

(b) 16-QAM modulation

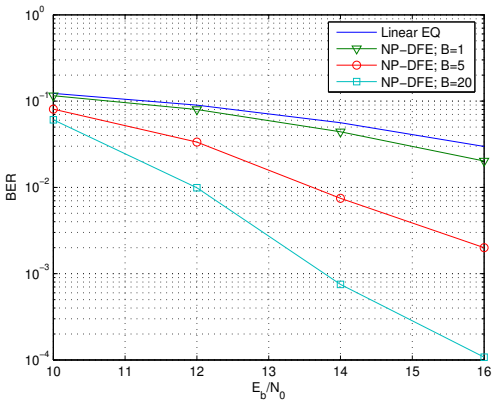

(c) 64-QAM modulation

Figure 4: LDPC-coded BER performance for different number of feedback taps, B =1, 5, 20. ML-based channel estimation with 384 symbol training sequence. LDPC code rate 3/4 and block length 3840.

[2] M. V. Clark, "Adaptive frequency-domain equalization and diversity combining for broadband wireless communications," *IEEE Journal on Selected Areas in Communications*, vol. 16, no. 8, pp. 1385–1395, Oct. 1998.

[3] H. Sari, G. Karam, and I. Jeanclaude, "Frequency-domain equalization of digital terrestrial tv broadcasting," *IEEE Communications Magazine*, pp. 100–109, Feb. 1995.

[4] A. Czyliwk, "Comparision between adaptive OFDM and single carrier modulation with frequency domain equalization," in *Proc. VTC*, Phoenix,AZ, May 1997, pp. 865–869.

[5] Y. Yang, T. Ihalainen, and M. Renfors, "Filter bank based frequency domain equalizer in single carrier modulation," in *Proceedings of 14th IST Mobile and Wireless Communications Summit*, Dresden, Germany, June 2005.

[6] ——, "Frequency domain equalization in single carrier transmission: Filter bank approach," submitted to EURASIP Journal of Applied Signal Processing, January 2006.

[7] N. Benvenuto and S. Tomasin, "On the comparison between OFDM and single carrier with a DFE using a frequency domain feedforward filter," *IEEE Transactions on Communications*, vol. 50, pp. 947–955, June 2002.

[8] C. A. Belfiore and J. H. Park, "Decision feedback equalization," Proc IEEE, pp. 1143–1156, Aug. 1979.

[9] M. V. Eyuboglu, "Detection of coded mudulation signals on linear, severely distorted channels using decision feedback noise prediction with interleaving," *IEEE Transactions on Communications*, vol. 36, pp. 401–409, Apr. 1988.

[10] J. G. Proakis, *Digital Communications, 4th Ed.* Mc Graw Hill, 2001.

[11] Y. Zhu and K. B. Letaief, "Single carrier frequency domain equalization with noise prediction for broadband wireless systems," in *Proc. of IEEE Globecom'04*, Dallas, Texas, USA, Dec. 2004, pp. 3098–3102.

[12] J. Alhava, A. Viholainen, and M. Renfors, "Efficient implementation of complex exponentially modulated filter banks," in *IEEE Int. Symp. Circuits and System*, Bangkok, Thailand, May 2003, pp. 157–160.

[13] A. Viholainen, J. Alhava, and M. Renfors, "Efficient implementation structures for complex modulated filter banks using cosine and sine modulated filter banks," accepted to *EURASIP Journal of Applied Signal Processing.*

[14] T. Ihalainen, T. H. Stitz, and M. Renfors, "Efficient per-carrier channel equalizer for filter bank based multicarrier systems," in *IEEE International Symposium on Circuits and Systems*, Japan, May 23-26 2005.

[15] A. Viholainen, T. Ihalainen, T. H. Stitz, Y. Yang, and M. Renfors, "Flexible filter bank dimensioning for multicarrier modulation and frequency domain equalization," submitted to 2006 IEEE Asia Pacific Conference on Circuits and Systems, May 2006.

[16] T. B. Sorensen, P. E. Mogensen, and F. Frederiksen, "Extension of the ITU channel models for wideband OFDM systems," in *Proc. IEEE Vehicular Technology Conf.*, Dallas, USA, Sept. 2005.

Publication P3

Y. Yang, M. Rinne and M. Renfors, "Noise Predictive Turbo equalization for a Filter Bank based Receiver in SC transmission System," in *Proc. IEEE 65th Vehicular Technology Conference Spring*, VTC'07, Dublin, Ireland, April 2007, pp. 2389-2393.

Noise Predictive Turbo Equalization for a Filter Bank Based Receiver in a SC Transmission System

Yuan Yang Tero Ihalainen Markku Renfors
Institute of Communications Eng.
Tampere University of Technology
{yang.yuan; tero.j.ihalainen; markku.renfors}@tut.fi

Mika Rinne
Nokia Research Center
Helsinki, Finland
mika.p.rinne@nokia.com

***Abstract*—For coded transmission over band-limited channels with inter-symbol interference, Douillard proposed the turbo equalization approach which has been studied widely. It is an iterative equalization/decoding algorithm and results in tremendous performance improvement. This paper studies a turbo equalization approach, which includes our recently proposed filter bank based frequency-domain equalizer, and a noise predictor inside of a decision-feedback loop, in coded single-carrier transmission. Its performance is simulated in a frequency-selective channel for QPSK and 16-QAM modulations. Different number of iterations and noise prediction orders are examined. The simulation shows that one iteration with 5-taps noise prediction filter is sufficient to obtain significant gain over linear equalizer.**

I. Introduction

Future wireless communications are required to support high-rate, high-quality data transmission. This requires a wide transmission bandwidth. However, there exist receiver design challenges due to highly frequency-selective channels, which are introduced by the multipath effects. Single-carrier transmission with frequency-domain equalization (FDE) has been considered as an alternative technique for broadband wireless communications [1], [2]. It may be derived from a multi-carrier (MC) transceiver by shifting the synthesis part from the transmitter to the receiver, thereby easing the processing requirements of the transmitter front-end. Moreover, single-carrier FDE is characterized by a block-wise transmission, where the equalization tasks are performed in frequency-domain. This leads to a remarkable complexity reduction compared to a time-domain realization.

Decision-feedback equalizer (DFE) outperforms linear equalizer (LE) for severely distorted wireless channels such as channels with spectral nulls [3], [4]. The advantage of DFE is the cancellation of intersymbol interference (ISI) with reduced noise enhancement, which results in better performance. Significant improvements can also be achieved using error correction codes, which have been devised for increasing the reliability of transmission. However, DFE cannot be applied directly to coded transmission because of the decoding delay. Eyuboglu [5] introduced a successive decoding scheme, where a time-interleaver/de-interleaver pair was used to re-arrange the received symbols for decoding within one transmitted frame, in such a way that the reliable detected symbols can be used in the feedback loop. In this scheme, short code length should be used because long code size causes excessive transmission latency [5], which would be difficult from the system design point of view when considering issues like power control, adaptive modulation and packet scheduling. The most common combined equalization/decoding method is the iterative decoding approach [6]–[8]. It is referred to as turbo equalization and the DFE function is realized by repeating the equalization and decoding tasks on the same frame of received data. The feedback information from the decoder is incorporated into the equalization process. The reliability of feedback symbols increases with the number of iterations. Both mentioned schemes are able to attain remarkable performance gains over LE.

In this paper, we consider the turbo equalization scheme, which incorporates a linear FDE [9] and a noise prediction (NP) [3] for decision feedback, along with Gallager's low-density parity check (LDPC) code [10]. The FDE utilizes exponentially modulated filter banks (EMFBs) as the core of the frequency-domain processing instead of commonly adopted FFT transform. Because of the lack of guard-interval overhead, such FB-FDE performance would exceed FFT-FDE, while the number of subbands needed can be significantly lower than in the FFT-FDE. In our recent work, NP-DFE with FB-FDE in uncoded modulation has been studied in [11], where the NP-DFE has shown the capability of achieving significant performance improvement with the perfect feedback assumption. This paper examines the practical performance gain utilizing turbo equalization with the NP-DFE structure in time dispersive multipath channel conditions.

This paper is organized as follows: Section II will introduce the FB-FDE structure and the used CFIR-FBEQ subband equalizer design. Section III will briefly describe the turbo equalization scheme, along with design of the NP filter. The simulation set-up and numerical results are given in Section IV. The conclusion is drawn in Section V.

II. Frequency-Domain Equalization with Filter Bank Transform

In this paper, we consider a synchronous, linear modulated and single-carrier data transmission systems over severe distorted wireless channel. The channel is assumed to have a time-invariant impulse response during each frame transmission. The block diagram of the studied system is shown in Fig. 1. The equalization is actually the combination of

1550-2252/$25.00 ©2007 IEEE

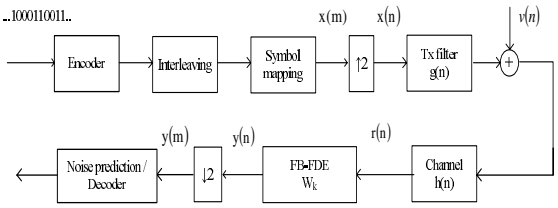

Fig. 1. Basic model for coded single-carrier transmission.

FB-FDE, a sort of feedforward filter in frequency-domain operating at $2\times$ symbol rate, and a time-domain NP operating at the symbol rate in the feedback loop. The FB-FDE performs the task of combating ISI efficiently, while NP intends to reduce the noise variance at the output of FB-FDE. This section will addresses FB-FDE, with emphasis on the design of the complex FIR subband equalizer.

With heavily frequency-selective channels, equalization with MSE criterion provides clearly better performance than ZF criterion, which would suffer from severe noise enhancement [4]. The frequency response of optimum fractionally-spaced equalizer with MSE criterion can be written as [1], [2], [9]

$$W_k = \frac{\sigma_x^2 C_k^*}{|\hat{C}_k|^2 \sigma_x^2 + \sigma_n^2} \qquad k = 0, 1, \ldots, 4M-1. \tag{1}$$

where we define C_k as DFT transform of impulse response of the cascade of real-valued RRC filter $g(n)$ and channel $h(n)$, and $|\hat{C}_k|^2 = |C_k|^2 + |C_{(2M+k)_{mod(4M)}}|^2$. The symbol $*$ denotes complex conjugate. The frequency index k is defined in such a way that $k = 0$ corresponds to DC and $k = 2M$ corresponds to the symbol rate $1/T$. $2M$ represents the total number of subbands for FB-FDE. σ_x^2 and σ_n^2 are the variances of data and additive white Gaussian noise, respectively.

In this paper, EMFBs with perfect reconstruction characteristics [12] are utilized for the time-frequency transform, instead of DFT. The important reason of using FB-FDE is that, the EMFBs not only can be used to combat channel distortion, but also used to implement part of the channel filtering with much higher performance than when using the FFT-FDE structures. In [13], [14], FB-FDE is shown to be an easily configurable structure for the final stage of the channel filtering chain, together with the channel equalization functionality.

As shown in Fig. 2, a 2x-oversampled analysis FB is applied. The received baseband equivalent complex I/Q signal $r(n)$ is split and decimated into $2M$ complex low-rate subband signals R_b ($b = 0, 1, \ldots, 2M-1$), which are equally spaced between $[0, 2\pi]$. After equalization, the real parts of the outputs are sufficient for synthesizing the time-domain equalized signal, using a critically sampled synthesis filter bank. The advantage of using 2x-oversampled analysis filter bank is that the channel equalization can be done within each subband independently of the other subbands. Assuming roll-off $\rho = 1.0$ in the filter bank design, the complex subband signals of the analysis bank are essentially alias-free.

The sampling rate reduction after FB-FDE can be realized efficiently by a folding operation in frequency-domain. It means that the synthesis transform size needs to be only half of the analysis transform. Practical design of the needed FB based system with $2M$-subbands analysis bank and M-subbands synthesis bank is discussed in [14].

As shown in Fig. 2, equalization takes place on the low-rate subband signals R_b. The number of subbands is selected in such a way that the channel is mildly frequency-selective within each individual subband. The subband equalizer responses are designed to cope with the channel responses within the subband. This is in contrast with FFT-FDE, where a simple complex coefficient per subband is used. Next we will address a low-complexity subband equalizer structure of FB-FDE, named as CFIR-FBEQ, together with the equalizer coefficient design.

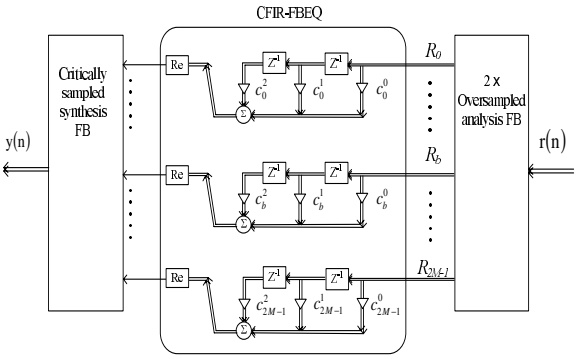

Fig. 2. Exponentially-modulated filter bank based frequency-domain equalizer.

Complex FIR type subband equalizer

In this paper, we used a 3-tap complex FIR filter (CFIR), $E(z) = c_b^0 + c_b^1 z^{-1} + c_b^2 z^{-2}$, to compensate the channel distortion within each subband. The number of subbands is selected in such a way that the channel frequency response is smooth within each individual subband. The equalizer response $E(e^{jw})$ is designed in a frequency-sampled manner, utilizing a number of selected frequency points within each subband. There are some differences between the odd and even subband processing because, at the low rate, the interesting subband is centered at $\pi/2$ and $-\pi/2$ for odd and even subbands, respectively. Here three frequency points $\omega = \{0\pi/\ 2\pi\ \}$ or $\omega = \{-\pi, -\pi/2, 0\}$ (normalized frequencies) are chosen to determine the subband equalizer response, which results in simplified calculations [9].

Suppose there are frequency points with indexes $k = 0, 1, \ldots, 4M-1$ for the subbands indexed by $b = 0, 1, \ldots, 2M-1$. At the low data rate after decimation, these frequency points are located for the even subbands at frequencies ω = $\{0\pi/\ 2\pi\ \}$, and for the odd subbands at ω

= $\{-\pi, -\pi/2, 0\}$ [12]. For notational convenience, we define the target frequency responses in term of the subband index $b = 0, 1, \ldots 2M-1$, instead of frequency point k. These target responses for subband b are denoted as η_b^i, with $i \in \{0,\ 1,\ 2\}$. In the following, the superscript indexes $0,\ 1,\ 2$ correspond to the subband lower edge, center, and upper edge, respectively. These are defined as:

$$\eta_b^i = W_{2b+i}. \tag{2}$$

The CFIR subband equalizer response at the target frequencies satisfy the following equations:
For even subband:

$$E_b(e^{j\omega}) = \begin{cases} c_b^0 + c_b^1 + c_b^2 = \eta_b^0, & (\omega = 0) \\ jc_b^0 + c_b^1 - jc_b^2 = \eta_b^1, & (\omega = \pi/2) \\ -c_b^0 + c_b^1 - c_b^2 = \eta_b^2, & (\omega = \pi) \end{cases} \tag{3}$$

For odd subband:

$$E_b(e^{j\omega}) = \begin{cases} -c_b^0 + c_b^1 - c_b^2 = \eta_b^0, & (\omega = -\pi) \\ -jc_b^0 + c_b^1 + jc_b^2 = \eta_b^1, & (\omega = -\pi/2) \\ c_b^0 + c_b^1 + c_b^2 = \eta_b^2, & (\omega = 0) \end{cases} \tag{4}$$

Then the 3-tap CFIR coefficients $\{c_b^0 c_b^1 c_b^2\}$ of the bth subband equalizer can be obtained as follows (signs + stand for even subbands and signs - for odd subbands):

$$\begin{aligned} c_b^0 &= \pm\tfrac{1}{2}\left(\frac{\eta_b^0 - \eta_b^2}{2} - j\left(\eta_b^1 - \frac{\eta_b^0 + \eta_b^2}{2}\right)\right) \\ c_b^1 &= \frac{\eta_b^0 + \eta_b^2}{2} \\ c_b^2 &= \pm\tfrac{1}{2}\left(\frac{\eta_b^0 - \eta_b^2}{2} + j\left(\eta_b^1 - \frac{\eta_b^0 + \eta_b^2}{2}\right)\right) \ . \end{aligned} \tag{5}$$

It should be noted that the order of CFIR-FBEQ and the number of used frequency points within one subband can be flexible [9]. For instance, first order CFIR-FBEQ would be viewed as a single complex gain determined from the channel frequency response at the subband center, and second order of CFIR-FBEQ can be derived from the frequency response at the passband edges, ω = $\{0\pi\ \}$ or $\omega = \{-\pi, 0\}$. The order of CFIR-FBEQ can be determined individually for each subband based on the channel estimates. This enables CFIR-FBEQ order to be controlled so that each subband response is equalized optimally at the minimum number of frequency points which can be expected to result in sufficient performance.

III. Turbo equalization with FB-FDE and NP-DFE

Classic turbo equalization, first proposed by Doulliard [6], utilizes maximum a posteriori probability (MAP) equalizer and suffers from high computational load for channels with long memory or large constellation sizes. Further development can be found in [7], where MAP equalizer was replaced by an LE and a DFE. In this paper, we apply a fractionally-spaced FB-FDE and a NP-DFE, where the filter coefficients are calculated using the MSE criterion. Moreover, the feedback symbols are updated based on soft output from the decoder, which may improve the system performance compared to hard-decision decoder. In this section, this iterative equalization/decoding scheme used in our studies will be briefly described. The optimum NP coefficients in the case of fractionally-spaced equalizer are presented.

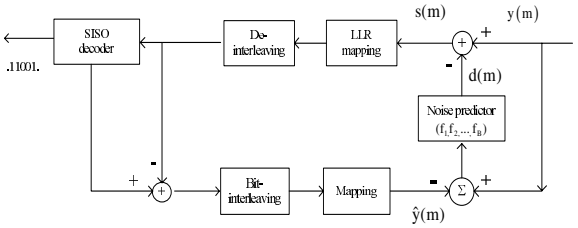

Fig. 3. Iterative noise prediction and soft decoding.

As shown in Fig. 1, a number of source information bits are fed into encoder at the transmitter, where LDPC code is applied. Then the coded bits are interleavered and mapped into QAM symbols. It should be emphasized that, in conventional single-carrier FFT-FDE system, the data stream is split into a number of transmission blocks, and a cyclic prefix (CP) is inserted between successive blocks for equalization purposes [1], [2]. This CP is used to mitigate interblock interference induced by the time dispersion of the channel. However, CP is not utilized in FB-FDE system, resulting in higher bandwidth efficiency over conventional FFT-FDE [9]. In Fig. 1, the index m represents symbol-spaced samples, while n represents fractionally-spaced samples. The oversampled received signal $r(n)$ can be written in frequency-domain as $R_k = C_k X_k + V_k$. Here V_k is the frequency-domain representation of additive white Gaussian noise $v(n)$. C_k is formulated as $C_k = G_k H_k$ and the optimum feedforward equalizer response W_k with MSE criterion was already present in equation (1). Using the NP-approach, the feedback filter design is actually decoupled from the design of the feedforward filter. The feedback filter order can be chosen independently from the feedforward filter. The important property of NP-DFE structure is that performance improvement can be adjusted by changing the order of NP in the feedback. This is clearly more flexible scheme than the conventional DFE method where the feedforward filter and feedback filter have to be designed jointly.

The feedback structure combining NP-DFE and decoding is shown in Fig. 3. De-interleaver is applied before the decoder, such that error bursts can be avoided within a block of data and therefore the quality of feedback symbols can be improved. In the case of soft decoder, bit-wise log-likelihood ratio (LLR) can be converted into probabilities that each of the received code bits takes on the value of zero or one. They will be updated every time after decoding. After interleaving, this updated bit LLR information is used to form more reliable feedback symbols $\hat{y}(m)$, which are used to predict the noise component $d(m)$. The sequence $s(m)$ contains the symbols

with reduced noise variance.

To predict the noise in the current symbol $y(m)$, the past reliable decision-feedback symbols $\hat{y}(m-l)$, $l = \{1, 2, \ldots, B\}$, are used. B is the order of noise predictor. The estimated noise component can be represented by $d(m) = \sum_{l=1}^{B} f(l)(y(m-l) - \hat{y}(m-l))$, where the feedback filter coefficients $f(l)$ can be obtained as the solutions of the following set of equations [3], [11]:

$$\sum_{l=1}^{B}\sum_{k=0}^{M-1} f(l)e^{j\frac{2\pi}{M}k(m-l)}D_k = \sum_{k=0}^{M-1} e^{j\frac{2\pi}{M}km}D_k \qquad m = 1, 2, \ldots, B, \tag{6}$$

D_k is the power spectrum of the total noise and ISI at the MSE linear equalizer output. For the fractionally-spaced structure, D_k can be written as:

$$D_k = \frac{\sigma_n^2}{|\hat{C}_k|^2\sigma_x^2 + \sigma_n^2}. \tag{7}$$

The feedforward filter coefficients in equation (5) and feedback filter coefficients in equation (6) are updated at regular intervals based on the channel estimates and knowledge of the receiver RRC filter frequency response. It is known that the order of the noise predictor and especially the number of iterations have strong influence on the receiver's processing complexity and delay time. The next section describes the system simulation set-up and presents the performance improvement obtained with different iterations and different orders of the noise predictor.

IV. Numerical Results

The basic system model is shown in Fig. 1. The parameters of the simulation model are presented in Table I. The transmit and receiver filters are real-valued RRC filters with roll-off of $\alpha = 0.22$. The EMFB designs in the model use roll-off $\rho = 1.0$, overlapping factor of $K = 5$, and $2M = 256$ subbands. The performance was tested using the extended Vehicular A channel model of ITU-R with the maximum excess delay of about $2.5\mu s$ [15]. Each frame contains 6912/13824 bits for QPSK/16-QAM modulation using Gray-Code in bit-mapping. During each transmission frame, we assumed the channel to be stationary and 4000 random channel instances were used to estimated the performance. MSE criterion was applied in both the linear and feedback equalizer design. The frame error rate (FER) is used as the performance metric.

Fig. 4(a) shows the performance of different number of iterations and with ideal feedback, when the order of noise prediction is fixed to $B = 20$. It is clearly visible that NP-DFE is capable of achieving over 1 dB gain for QPSK modulation, and nearly 2 dB gain for 16-QAM at FER of 10^{-1}, compared to LE with interleaving (LEI). Even more gain is obtained when comparing with LE without interleaving. The number of iterations improves the reliability of feedback symbols gradually, and consequently also the FER performance. In the most interesting FER region $1\% - 10\%$, about 0.8 dB/1.4 dB gain can be obtained for QPSK/16-QAM with two iterations.

TABLE I
System Parameters of the Simulation

Symbol rate	15.36 MHz	
RRC roll-off	0.22	
Signal bandwidth	18.74 MHz	
No. of subbands	256	
Data symbols per frame	3456	
Training symbols	384	
Total symbols	3840	
Frame duration	250 μs	
Error correction coding	LDPC with code rate 2/3	
QAM Modulation	QPSK	16-QAM
Transmit bits (Coded)	6912	13824
Source bits	4608	9216

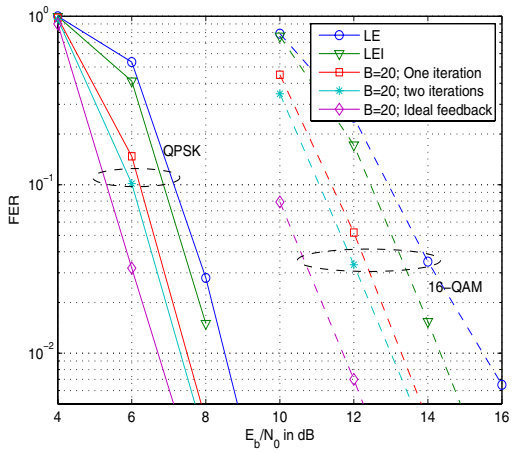

(a) Performance improvement by one or two iterations with a fixed order of noise predictor (B=20)

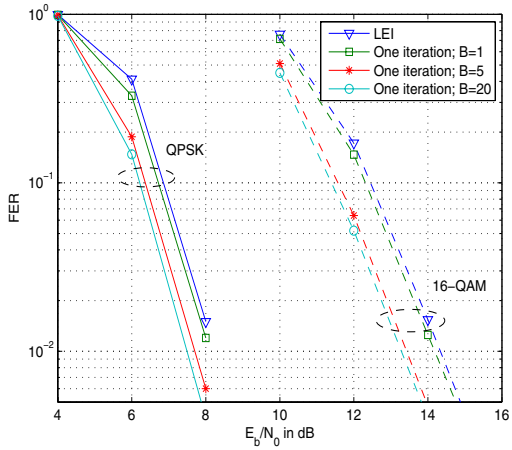

(b) Performance improvement by different orders of noise predictor with one iteration

Fig. 4. Performance evaluations on different number of iterations and the order of noise predictor.

Moreover, it is seen that already one iteration can provide significant gain.

The performance with one iteration and different orders of noise predictor, $B = \{1, 5, 20\}$, are examined in Fig. 4(b). It is seen that $B = 1$ has only marginally better performance than LEI. Furthermore, $B = 5$ can achieve most of the performance gain, which would be a good performance/complexity tradeoff, while $B = 20$ gives only marginally better performance over $B = 5$ for both QPSK and 16-QAM modulations.

V. Conclusion

Single-carrier transmission with frequency-domain equalization has been considered a promising alternative to orthogonal frequency division multiplexing systems for broadband wireless communications. With mildly frequency-selective subband processing and modest number of subbands, filter bank based frequency-domain equalization can provide better performance than conventional FFT-based approaches with a higher number of subbands. In this work, we added turbo equalization idea into the coded single-carrier system, which utilizes our exponentially-modulated filter bank based frequency-domain equalizer and noise prediction as feedforward and feedback filters, respectively. The simulation results show that this combined equalization/decoding scheme can obtain significant performance improvement over linear equalizer in time dispersive multipath channels. Moreover, one iteration with the order of noise predictor $B = 5$ is sufficient to achieve most processing gain of two iterations with $B = 20$, while yet maintaining an affordable complexity.

References

[1] D. Falconer, S. L. Ariyavisitakul, A. Benyamin-Seeyar, and B. Eidson, "Frequency domain equalization for single-carrier broadband wireless systems," *IEEE Communications Magazine*, vol. 40, no. 4, pp. 58–66, Apr. 2002.

[2] M. V. Clark, "Adaptive frequency-domain equalization and diversity combining for broadband wireless communications," *IEEE Journal on Selected Areas in Communications*, vol. 16, no. 8, pp. 1385–1395, Oct. 1998.

[3] C. A. Belfiore and J. H. Park, "Decision feedback equalization," *Proc. IEEE*, vol. 67, pp. 1143–1156, Aug. 1979.

[4] J. G. Proakis, *Digital Communications, 4th Ed.* McGraw-Hill, 2001.

[5] M. V. Eyuboglu, "Detection of coded mudulation signals on linear, severely distorted channels using decision feedback noise prediction with interleaving," *IEEE Transactions on Communications*, vol. 36, pp. 401–409, Apr. 1988.

[6] C. Douillard, M. Jezequel, and C. Berrou, "Iterative correction of intersymbol interference: Turbo–equalization," *European Transactions on Telecommunications*, vol. 6, pp. 507–511, Sept. 1995.

[7] M. Tuchler, R. Koetter, and A. Singer, "Turbo equalization: Principles and new results," *IEEE Transactions on Communications*, vol. 50, pp. 754–767, May 2002.

[8] R. Koetter, A. C. Singer, and M. Tuchler, "Turbo equalization," *IEEE Signal Processing Magazine*, vol. 21, pp. 67–80, Jan. 2004.

[9] Y. Yang, T. Ihalainen, M. Rinne, and M. Renfors, "Frequency-domain equalization in single-carrier transmission: Filter bank approach," *EURASIP Journal on Advances in Signal Processing*, vol. 2007, pp. Article ID 10 438, 16 pages, 2007, doi:10.1155/2007/10438.

[10] R. G. Gallager, *Low Density Parity Check Codes.* Cambridge, MIT Press, 1963.

[11] Y. Yang, M. Rinne, and M. Renfors, "Filter bank based frequency-domain equalization with noise prediction," in *Proc. 17th Annual IEEE international symposium on personal, indoor and mobile radio communications*, Helsinki, Finland, Sept. 2006.

[12] A. Viholainen, J. Alhava, and M. Renfors, "Efficient implementation of 2x oversampled exponentially modulated filter banks," *IEEE Transactions on Circuits and Systems II*, vol. 53, pp. 1138–1142, Oct. 2006.

[13] Y. Yang, T. H. Stitz, M. Rinne, and M. Renfors, "Mitigation of narrowband interference in single carrier transmission with filter bank equalization," in *Proc. 2006 IEEE Asia Pacific Conference on Circuits and Systems*, Singapore, Dec. 2006, pp. 749–752.

[14] A. Viholainen, T. Ihalainen, T. H. Stitz, Y. Yang, and M. Renfors, "Flexible filter bank dimensioning for multicarrier modulation and frequency domain equalization," in *Proc. 2006 IEEE Asia Pacific Conference on Circuits and Systems*, Singapore, Dec. 2006, pp. 451–454.

[15] T. B. Sorensen, P. E. Mogensen, and F. Frederiksen, "Extension of the ITU channel models for wideband OFDM systems," in *Proc. IEEE Vehicular Technology Conf.*, Dallas, USA, Sept. 2005.

Publication P4

Y. Yang and M. Renfors, "Channel equalization in wideband single-carrier transmission using a filter bank transform and a block interleaved DFE," in *Proc. IEEE 8th International Workshop on Signal Processing Advances for Wireless Communications*, SPAWC'07, Helsinki, Finland, June 2007.

CHANNEL EQUALIZATION IN WIDEBAND SINGLE-CARRIER TRANSMISSION USING A FILTER BANK TRANSFORM AND A BLOCK INTERLEAVED DFE

Yuan Yang *Markku Renfors*

Institute of Communications Engineering
Tampere University of Technology
P. O. Box 553, FI-33101 Tampere, Finland
{yang.yuan; markku.renfors}@tut.fi

ABSTRACT

This paper explores a low-complexity decision feedback equalization/decoding scheme, which uses filter bank frequency-domain equalizer and noise prediction in feedforward and feedback filter, respectively. Its performance is evaluated with extended Vehicular A channel model of ITU-R in LDPC coded single-carrier modulation. Simulation results show that the equalization/decoding scheme with symbol-wise block interleaver can achieve a considerable performance improvement over linear equalizer. Moreover, its performance comparison to widely-used turbo equalizer approach is also included, showing minor performance degradation with considerably reduced complexity.

I. INTRODUCTION

Single-carrier frequency-domain equalization (SC-FDE) has been discussed as a promising technology to cope with large multipath delay spread in broadband wireless channels [1], [2]. It is characterized by block-wise transmission, where the channel estimation and equalization tasks are performed in frequency-domain. This leads to a remarkable complexity reduction compared to time-domain realizations. For the mitigation of the channel frequency response with deep spectral fading, the decision-feedback equalizer (DFE) provides better performance than the linear equalizer (LE) [3], [4]. The advantage of DFE is the cancelation of intersymbol interference (ISI) with reduced noise enhancement.

Error correction codes have been devised for increasing the reliability of transmission. The most common combined equalization/decoding method is the iterative decoding approach [5]. It is referred to as turbo equalization and the DFE function can be realized by performing the equalization and decoding tasks iteratively on the same frame of received data. The feedback information from the decoder is incorporated into the equalization process.

In a recent work [6], we presented a low-complexity iterative receiver structure for coded single-carrier transmission, which incorporates a filter bank frequency-domain equalizer (FB-FDE) [7] and a noise predictor (NP) [3] for decision feedback, along with Gallager's low-density parity check (LDPC) code [8]. The FDE utilizes exponentially modulated filter banks (EMFBs) instead of commonly adopted FFT transform. An important property of FB-FDE is that the EMFBs not only can be used to perform channel equalization task, but also used to implement part of the channel filtering. Moreover, it is shown that with mildly frequency selective subband processing and modest number of subbands, FB-FDE can provide better performance than conventional FFT-FDE approaches with a higher number of subbands [7]. The performance gain is due to the absence of cyclic prefix (CP) overhead of the FFT-FDE schemes. Furthermore, FB-FDE can be used for any communications waveform, no matter whether CP is specified in the system or not.

This paper continues to apply such FB-FDE in the feedforward filter and NP in the feedback filter, but now we use a different scheme to get reliable symbol decisions to the feedback. A simple symbol-wise block interleaver/deinterleaver pair is utilized to re-arrange the received symbols for decoding, in such a way that previous detected symbol blocks can be used to predict the noise variance of next block. A short code block is used so as to have more reliable detected feedback for noise prediction. In this paper, we refer to the studied scheme as block DFE. The main objective is to build such a block DFE with the common FB-FDE configuration. Its performance is examined in comparison with the turbo scheme introduced in [6].

This paper is organized as follows: Section II will shortly describe the coded data transmission system with the block DFE scheme. The idea of FB-FDE will be presented. Section III will describe the receiver of the block DFE scheme, along with comparison to the turbo scheme. The simulation set-up and performance comparisons are given in Section IV. The conclusion is drawn in Section V.

II. FB-FDE MODEL

The block diagram of the studied system is shown in Figure 1. The FB-FDE operates at $2\times$-symbol rate, which

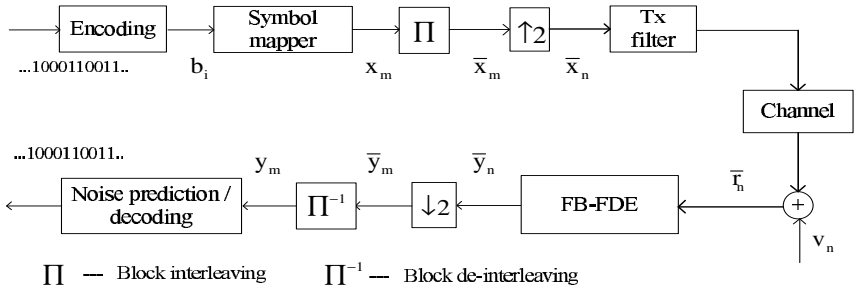

Fig. 1. Basic model for coded single-carrier transmission.

provides robustness to the sampling phase and the receiver filter can be implemented efficiently in frequency-domain without additional complexity. In this paper, we define that the capital letter denotes samples in frequency-domain while lower case represents time-domain samples. The subscripts m and n represent symbol rate and fractionally-spaced samples, respectively; the subscripts k, b and i denote the index of frequency point, subband, bit-wise order, respectively; the symbol $*$ denotes complex conjugate and $\bar{(.)}$ represents the interleaved samples.

The interleaved and oversampled received signal $\bar{r}_n$ can be written as $\bar{r}_n = c_n \otimes \bar{x}_n + v_n$, where v_n is additive white Gaussian noise and c_n is the impulse response of the cascade of the real-valued RRC transmit filter and channel $h(n)$. The symbol $\otimes$ denotes convolution. The frequency response of the fractionally-spaced FDE with MSE criterion can be described as [1]

$$\begin{aligned} W_k &= \frac{\sigma_x^2 C_k^*}{|\hat{C}_k|^2 \sigma_x^2 + \sigma_n^2} \\ & k = 0, 1, ..., 4M-1. \end{aligned} \tag{1}$$

where $|\hat{C}_k|^2 = |C_k|^2 + |C_{(2M+k)_{mod(4M)}}|^2$ and σ_x^2 and σ_n^2 are the variances of data and additive white Gaussian noise, respectively.

With our choice of the parameters, an FFT-FDE would use an FFT size of $4M$. Our FB-FDE uses $2M$ subbands, together with low-complexity subband processing to achieve the same frequency resolution. In both cases, the FDE operation can be formulated as

$$\bar{Y}_k = W_k \bar{R}_k + W_{(2M+k)_{mod(4M)}} \bar{R}_{(2M+k)_{mod(4M)}}. \tag{2}$$

Here the frequency-domain folding operation, characteristic to fractionally-spaced FDE, is included. Notice that in (2), depending on the RRC roll-off factor α, $W_k = 0$ in the stopband region. The time-domain signal is synthesized using an M-channel filter bank [7], [9], or $2M$-point FFT in the FFT-FDE case [1].

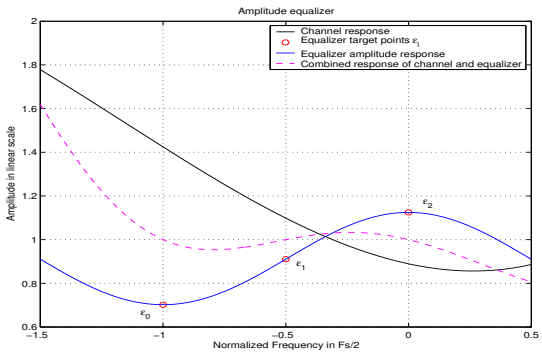

Fig. 2. Subband amplitude responses of channel and equalizer in FB-FDE (ZF criterion).

Complex FIR type subband equalizer

We use a 3-tap complex FIR filter (CFIR), $E(z) = c_b^0 + c_b^1 z^{-1} + c_b^2 z^{-2}$, to equalize the subband signals R_b. The equalizer response $E(e^{jw})$ is designed in frequency-sampled manner based on (1), as indicated in Figure 2.

Given three selected frequency points within each subband, i.e., subband lower edge, center and upper edge frequencies, the 3-tap CFIR coefficients of the subband equalizer can be obtained as (signs + stand for even subbands and signs - for odd subbands):

$$\begin{aligned} c_b^0 &= \pm\tfrac{1}{2}\left(\frac{\eta_b^0 - \eta_b^2}{2} - j\left(\eta_b^1 - \frac{\eta_b^0 + \eta_b^2}{2}\right)\right) \\ c_b^1 &= \frac{\eta_b^0 + \eta_b^2}{2} \\ c_b^2 &= \pm\tfrac{1}{2}\left(\frac{\eta_b^0 - \eta_b^2}{2} + j\left(\eta_b^1 - \frac{\eta_b^0 + \eta_b^2}{2}\right)\right), \end{aligned} \tag{3}$$

where η_b^i, $i \in \{0,\ 1,\ 2\}$, represent these target frequency responses for bth subband, (superscript indexes 0, 1, 2 correspond to the subband lower edge, center, and upper edge, respectively). The relationship between η_b^i and W_k is

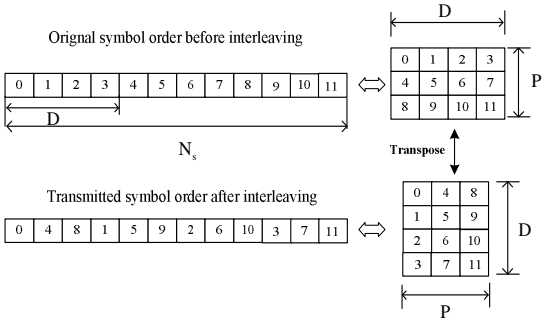

Fig. 3. Block interleaver.

described as $\eta_b^i = W_{2b+i}$.

It should be noted that the order of CFIR and the number of used frequency points within one subband can be flexible. For instance, 0-th order CFIR would be viewed as a single complex gain determined from the channel frequency response at the subband center, and first order of CFIR can be derived from the frequency response at the passband edges. The order of CFIR can be determined individually for each subband based on the channel estimates.

III. COMBINED EQUALIZATION/DECODING

The most popular combined equalization/decoding scheme is turbo equalization. Generally, a turbo system can utilize the different structures for the equalization task: the optimal MAP equalizer was used in [5], while linear and nonlinear equalizers were applied in [10], motivated as low-complexity alternative to the MAP equalizer. In [6], we presented a low-complexity turbo equalizer based on FB-FDE. In this paper, we study another equalization/decoding scheme which employs a block interleaver. The differences compared to the turbo scheme are also discussed.

III-A. Block interleaver

The basic idea of the block interleaver used in coded DFE system has been presented in [11], where the interleaver/de-interleaver were designed according to some special algorithms. And this results in long processing delay by the interleaver/de-interleaver operation. In this paper, we use the common block interleaver [4] to re-arrange the order of the transmitted symbols, so that the decoding decisions of the previous block can be used to predict the noise components of the next block of symbols. Furthermore, this scheme can be realized efficiently and it does not introduce additional delays by the interleaver/de-interleaver operation.

Block interleaving is an example of periodic interleaving, which introduces a fixed delay of D between original symbols, as illustrated in Figure 3. In our application, the value of D is equal to the length of code block. From its matrix representation, it is easy to find that after interleaving/de-interleaving, the first block of symbols, $\{x_m, m = 0, 1, 2, 3\}$, can be fed back to cancel ISI effects of other symbols on the same row. Another important function of block interleaver is that error bursts can be avoided and therefore the quality of feedback symbols can be improved.

It is visible from Figure 3 that the maximum number of possible feedback taps is equal to $P - 1$, so it is determined by the number of columns. This is in contrast to the turbo equalization, where the whole transmitted frame is first decoded and the possible feedback taps can be selected as high as $N_s - 1$, where N_s is the interleaver size. Even for one iteration of turbo equalization, each block has to be decoded twice before the final decision. While block DFE scheme is a successive decoding scheme, each block of symbols is decoded only once, and the previous blocks of symbols are used to combat the ISI effect of the next block. Then it naturally has a low-complexity property over the turbo scheme.

III-B. Noise prediction in block DFE

The feedback loop combining NP and decoding blocks is depicted in Figure 4. A soft-input-soft-output (SISO) decoder [12] is applied. Let's define a symbol block as a vector $\mathbf{x}^p = \{x_0^p, ..., x_{D-1}^p\}$, where $p = 1, ..., P$ denotes the block index. ISI mitigation of symbol $y_d^{p_2}$, $d = 0, ..., D-1$, would utilize the corresponding feedback symbols in previous blocks $\{\hat{x}_d^{p_1}, 1 \le p_1 < p_2 \le P\}$.

The procedure is illustrated below:

1) The received samples $\{\bar{r}_m, m = 0, ..., N_s - 1\}$ are equalized using linear FB-FDE introduced in Section II. After downsampling and de-interleaving, the signal $\{y_m\}$ is divided into a number of blocks, $\{\mathbf{y}^p, p = 1, ..., P\}$, which are fed to the equalization/decoding loop in the block order.
2) For first block, $\hat{\mathbf{y}}^1 = \mathbf{y}^1$ due to absence of feedback information. The symbol demapper generates a block of bit-wise LLRs $\{L^E(c_i), i = 0, ..., Q \times (D-1)\}$ based on the block $\hat{\mathbf{y}}^p$, where Q is the number bits per symbol. For QPSK modulation, the LLR values of coded bits can be obtained as:
$$L^E(b_{2m}) = \text{Re}\{\hat{y}_m^p\}, \quad L^E(b_{2m+1}) = \text{Im}\{\hat{y}_m^p\}. \quad (4)$$
3) Based on $\{L^E(b_i)\}$, the SISO decoder produces a block of soft LLR information $\{L^D(b_i)\}$, as well as a block of final hard decisions of the transmitted bits. The block of LLR values will be further fed to the symbol mapper.
4) From the knowledge of $\{L^D(b_i)\}$, the symbol mapper can generate a block of estimated symbols $\hat{\mathbf{x}}^p$. In the case of QPSK modulation, the mapping can be done by
$$\hat{x}_m^p = \frac{e^{L^D(b_{2m})} - 1}{e^{L^D(b_{2m})} + 1} + j\frac{e^{L^D(b_{2m+1})} - 1}{e^{L^D(b_{2m+1})} + 1}. \quad (5)$$

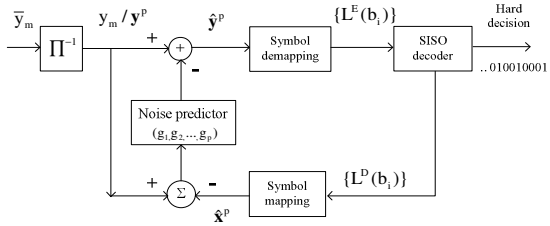

Fig. 4. Block DFE with noise prediction and SISO decoder.

5) The reliable block $\hat{\mathbf{x}}^p$ is then fed back to cancel ISI effect on the next block $\hat{\mathbf{y}}^{p+1}$, which can be updated as $\hat{y}_d^{p+1} = y_d^{p+1} - \sum_{l=1}^{p} g_l(y_d^p - \hat{x}_d^p), d = 0, ..., D-1$.
6) Repeat from step 2 until the last block, P.

The number of feedback grows with the number of processed blocks p. The NP coefficients $\{g_p, p = 1, 2, ..., P-1\}$ can be obtained by equations [3], [13]:

$$\sum_{p=1}^{P-1}\sum_{k=0}^{M-1} g_p \frac{\sigma_n^2 e^{j\frac{2\pi}{M}k(l-p)}}{|\hat{C}_k|^2\sigma_x^2 + \sigma_n^2} = \sum_{k=0}^{M-1} \frac{\sigma_n^2 e^{j\frac{2\pi}{M}kl}}{|\hat{C}_k|^2\sigma_x^2 + \sigma_n^2}$$
$$l = 1, 2, ...P-1,$$

The symbol mapper/demapper for higher order modulation can be found in [14]. In the basic scheme, the first block of symbols can only be linear equalized and the subsequent blocks use the decision feedbacks with increasing order. The straightforward way to improve the symbol decisions and reduce the error propagation is the utilization of known reference symbols in the first block. It will be shown in Section IV that a significant performance gain can be achieved, while the price of reference block would be some reduction of data rate and spectral efficiency.

IV. NUMERICAL RESULTS

In this section, we study the performance of a single-carrier data transmission systems with linear modulation in fading multipath wireless channels. The basic system model is shown in Figure 1. The signal bandwidth is 18.74 MHz. The transmit and receiver filters are real-valued RRC filters with roll-off of $\alpha = 0.22$. The EMFB designs in the model use roll-off $\rho = 1.0$, overlapping factor of $K = 5$ and $2M = 256$ subbands. The performance was tested using the extended Vehicular A channel model of ITU-R with the maximum excess delay of about 2.5 μs [15]. We assumed the channel to be time-invariant during each frame transmission and 5000 random channel instances were used to estimated the performance. The MSE criterion was applied in both the linear and feedback equalizer design.

Each frame contains 3840 symbols, which includes 384 training symbols for channel estimation and $N_s = 3456$ data symbols. The CP commonly used in the FFT-FDE system is not included [7]. LDPC with code rate of $R = 2/3$ was used. The length of the block code D in this paper is 576 bits, corresponding to 288/144 symbols for QPSK/16-QAM. It allows the maximum number of NP, $B = 12/24$, for QPSK/16-QAM. Here we only consider $B = \{1, 5\}$ because it has been shown in [6] that DFE with $B = 5$ can achieve most of the available performance gain. The frame error rate (FER) and bit error rate (BER) performance are measured.

IV-A. Performance of the LDPC coded block-DFE

Figures 5(a) and 5(b) demonstrate significant performance improvement over LE with 5 feedback taps for both QPSK and 16-QAM modulations. For the FER of 10^{-1}, there is over 0.5 dB benefit for QPSK and over 1 dB for 16-QAM in the case of $B = 5$ without reference symbols. The use of known reference symbols in the first code block gives also a clear further improvement, with the cost of about 8% or 5% reduction in user data rate for QPSK and 16-QAM, respectively.

IV-B. Performance comparison of the block DFE with the turbo DFE

Figure 5(c) shows the performance comparison for 16-QAM modulation between block DFE with reference symbols and turbo DFE when the same moderate length of block code ($D = 576$ in bits) is applied. Both DFEs use one tap or maximum 5 feedback taps for ISI mitigation. It is shown that the block DFE achieves almost the same FER performance as the turbo DFE with one iteration, whereas it is worse than turbo DFE with two or more iterations. It is also visible that the block DFE has a clearly better BER performance. This is due to the following facts: (1) Block DFE has the known symbols in the first block, which helps to correctly estimate the subsequent symbols. (2) Error propagation caused by wrong decisions in turbo DFE is more severe than in block DFE, because the number of symbols which use the maximum number of feedback taps in turbo DFE is much larger than in block DFE.

V. CONCLUSION

This paper has studied a hybrid frequency-time domain equalization structure in coded single-carrier modulation, which utilizes filter bank frequency-domain equalizer and noise prediction as feedforward and feedback filters, respectively. A block interleaver/de-interleaver was applied so that the previous reliable decisions can be used for ISI cancelation. The simulation results show that this interleaved DFE scheme with five feedback taps, along with first reference block insertion, can achieve a significant performance improvement over linear equalizer in time dispersive multipath wireless channels. Moreover, this block DFE achieves a similar performance as the turbo DFE with one iteration, while it has clearly lower complexity.

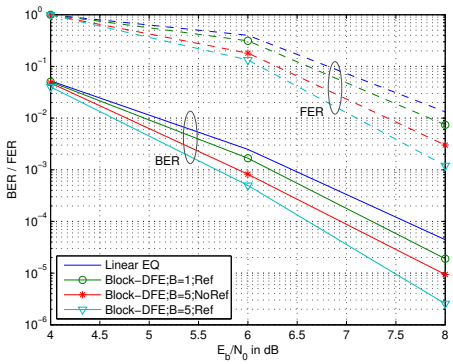

(a) Performance with QPSK modulation

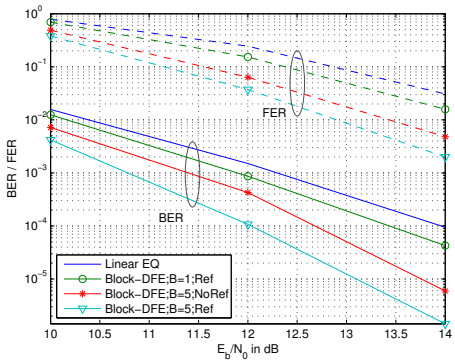

(b) Performance with 16-QAM modulation

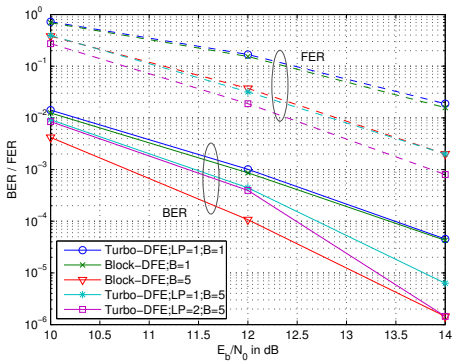

(c) Performance comparison for 16-QAM between block DFE with known reference symbols and turbo DFE with the number of iterations LP=1,2;

Fig. 5. Block DFE performance with LDPC code rate $R = 2/3$ and code length block length in bits $D = 576$; the number of feedback taps $B = 1$ or 5;

The drawback of block DFE is that significantly higher code block lengths are not feasible. This is because, if the code block length is increased while keeping the interleaver block size fixed, the performance is degraded due to reduced average number of feedback taps. Also the overhead due to reference symbols grows with the code block length. On the other hand, the interleaver depth cannot be increased significantly in wireless communication systems with moderate or high mobility.

ACKNOWLEDGMENT

This research work was supported by Nokia. The authors would like to acknowledge Mika Rinne from Nokia Research Center for the constructive comments during the work.

VI. REFERENCES

[1] D. Falconer, S. L. Ariyavisitakul, A. Benyamin-Seeyar, and B. Eidson, "Frequency domain equalization for single-carrier broadband wireless systems," *IEEE Communications Magazine*, vol. 40, no. 4, pp. 58–66, Apr. 2002.

[2] M. V. Clark, "Adaptive frequency-domain equalization and diversity combining for broadband wireless communications," *IEEE Journal on Selected Areas in Communications*, vol. 16, no. 8, pp. 1385–1395, Oct. 1998.

[3] C. A. Belfiore and J. H. Park, "Decision feedback equalization," *Proc. IEEE*, vol. 67, pp. 1143–1156, Aug. 1979.

[4] John G. Proakis, *Digital Communications, 4th Ed.*, McGraw-Hill, 2001.

[5] C. Douillard, M. Jezequel, and C. Berrou, "Iterative correction of intersymbol interference: Turbo–equalization," *European Transactions on Telecommunications*, vol. 6, pp. 507–511, Sept. 1995.

[6] Y. Yang, M. Rinne, and M. Renfors, "Noise predictive turbo equalization for a filter bank based receiver in a sc transmission system," accepted to *2007 IEEE 65th Vehicular Technology Conference, VTC2007-Spring*, Apr. 2007.

[7] Y. Yang, T. Ihalainen, M. Rinne, and M. Renfors, "Frequency-domain equalization in single-carrier transmission: Filter bank approach," *EURASIP Journal on Advances in Signal Processing*, vol. 2007, pp. Article ID 10438, 16 pages, 2007, doi:10.1155/2007/10438.

[8] R. G. Gallager, *Low Density Parity Check Codes*, Cambridge, MIT Press, 1963.

[9] A. Viholainen, T. Ihalainen, T. Hidalgo Stitz, Y. Yang, and M. Renfors, "Flexible filter bank dimensioning for multicarrier modulation and frequency domain equalization," in *Proc. 2006 IEEE Asia Pacific Conference on Circuits and Systems*, Singapore, Dec. 2006, pp. 451–454.

[10] M. Tuchler, R. Koetter, and A. Singer, "Turbo equalization: Principles and new results," *IEEE Transactions on Communications*, vol. 50, pp. 754–767, May 2002.

[11] M. Vedat Eyuboglu, "Detection of coded mudulation signals on linear, severely distorted channels using decision feedback noise prediction with interleaving," *IEEE Transactions on Communications*, vol. 36, pp. 401–409, Apr. 1988.

[12] L. R. Bahl, J. Cocke, F. Jelinek, and J. Raviv, "Optimal decoding of linear codes for minimizing symbol error rate," vol. IT-20, pp. 284–287, Mar. 1974.

[13] Y. Yang, M. Rinne, and Markku Renfors, "Filter bank based frequency-domain equalization with noise prediction," in *Proc. 17th Annual IEEE international symposium on personal, indoor and mobile radio communications*, Helsinki, Finland, Sept. 2006.

[14] C. Laot, A. Glavieux, and J. Labat, "Turbo equalization: adaptive equalization and channel decoding jointly optimized," vol. 19, pp. 1744–1752, Sept. 2001.

[15] T. B. Sorensen, P. E. Mogensen, and F. Frederiksen, "Extension of the ITU channel models for wideband OFDM systems," in *Proc. IEEE Vehicular Technology Conf.*, Dallas, USA, Sept. 2005.

Publication P5

Y. Yang, T. H. Stitz, M. Rinne and M. Renfors, "Mitigation of narrowband interference in single carrier transmission with filter bank equalization," in *Proc. IEEE Asia Pacific Conference on Circuits and Systems*, APCCAS'06, Singapore, December, 2006, pp. 748–751.

Mitigation of Narrowband Interference in SC Transmission with Filter Bank Equalization

Yuan Yang*, Tobias Hidalgo Stitz*, Mika Rinne†and Markku Renfors*
*Institute of Communications Engineering, Tampere University of Technology
P. O. Box 553, FIN-33101 Tampere, Finland
Email: {yang.yuan; tobias.hidalgo; markku.renfors}@tut.fi
†Nokia Research Center
P. O. Box 407, FIN-00045 Helsinki, Finland
Email: mika.p.rinne@nokia.com

***Abstract*— Filter bank based frequency domain equalization provides an attractive scheme for single-carrier transmission of broadband wireless communications. With mildly frequency-selective subband processing and a modest number of subbands, it is able to provide better performance than conventional FFT approach with a higher number of subbands. Another benefit of this approach is that the same filter bank can be utilized to implement a significant part of the baseband channel selection filtering task. This paper proposes a technique for tuning the filter bank equalizer to mitigate narrowband interference without additional complexity. Simulation results show that the proposed scheme is effective and can provide better performance than the basic complete subband elimination approach when moderate interference is present.**

***Keywords*—frequency-domain equalization, filter bank, narrowband interference, broadband wireless communications**

I. Introduction

Future wireless communications are targeting at increasingly high data rates to satisfy the demands for broader content delivery with improved quality. The use scenarios also include increasingly fast mobile velocities. The efficiency can be improved by optimally utilizing the available spectrum for transmission and by reducing the complexity of the signal processing tasks. Multirate signal processing has shown to provide very good solutions in this sense. Multicarrier (MC) transmission schemes have many advantageous properties. Among them we count flexible and efficient spectral use, robustness in case of frequency selective channels, offering the possibility of simple equalization, simple time synchronization, as well as insensitivity to narrowband interference (NBI). NBI is a distorting signal that may be present in a number of scenarios. For example, in ultra-wideband (UWB) systems the reason can be overlaid spectrum, i.e., a narrowband signal using the same frequencies as part of the UWB communication. Other sources may be spurious emissions due to own or nearby transceiver, or even intentional jamming.

Single-carrier frequency domain equalization (SC-FDE) may be derived from a MC transceiver by shifting the synthesis part from the transmitter to the receiver, thereby moving

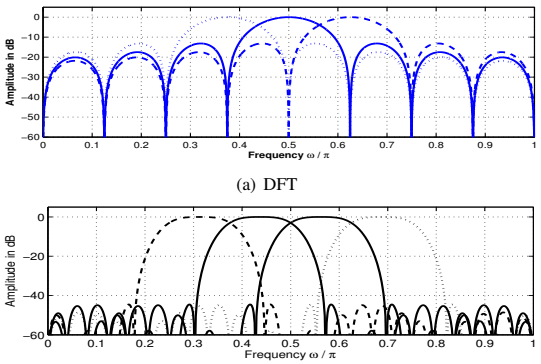

(a) DFT

(b) EMFB

Fig. 1. Comparison of the subband frequency responses of DFT and EMFB.

complexity to the receiver while maintaining many advantages of MC communications. Several SC-FDE schemes have been proposed, some based on FFT [1] and some based on filter banks (FBs) [2]. We follow the latter approach because the advantage of FBs makes them a suitable candidate for highly spectral efficient communications. Fig. 1 illustrates this advantage compared to a DFT based subband transform. It is clear that the DFT filter bank has a larger degree of spectral overlapping, which can lead to severe distortion and spectral leakage in case of NBI. Further, in [2] it has been demonstrated that FB-FDE with a modest number of subbands and subband-wise amplitude and phase equalization approach (referred as AP-FBEQ) can outperform FFT-FDE with a high number of subbands, in which the equalizer is a simple complex coefficient. On the other hand, in [3] and [4], it has been shown that FBs are well suited for combating NBI, overcoming the limitations of FFT-based NBI mitigation.

The paper is structured as follows: Section II briefly introduces the considered single-carrier FB-FDE and the subband-wise amplitude and phase equalization approach. Section III illustrates how the AP-FBEQ can be tuned to

1–4244–0387–1/06/$20.00

mitigate NBI. Section IV presents our simulation setup and results, and Section V draws the conclusions.

II. Single-carrier FB-FDE model

In this paper we consider a synchronous, linearly modulated, single-carrier transmission system operating over linear band-limited channels with additive white Gaussian noise (AWGN). The block diagram of a communication link with FB-FDE is shown in Fig. 2. EMFBs with perfect reconstruction are utilized to transform the signal between frequency and time domains [2], [5]. At the receiver, a 2x-oversampled analysis FB is applied, which splits and decimates the received baseband equivalent complex I/Q signal into $2M$ complex low-rate subband signals, equally spaced between 0 and 2π. Equalization takes place subband-wise. The real part of the equalized subband signals is fed to the critical sampled synthesis FB and transformed to a complex time-domain signal.

The advantage of using the 2x-oversampled analysis FB is that the channel equalization can be done within each subband independently of the other subbands [2]. Assuming roll-off $\rho = 1.0$ in the EMFB design, the complex subband signals of the analysis bank are essentially alias-free. This is because the aliasing signal components are attenuated by the stopband. Subband-wise equalization compensates the channel frequency response over the whole subband bandwidth, including the passband and transition bands. After this, the real parts of the equalizer outputs are sufficient for synthesizing the time-domain equalized signal, using a critically sampled synthesis filter bank.

Subband equalizer: AP-FBEQ

The AP-FBEQ from Fig. 2 is a fractionally-spaced equalizer [2], which is robust to sampling phase offsets. In addition, the receiver root raised cosine (RRC) filtering can be implemented efficiently by the equalizer, without introducing additional complexity. When assuming that the channel frequency response H^l_{ch} and RRC frequency response H^l_{RRC} are perfectly known, the optimum MSE linear equalizer responses can be written as [1]

$$W_l = \frac{C^*_l}{|C_l|^2 + \sigma^2}. \tag{1}$$

where σ^2 represents the noise to signal ratio, $C_l = H^l_{ch} H^l_{RRC}$ is the combined response of channel and RRC filter. The frequency index $l = 0, 1, ..., 4M-1$ covers the entire spectrum $[0, 2\pi]$ as $H^l_x = H_x(e^{j\omega})$ at $\omega = 2\pi l/4M$. We concentrate on an AP-FBEQ Case 3 as defined in [2]: each subband equalizer is determined by the channel frequency responses at three frequencies, one at the subband center frequency, the other two at the subband edges. For the $2M$ subbands, there are $4M$ frequency points. For notational convenience, we define the target frequency responses in terms of the subband index $k = 0, 1, ..2M-1$, instead of frequency point l. The amplitude and phase response target values for subband k are denoted as ϵ_{ik} and ς_{ik}, respectively,

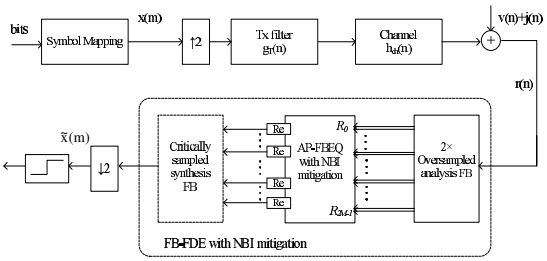

Fig. 2. Filter bank based frequency domain equalizer

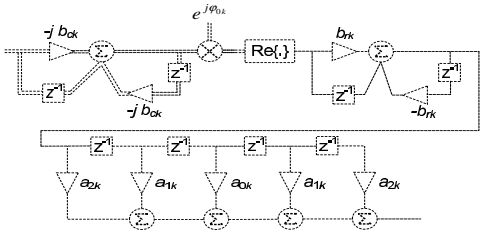

Fig. 3. Subband equalizer structure for AP-FBEQ Case 3.

with $i \in \{0,\ 1,\ 2\}$. Here indexes $0,\ 1,\ 2$ correspond to the subband lower edge, center, and upper edge, respectively. These are defined as

$$\epsilon_{ik} = |W_{2k+i}| \qquad \varsigma_{ik} = \arg(W_{2k+i}). \tag{2}$$

The proposed NBI mitigation scheme is based on this AP-FBEQ with three target frequencies per subband and tuning these target amplitude responses.

The AP-FBEQ Case 3 realization, shown in Fig. 3, includes a first-order complex allpass section and a first order real allpass section in the phase equalizer together with the phase rotator, and a 5-tap linear-phase FIR filter as the amplitude equalizer. The equalizer amplitude and phase responses for the kth subband can then be written as [2]

$$\begin{aligned} \left|H_k(e^{j\omega})\right| &= |a_{0k} + 2a_{1k}\cos\omega + 2a_{2k}\cos 2\omega| \\ \arg[H_k(e^{j\omega})] &= \varphi_k + 2\arctan(\frac{-b_{ck}\cos\omega}{1+b_{ck}\sin\omega}) \\ &\quad +2\arctan(\frac{b_{rk}\cos\omega}{1+b_{rk}\sin\omega}), \end{aligned} \tag{3}$$

where a_{0k}, a_{1k}, a_{2k} are the symmetric 5-tap FIR coefficients, and $\varphi_k, b_{ck}, b_{rk}$ are the phase equalizer coefficients. They can be derived from the target response values ϵ_{ik} and ς_{ik} as follows:

$$\begin{aligned} \varphi_k &= \tfrac{\zeta_{0k}+\zeta_{2k}}{2} & a_{0k} &= \tfrac{\epsilon_{0k}+2\epsilon_{1k}+\epsilon_{2k}}{4} \\ b_{ck} &= \pm\tan(\tfrac{\zeta_{2k}-\zeta_{0k}}{4}) & a_{1k} &= \pm(\tfrac{\epsilon_{0k}-\epsilon_{2k}}{4}) \\ b_{rk} &= \pm\tan(\tfrac{\zeta_{1k}-\zeta_{0k}}{2}) & a_{2k} &= \pm(\tfrac{\epsilon_{0k}-2\epsilon_{1k}+\epsilon_{2k}}{8}). \end{aligned} \tag{4}$$

Here the + signs stand for odd subbands and - signs for even subbands.

III. Narrowband interference mitigation

In this paper, the NBI is characterized as a single tone. In the presence of NBI, the received signal in frequency domain can be written as

$$R_k = X_k + V_k + J_k, \tag{5}$$

and it consists of the desired subband signal X_k, the noise term V_k and the NBI J_k. In absence of NBI, the target MSE equalizer responses are obtained from (1). When NBI appears in the signal band, the equalization can be tuned to mitigate the NBI by slightly modifying equation (1)

$$\hat{W}_l = \frac{C_l^*}{|C_l|^2 + \sigma^2 + \eta_l^2}, \tag{6}$$

where η_l^2 is the estimated NBI power at the target frequencies.

In the AP-FBEQ [2], each subband equalizer response ϵ_{ik}, $i \in \{0,\ 1,\ 2\}$ can be designed to cope with the NBI power within the subband. Fig. 4 illustrates an example case where the channel response is assumed to be flat and NBI is located exactly at the edge frequency f_{2k+2} between two subbands R_k and R_{k+1}. Both subband signals would be badly distorted by the NBI. The AP-FBEQ Case 3 can attenuate the frequency f_{2k+2} while maintaining the frequency contents of f_{2k+1} and f_{2k+3}. This is in contrast to complete subband elimination, where some NBI-free frequency components would be also removed. Next we address a novel method to estimate the NBI power and its frequency location within a subband.

NBI estimation

In order to apply equation (6), it is necessary to obtain an estimate of the interferer power and its frequency. This could be done during estimation of the training sequence or even simultaneously with the data reception. In this paper we propose a method where the NBI power and its frequency is obtained by calculating the difference between the measured and the expected subband power.

A good estimate of the expected subband signal power is obtained from the channel magnitude estimates. Taking into account that each subband contains three estimation points in the AP-FBEQ Case 3, we can write

$$\hat{P}_k = \frac{|C_{0k}|^2 + 2|C_{1k}|^2 + |C_{2k}|^2}{4} + \sigma^2. \tag{7}$$

Here three combined responses C_l from equation (1) within one subband are applied, but with the subband index notation used in equation (2).

The measured kth subband power is denoted as P_k. If the difference power $\Delta_k = P_k - \mu\hat{P}_k$ surpasses zero (μ is the threshold factor), then we can declare the subband signal to be contaminated by an interferer. Assuming only one NBI, the sum of the contaminated subbands, $\sum \Delta_k$, is the estimate of NBI power η^2. As seen in equation (6), η_l^2 acts as an attenuation factor on the different frequencies. The main purpose is to impose most attenuation on the frequency close to the NBI, while attenuating other frequencies as little as possible. Next an estimate of NBI frequency location is presented.

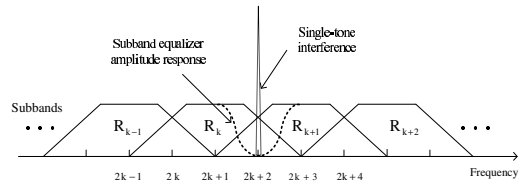

Fig. 4. Single-tone interference and equalized subband responses

Since only one or two subband signals would be significantly distorted by a single-tone interferer, the ratio of two consecutive estimated NBI powers $G_k = \Delta_k/\Delta_{k+1}$ can be used to perform a rough estimate of the position of single-tone interferer within the subband. For example, $G >> 1$ indicates that the interferer is close to the center of subband k, and $G \approx 1$ hints that an NBI is located at the edge between subbands k and $k+1$. Our current simulation model includes estimation of three different frequency location within a subband, namely: center, edge and halfway between center and edge. However, it should be noted that an AP-FBEQ Case 3 would be capable of complete NBI suppression only at the subband center and edges, while it can only alleviate its effect at other frequencies, even though the intermediate frequency could be estimated successfully. In future studies, G could be used to define an equalization point to be notched out. However, this would increase the complexity of the AP-FBEQ coefficient calculation, compared to equation (4).

For AP-FBEQ Case 3 NBI scheme, it would be sufficient to tune up to 5 consecutive target frequencies as a single-tone interferer would significantly affect two subband signals at most. As illustrated in Fig. 4, the heaviest attenuation is placed closest to the estimated interference and the adjacent attenuation factors would be decreased and determined by the NBI power leakage ratio G_k. In the case of an interferer located at halfway between the center and the edge of a subband, we notch out the two closest frequencies. The next section presents the performance when NBI appears at these three different locations within a subband, along with more generic cases with random-frequency interferer.

IV. Simulation results and analysis

The block diagram of a communication link with the FB-FDE is shown in Fig. 2. The pulse shaping filters at Tx and Rx are real-valued RRC filters with roll-off $\alpha = 0.22$. Three important design parameters of the EMFB are applied in the model: roll-off parameter ρ, overlapping factor K and the number of subbands $2M$. The choice of $\rho = 1.0$ means that only the neighboring subbands are overlapping with each other, and the overall subband bandwidth (passband and transition bands) is twice the subband spacing. In this paper, $K = 5$ determines the EMFB subfilter length, and results in 50 dB stopband attenuation. $2M = 256$ specifies

the total number of subbands in the region $[0, 2\pi]$. The transmitted signal occupies 32 subbands at the receiver, simulating a hypothetical user in a frequency-domain multiplex. One single-tone interference is assumed to appear within the transmitted bandwidth, at a fixed frequency location (Fig. 5(a)) or random frequency locations (Fig. 5(b)). The AP-FBEQ scheme with estimated NBI power and location, as discussed in Section IV, was applied for NBI mitigation with threshold factor $\mu = 1.1$.

The performance was estimated as a function of the signal to interference ratio (SIR) in a channel following the ITU-R Vehicular A model, using 4.685 MHz system bandwidth for 32 subbands. During each transmission block, we assumed the channel to be stationary and 1000 different channel realizations were used to obtain the average performance. The BER performance was evaluated for QPSK modulation with energy per source bit to noise ratio $E_b/N_0 = 9$ dB.

Fig. 5 illustrates the BER performance of two NBI mitigation schemes: the proposed AP-FBEQ based scheme and a basic scheme which directly suppresses the affected subbands completely. Two reference curves are used to evaluate the performance: One is the performance with no NBI in signal band and the other is the worst-case performance with no suppression imposed on an interferer present in the signal band. Fig. 5(a) shows that the AP-FBEQ scheme is capable of suppressing the NBI sufficiently at the subband edge and center frequencies. We can also see that it performs worst when the NBI is exactly in the middle of the center and edge frequencies, since we cannot locate a notch directly over the NBI. Further, at around 10 dB signal to interference ratio, the NBI detection approach fails to detect NBI located exactly at the edge between two subbands and therefore almost no gain is obtained since NBI is not suppressed.

Fig. 5(b) shows the case in which the interference is randomly changing its frequency position at each channel realization. For moderate NBI powers up to 0 dB SIR, the proposed AP-FBEQ coefficient tuning yields better performance than complete suppression of the affected subbands.

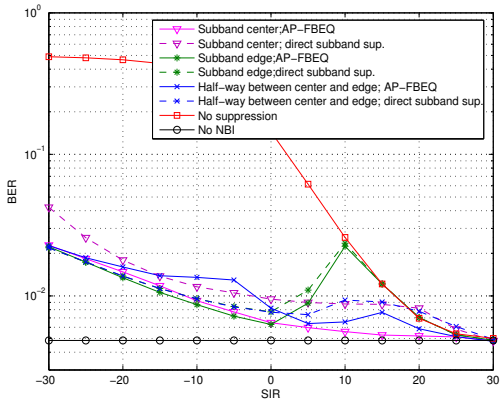

(a) Fixed interfering signal frequency

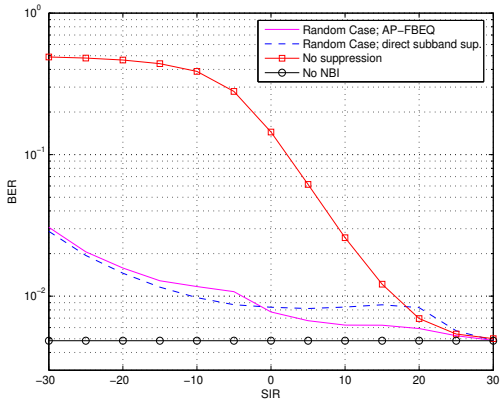

(b) Random interfering signal frequency

Fig. 5. The suppression method comparisons with frequency selective channel model; QPSK system; $E_b/N_0 = 9$ dB; AP-FBEQ with $2M = 256$ and $K = 5$; 32 subbands utilized

V. Conclusions

Filter bank based narrowband interference mitigation is very effective because of its ability to compactly represent the interfering signal energy in the transform domain. This paper has examined a narrowband interference mitigation scheme in an FB-FDE system that uses the AP-FBEQ Case 3 structure, which is slightly tuned with marginal additional complexity. The method is especially suitable in FDMA multi-user cases where the signal bandwidth allocated to a single user fits in a low or moderate number of subbands. The proposed approach always gives a clear gain compared to no suppression case. It is safe to use also in cases where the probability of NBI is low. In contrast, with low number of subbands, the complete subband elimination performs worse than no suppression for low NBI power. Based on the NBI power estimates, it would be best to switch to complete subband suppression when the SIR is below 0 dB.

References

[1] D. Falconer, S. L. Ariyavisitakul, A. Benyamin-Seeyar, and B. Eidson, "Frequency domain equalization for single-carrier broadband wireless systems," *IEEE Communications Magazine*, vol. 40, no. 4, pp. 58–66, Apr. 2002.

[2] Y. Yang, T. Ihalainen, M. Rinne, and M. Renfors, "Frequency domain equalization in single carrier transmission: Filter bank approach," submitted to *EURASIP Journal of Applied Signal Processing*, Jan. 2006.

[3] S. Hara, T. Matsuda, K. Ishikura, and N. Morinaga, "Co-existence problem of TDMA and DS-CDMA systems-application of complex multirate filter bank," in *Proc. of IEEE Globecom'06*, vol. 2, London, UK, Nov. 1996, pp. 1281–1285.

[4] T. H. Stitz and M. Renfors, "Filter-bank-based narrowband interference detection and suppression in spread spectrum systems," *EURASIP Journal on Applied Signal Processing*, vol. 2004, no. 8, pp. 1163–1176, 2004.

[5] A. Viholainen, J. Alhava, and M. Renfors, "Efficient implementation of complex modulated filter banks using cosine and sine modulated filter banks," *EURASIP Journal on Applied Signal Processing*, vol. 2006, pp. Article ID 58 564, 10 pages, 2006.

Publication P6

Y. Yang, T. Ihalainen, J. Alhava and M. Renfors, "DSP Implementation of Low-Complexity Equalizer for Multicarrier Systems," in *Proc. 7th International Symposium on Signal Processing and Its Applications,* ISSPA'03, Paris, France, July 2003, vol. 2, pp. 271-274

DSP IMPLEMENTATION OF LOW-COMPLEXITY EQUALIZER FOR MULTICARRIER SYSTEMS

Yuan Yang, Tero Ihalainen, Juuso Alhava, Markku Renfors

Institute of Communications Engineering, Tampere University of Technology
P. O. Box 553, FIN-33101, Tampere, Finland
{yuan.yang; tero.j.ihalainen; juuso.alhava; markku.renfors}@tut.fi

ABSTRACT

Efficient complex perfect reconstruction filter bank structures based on cosine and sine modulated filter bank sections have recently been introduced. In the transmultiplexer configuration, these filter banks can be used as a basis when developing filter bank based multicarrier systems for wireless communications. Also a simple channel equalization concept for such systems has been proposed recently. This so-called ASCET structure uses an oversampled analysis bank in receiver end to be able to do the equalization in per-carrier way. In this paper we explore the possibilities of implementing the receiver bank and equalizer sections with a digital signal processor (DSP), using the TMS320C5510 as the platform. Both single-processor and two-processor designs are considered. With realistic filter bank parameters, about 1 MHz and 2 MHz sampling rates are possible in the two cases, respectively

1 INTRODUCTION

Multicarrier techniques are gaining increasing importance as they are being applied in more and more existing and emerging communication systems, like ADSL/VDSL, DVB-T, WLAN [1]. They can reach high efficiency in frequency selective channels with simple equalization methods. Other advantages include robust timing synchronization and insensitivity to limited narrowband interference. Orthogonal frequency division multiplexing (OFDM) is the most prominent one among the different kinds of MC techniques.

Filter bank based multicarrier (FBMC) systems have a number of benefits over OFDM. Firstly, the bank selectivity is a design parameter for precise spectrum control. This provides resistance against narrowband interference and allows the use of very narrow guard bands around the multicarrier signal. Secondly, the guard period applied in OFDM systems to combat ISI becomes unnecessary. This saves some bandwidth for data transmission. Furthermore, FBMC approach allows the use of considerably lower number of subcarriers than OFDM techniques, which helps to reduce the problems in OFDM due to high peak-to-average power ratio [2]. However, efficient channel equalizer techniques for FBMC systems are still under research. Recently we presented a complex modulated critically sampled filter bank based on cosine- and sine-modulated filter banks sections [4]. It is used here as a transmultiplexer, together with a low complexity equalizer called 0^{th}-order ASCET to compensate the channel distortion [3][5].

In this paper, we explore the DSP implementation of 0^{th}-order ASCET on Texas Instrument DSP platform TMS320C5510, which is fixed-pointed 16-bit DSP with 200 *MHz* clock rate. Section II describes the ASCET structure, and briefly addresses the cosine- and sine-modulated filter banks, as well as the simple equalizer. Its DSP implementation requirements and considerations are explained in Section III. ASCET performance in the processor implementation and conclusions are present in Sections IV and V, respectively.

2 TRANSMULTIPLEXER STRUCTURE

The structure shown in Fig. 1 is the 0^{th}-order ASCET.

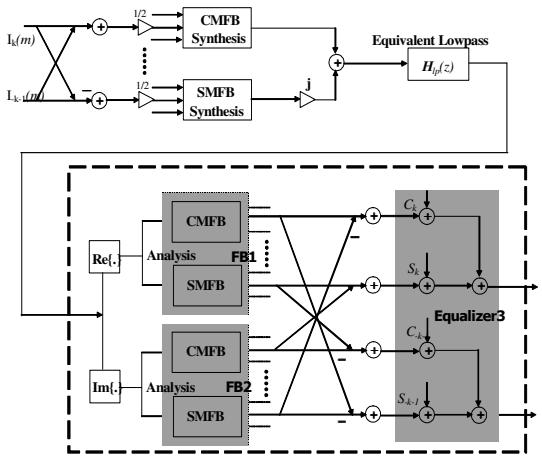

Figure 1. The 0^{th}-order ASCET equalizer structure in complex FBMC system.

The synthesis filter bank is used to combine 2*M* real low-rate signals into a single complex high-rate signal. In the receiver end, analysis filter bank separates the subchannels signals. The synthesis and analysis filter banks should satisfy the perfect reconstruction (PR) condition [6] which guarantees error-free transmission of the subchannel signals in case of an ideal channel. In this paper, the focus is on examining the DSP implementation of the receiver end of a complex ASCET system, shown as the dashed block in the figure. It consists of sine- and cosine-modulated filter bank blocks and a simple equalizer.

2.1 Sine/Cosine-Modulated Filter Banks

The subchannel filters (both the analysis and synthesis filters) are derived from a prototype filter by complex modulation, which can be implemented using cosine-and sine-modulated filter bank sections. Cosine-modulation translates the frequency response of a prototype filter into new center frequency. By modulating a real lowpass prototype filter $h_p(n)$ with a cosine sequence, the synthesis filter can be written as

$$f_k^{\cos} = h_p(n)\sqrt{\frac{2}{M}}\cos\left[\left(n+\frac{M+1}{2}\right)\left(k+\frac{1}{2}\right)\frac{\pi}{M}\right] \qquad (1)$$

where $n = 0,1,.....N-1$ and $k = 0, 1,..., M-1$.

The analysis filter bank consists of time-reversed versions of these filters. Furthermore, the analysis bank is implemented in a 2-times oversampled form by taking the complex subchannel signals (instead of real parts of those that would be enough in the critically sampled case [4]). The use of oversampled subchannel signals allows to do the channel equalization independently for each subchannel. On the other hands, it increases the complexity as two CMFB and SMFB blocks are needed in the receiver.

It is assumed that $N=2KM$ is an even integer multiple of M. K is the overlapping factor of the transform and can be used as a design parameter as it effects on how much stopband attenuation we can achieve. In the following, we consider the cases with 100% roll-off and K = 3 or 4, giving 40 … 50 dB stopband attenuation.

The synthesis and analysis sine-modulated filter banks are also obtained in the same manner as CMFB, only sine-modulation is used instead of cosine-modulation. The k-th synthesis sine-modulated filter is

$$f_k^{\sin} = h_p(n)\sqrt{\frac{2}{M}}\sin\left[\left(n+\frac{M+1}{2}\right)\left(k+\frac{1}{2}\right)\frac{\pi}{M}\right]. \qquad (2)$$

CMFBs have efficient implementation structures based on the extended lapped transform (ELT) [6]. The basic idea behind a fast ELT algorithm is to implement the polyphase component matrix as a cascade of two kinds of matrices, zero-delay orthogonal factor and pure delays [6][7]. The structure for the fast ELT is shown in Fig 2. The basic factor of fast ELT structure are the symmetrical butterfly matrices D_k, which are defined by

$$D_k \equiv \begin{pmatrix} -C_k & S_k J \\ J S_k & J C_k J \end{pmatrix} \qquad (3)$$

where

$$C_k \equiv diag\{\cos\theta_{0k}, \cos\theta_{1k}, ... \cos\theta_{M/2-1,k}\}$$
$$S_k \equiv diag\{\sin\theta_{0k}, \sin\theta_{1k} .... \sin\theta_{M/2-1,k}\}$$

and $\boldsymbol{J}$ is the reversal matrix. After the butterfly matrices and the delays, the last factor of the ELT structure is a type-IV DCT operator.

Same kind of fast ELT structure with type-IV DST can also be applied to the sine-modulated filter bank.

2.2 Equalizer

In 0^{th}-order ASCET, single complex coefficient is applied to each complex subchannel, adjusting the amplitude and phase of each subchannel. As shown in Fig. 1, the outputs of each cosine/sine-modulated analysis subband filter pair are properly weighted by real coefficients c_k and s_k.. Optimal weights are related to the channel amplitude and phase responses within each particular subband. They can written in the following forms.

$$c_k \approx \frac{1}{A_{ch}(\omega_k)}\cos(\phi_{ch}(\omega_k)) \qquad (4)$$

$$s_k \approx \frac{1}{A_{ch}(\omega_k)}\sin(\phi_{ch}(\omega_k)) \qquad (5)$$

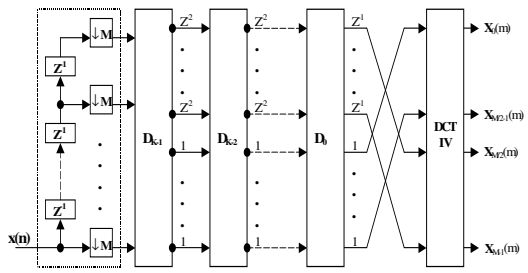

Figure 2. Implementation of analysis CMFB using ELT.

Higher order ASCETs are obtained by including low-order FIR filter stages for each of the subchannels. It would be a waste of resources, if higher order ASCET is used for low SNR subchannels. The 0^{th}-order ASCET performs fairly well in the range of SNR values that we expect to experience in practice in wireless communication systems [2].

3 DSP IMPLEMENTATION CONSIDERATION

The 0^{th}-order ASCET receiver end structure of Fig. 1 can be divided into three components: FB1, FB2 and Equalizer. FB1 and FB2 take the real and imaginary parts of the complex input sequence separately, and each FB includes CMFB and SMFB sections. Those two FBs have the same calculation complexity. We start with a single DSP implementation, and evaluate the basic system requirements to get a picture of calculation complexity of those three parts on DSP. The platform we selected to implement ASCET is TMS320C5510. Details of this DSP can be found in [8].

3.1 Memory

The C5510 device has a 160*k* words on-chip memory. There are two kind of internal memory, a Dual-Access RAM (DARAM) of 4*8*k* words, and a Single-Access (SARAM) of 16*8*k* words [8]. DARAM allows two read, or two write, or one read and one write operation in single cycle. SARAM allows one read or one write. To maximize the speed, all the constant tables and intermediate data are allocated in the DARAM if possible.

Managing efficiently all the data stored in the internal memory is the best way to speed up the processing. It is easy to find out that the number of subchannel, *M*, and the overlapping factor, *K,* have impact on data memory requirements. The bigger *K* and *M* are, the more data memory required.

Constants

All the coefficients have 12 bit word length, except that the FFT twiddle factors are 16 bit signed integers. They are stored in the same DARAM without any memory conflicts. If there is not enough DARAM, separate SARAM blocks are used.

Stack

Space for all locally declared objects are allocated in stacks. There are two software stacks on the C5510, data stack and system stack. Data in the stack is often accessed during the time when a function call/return occurs. To avoid memory conflicts, also potentially reduce the execution time, both stacks have to be located in the same DARAM or separate SARAMs. Setting the stack size as 8192 words is enough for our cases.

Table 1 shows the analysis of memory requirements for different cases. When *M* is larger than 512, the minimum required memory is larger than 32*k* words, which cannot allocated in the DARAM bank, and SARAM will be used, which will slow down the processing somewhat.

Table 1. Data Memory Requirements (in words)

	M=128	M=256	M=512	M=1024
K=3	14976	21504	33792	56320
K=4	15360	23040	36864	59392
K=5	16896	24576	39936	70656

3.2 Input and Output

Fig. 3 shows the basic data flow on the DSP. The incoming data sequences are acquired by the serial port. Data transfer from the serial port to the specific memory address can be accomplished by DMA, which greatly relieves the DSP core involvement. As it will be indicated in the end of this paper, the incoming sampling frequency may be up to about 2 *MHz*, which means (it requires) at least 32 *MHz* serial ock rate. The C5510 DSP may have as high as 100 *MHz* serial clock rate, which is quite applicable for this acquisition. The DMA event is triggered by serial port receiver full condition. The whole processing can be synchronized to the incoming data stream by polling of the DMA status, so that DMA continues to acquire data during the algorithm processing.

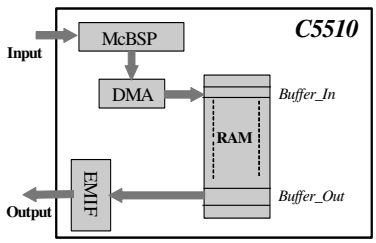

Figure 3. Single DSP implementation

4 PERFORMANCE EVALUATION

From the above section, we can assume that all the program code and data are allocated in the internal memory, and the input sampling is synchronized with signal processing. We build the algorithm in C language, compile the C code with option *–g –k -pm –o3* [8], and run the code in the TI simulation tool CCS 2.0 environment. Table 2 shows the number of needed execution cycles for different cases, as well as the maximum possible sampling rates

$$R_{\max} = \frac{samples \times 10^{-3}}{cycles \times 5 \times 10^{-9}} \quad (kHz)$$

Table 2 Excution times and sampling rates for single DSP case.

Samples	*M*	*K*	*Cycles*	*Rate (kHz)*
128	64	4	27334	936.56
128	64	3	23938	1069.43
256	128	4	53820	951.32
256	128	3	47288	1082.73
512	256	4	107368	953.73
512	256	3	94564	1082.86
1024	512	4	216404	946.38
1024	512	3	191056	1071.94

When compare the computational complexity of the three parts FB1, FB2, and equalizer, it turns out that FB1 and FB2 consume almost all the calculation power, about 48 percent each, whereas the equalizer takes only about 4 percent. A simple way to increase the achievable rate is to split the algorithm into two DSPs, one processor (DSP1) performing FB1, and another (DSP2) running FB2 and equalizer. The simple two DSP system is shown in Fig. 4. The series port is used to receive two incoming sequences through the DMA channel. FIFO1 handles the data connection between the two DSPs. The maximum overall sampling rate depends on DSP2 processing. In parallel with signal processing, reading A/D converter and storing the samples in an acquisition buffer or sampling I/O ports may cause interrupt and bus collisions. These impacts, which may slightly increase the parallel processing execution time, will not be considered in our evaluation.

Based on the above discussion, the possible sampling rates for different cases are show in Table 3. It is clear that the two DSP implementation speeds up the sampling rates by almost two times. The 2 *MHz* sampling rate is achievable for all cases with overlapping factor $K = 3$.

Table 3. Execution times and sampling rates for two DSP case

Samples	*M*	*K*	*Cycles*	*Rate (kHz)*
128	64	4	13823	1851.99
128	64	3	12161	2105.09
256	128	4	27450	1865.21
256	128	3	24220	2113.96
512	256	4	54977	1862.60
512	256	3	48626	2105.87
1024	512	4	111046	1844.28
1024	512	3	98408	2081.13

5 CONCLUSION

The DSP implementation of an adaptive sine/cosine modulated equalizer for transmultiplexer was explored. About 1 MHz sampling rate is possible with a single DSP implementation, almost independently of the number of subchannels, and the speed can be almost doubled by using two processors.

6 REFERENCES

[1] R. van Nee and R. Prasad, *OFDM Wireless Multimedia Communications*. Artech House, London, 2000.

[2] T. Ihalainen, J. Alhava, A. Viholainen, X. Hongnian, J. Rinne, M. Renfors, "On the performance of filter bank based multicarrier systems in xDSL and WLAN applications," in Proc. Int Conf. On Communications, New Orleans, Louisiana, USA, pp. 1120-1124, June 18-22, 2000

[3] J. Alhava and M. Renfors, "Adaptive sine-modulated/cosine-modulated filter bank equalizer for transmultiplexiers," European Conf. On Circuit Theory and Design, Espoo, Finland, pp III/337-340, Aug 28-31, 2001

[4] A. Viholainen, T. Hidalgo S., J. Alhava, T. Ihalainen, M. Renfors, "Complex modulated critically sampled filter banks based cosine and sine modulation," IEEE International Symposium on Circuits and Systems, ISCAS 2002, Vol. 1, pp 833 –836, 2002

[5] A. Viholainen, T. Saramäki, and M. Renfors, "Cosine modulated filter bank design for VDSL modems," *IEEE Int. Workshop on Intelligent Signal Processing and Communications Systems*, Melbourne, Australia, pp. 143-147, Nov. 1998

[6] H. S. Malvar, "Extended lapped transform: properties, application, and fast algorithms". *IEEE Transaction on Signal processing*. Vol.40, No. 11, November 1992

[7] P. P. Vaidyanathan, Multirate Systems and Filter Banks, Prentice Hall, NJ, 1993

[8] Texas Instrument: http://www.ti.com

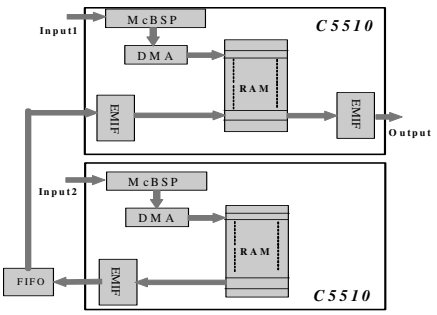

Figure 4. Two DSP implementation

Publication P7

Y. Yang, T. H. Stitz and M. Renfors, “Implementation of a Filter Bank based Narrowband Interference Suppression Algorithm on a DSP Processor,” in *Proc. International Conference on Telecommunications*, ICT’02, Beijing, China, June 2002, pp. 608-611.

Implementation of a Filter Bank Based Narrowband Interference Suppression Algorithm on a DSP Processor

Yuan Yang, Tobias Hidalgo Stitz, Markku Renfors

Institute of Communications Engineering
Tampere University of Technology
P.O. Box 553, FIN-33101, Tampere, Finland
e-mail: {yang, hidalgo, mr}@cs.tut.fi

ABSTRACT

High power narrow-band interferences, jammers, will degrade the performance in wideband Spread Spectrum Systems. To eliminate these effects, Filter bank based interference suppression method in a CDMA system is presented. In this paper, a modern VLIW programmable fixed-point digital signal processor (TMS320C6414) is used to implement the suppression algorithm.

1. INTRODUCTION

Code Division Multiple Access (CDMA) is a hot topic today because it is a core technology in many communication systems, like satellite systems (e.g. GPS), wireless local area networks (W-LAN), and the coming 3G mobile communication systems [1]. CDMA has several advantages, like low power spectral density, privacy of the communications and capability of coexistence with other communications sharing the spectrum.

The CDMA systems have an inherent immunity to narrowband interference, because of the spreading and despreading principle. But this immunity is only effective to a certain interference power, making it necessary to apply additional techniques to suppress the effect of strong narrowband interferences. Several interference suppression techniques have been proposed to process the signal in the time domain, in the transform domain, and in the spatial domain [2]. In the situations, in which the interfering environment changes quickly, time domain techniques are not suitable. In these cases, frequency domain techniques have better performance.

One good approach to frequency domain processing is based on filter bank as in Figure 1. The division of the incoming signal into *M* different frequency subbands is achieved by filtering it with parallel bandpass filters, which are centred at adjacent frequencies in such a way that the whole filter bank covers the entire bandwidth of the received signal [3]. The filters in the filter bank can be designed to fulfill the requirements of the application, e.g., filters with very low side lobes may be implemented. From there on, the signals can be processed independently. To remove the jammer, the signal energy of each subband can be computed to determine whether a jammer is present, and the further operations can be subsequently applied.

A filter bank based narrowband interference suppression method has been developed by our group. It uses cosine and sine modulated analysis-synthesis filter bank techniques [4][5]. The use of filter bank with a highly selective subband filter prototype, in combination with a newly developed excision algorithm [6], gives a clearly better performance than FFT-based reference systems. It also offers a solution with efficient implementation.

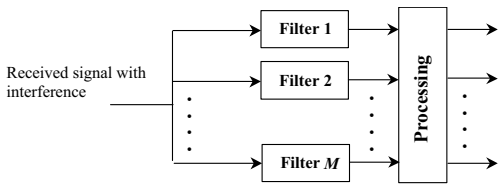

Figure 1. Filter Bank Processing

Within this paper, we will consider a moden Digital Signal Processor by Texas Instruments, TMS320C6414. The device is based on the second-generation high-performance, advanced VelociTI "Very-Long-Instruction-Word" (VLIW) architecture. With performance of up to 4800 million instructions per second (MIPS) at a clock rate of 600 MHz, the C6414 device offers cost-effective solutions to high-performance DSP applications. The C6414 also has a complete set of development tools which includes: a C compiler, an assembly optimizer, and a Windows debugger interface for visibility into source code execution. These tools make it simple to build algorithms on target DSP with high-level C programming language and simulate the performance in the software environment.

The rest of the paper is organized as follows: Section 2 introduces the basic structure of our filter bank based interference suppression method. Efficient

This work was carried out in the project "Digital and Analog Techniques in Flexible Receivers" funded by the National Technology Agency of Finland (Tekes).

implementation structure based on ELT will be described in Section 3. Requirements and the final performance on the DSP will be studied in Section 4. Conclusion is made in Section 5.

2. FILTER BANK BASED INTERFERENCE SUPPRESSION METHOD

The basic idea of narrowband interference removal in frequency domain is illustrated in Figure 2. The narrowband interference appears as a peak on the relatively flat wideband SS signal in the frequency domain. By the mean of a threshold, the peak value is detected, and either set to zero or equalized to the flat level.

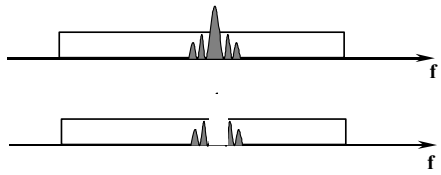

Figure 2 Removal of the narrowband jammer in a SS signal

Here we use the decimated analysis and synthesis filter banks for the frequency domain processing as shown in the Figure 3. The signal is first filtered by a set of analysis filters, obtaining the division into *2M* subchannels, and then interference detection and suppression algorithm is performed. After removing the interference, the subchannel signals are combined together for further processing. These analysis-synthesis filter banks are designed using the cosine modulation principle. A prototype filter with the desirable characteristics is modulated multiple times to get its frequency response uniformly shifted in the frequency domain. These shifted version are the subchannel filters, which build the subband systems. The impulse response of the *k-th* subchannel analysis filter is:

$$h_k(n) = P(n)e^{j(((2k-1)\frac{\pi}{2M}(n-1)-\frac{N-1}{2})+(-1)^{k-1}\frac{\pi}{4})}$$

and the impulse response of the *k-th* subchannel synthesis filter is:

$$f_k(n) = P(n)e^{j(((2k-1)\frac{\pi}{2M}(n-1)-\frac{N-1}{2})-(-1)^{k-1}\frac{\pi}{4})}$$

where *N=2KM*, *P(n)* is the prototype filter impulse response.

The prototype filter is designed in such a way that the analysis and synthesis filters are matched filter pairs and the filter bank provides perfect reconstruction of the signal after decimation and interpolation [7][8]. We have used different prototype filters designed for ELT implementation of cosine modulated filter banks with overlapping factors K = 3, 4, 5. With higher overlapping factors, the bank provides better stopband attenuation. However, the higher overlapping factor is used, the higher computing complexity becomes.

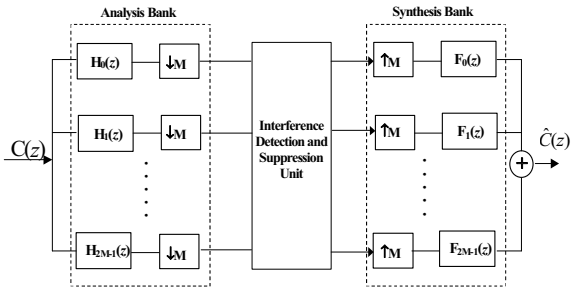

Figure 3. Analysis-Synthesis Filter Bank and Interference Rejection

3. EFFICIENT IMPLEMENTATION

The method chosen to implement the filter bank for narrowband interference detection and suppression on a single C6414 device is illustrated in the Figure 4. The input sequences are the in-phase and quadrature parts of the complex signal. The cosine and sine modulated filter banks and the bufferfly structures effectively allow to implementing a complex critically sampled perfect-recontruction filter bank [5]. The next step is the interference detection and suppression block, where the actual estimation of jammer localization on the frequency axis takes place.

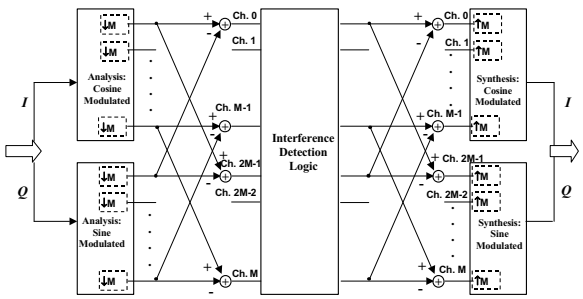

Figure 4. Realisation of the Complex Modulated Filter Bank Using Sine and Cosine Modulated Filter Bank

❑ Cosine Modulated and Sine Modulated Filter Bank Implementation

Cosine filter bank has efficient VLSI implementation based on the structure of ELT [9]. The basic idea behind a fast ELT algorithm is to implement the polyphase component matrix as a cascade of two kinds of matrices, zero-delay orthogonal factor and pure delays. The structure for the fast direct ELT is shown in Figure 5. The basic blocks of fast ELT structure are the symmetrical butterfly matrices D_k, which are defined by

$$D_k \equiv \begin{pmatrix} -C_k & S_k J \\ JS_k & JC_k J \end{pmatrix}$$

where

$$C_k \equiv diag \{\cos \theta_{0k}, \cos \theta_{1k}, \ldots \cos \theta_{M/2-1,k}\}$$

$$S_k \equiv diag \{\sin \theta_{0k}, \sin \theta_{1k} \ldots \sin \theta_{M/2-1,k}\}$$

and J is the reversal matrix. It performs a reversing operation. M is the number of channels and K is the overlapping factor. After the butterfly matrices and the pure delays, the last factor of the ELT structure is a type-IV DCT operator.

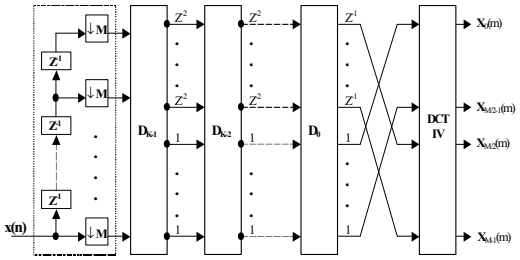

Figure 5. Fast Implementation of Cosine Modulated Analysis Filter Bank

The matrices D_n are the butterfly matrices with nonzero elements on diagonal and antidiagonal direction. With this property, we could scale all the coefficients in the bufferflies D_1 to D_{K-1} , such that all the diagonal entries would be equal to 1 or –1, and the necessary inverse scaling would be applied to D_0. Thus it saves computation complexity. More details on reducing ELT computation are presented in [10].

The sine modulated filter bank has the same computation complexity as the cosine filter bank. In the following Figure 6, an efficient implementation structure for analysis cosine and sine filter banks with M = 4 subchannels, and overlapping factor K = 2 is presented.

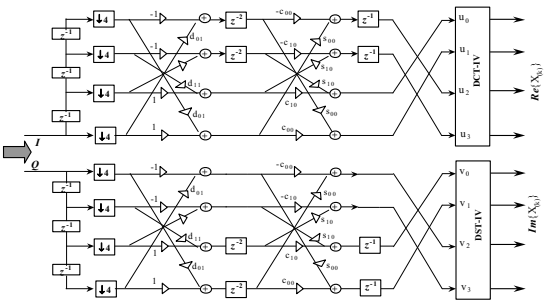

Figure 6. Fast Implementation of cosine and sine Modulated analysis Filter Bank with M = 4, K = 2

❑ **Interference Detection and Suppression**

To implement the detection of interference, the power of the individual subchannels are compared to a threshold and the ones above that threshold value will be suppressed. There are many methods for detection by allowing the threshold to change according to the conditions. Different adaptive threshold calculation methods for FFT-based systems have been studied [11]. In our case, the power of each subchannel is measured, a mean value of them is calculated and then multiplied by a factor to set up the threshold. Each channel power is compared to the threshold. The channel that surpasses the threshold value will be suppressed by not adding them to the output signal. The same process will be repeated in the left channels until all the remaining channels are all under the threshold, see Figure 7. When all channel powers are below the threshold, synthesis filter bank combined the remaining subchannel signals [6].

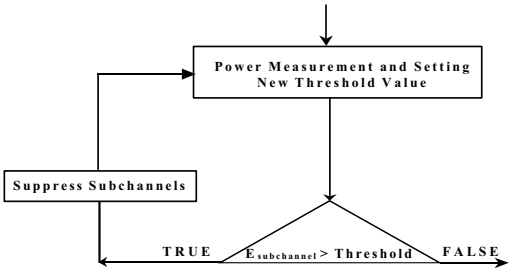

Figure 7. Recursive Interference Detection

4. SYSTEM CONSIDERATIONS AND PERFORMANCE ANALYSIS ON DSP

Using the model stated in the previous section, the system is capable of detecting and removing the interference. In our test, the interference is modeled as a single tone, which has a fixed frequency position at a certain pace.

In our DSP implementation, the codes are built with C and assembly codes. Much effort was devoted to improving the speed with good output accuracy. Auto-scale technique is applied to the DCT IV, DST IV and matrices D_k computation [12][13]. The space requirement of data memory varies with the parameters, such as number of channels, overlapping factor, block size in data acquisition. For the case of M = 128 channels, and overlapping factor K = 4, the maximum memory we used can be seen from Table 1, and it can all be allocated into the memory of Device C6414, which has 16kB internal program memory, and 16kB internal data memory. But as we have seen, there is not much free space left for data memory. In order to make all data running in the internal data memory in the case of K=5, M=128, we have to reduce the length of signal block for which interference suppression is carried out.

Table 1. Memory requirement

	Bytes
Program	**14912**
Data	**15012**

After successfully implementing the interference detection and suppression algorithm and running on the code composer studio for C6414 device, we get the graphics as shown in Figure 8, displaying that the single tone jammer at the fixed frequency location was removed.

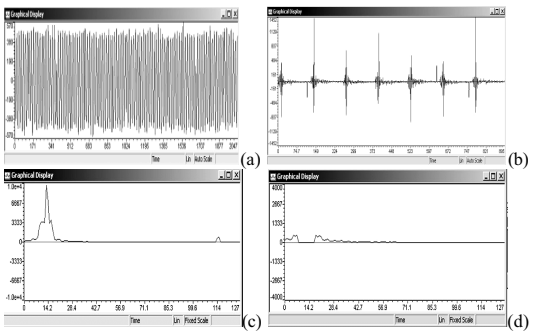

Figure 8. Simulation Graphic Results. M = 128, K = 4. a) Input Time-domain Sequences. b) The Frequency-domain Channel Sequence. c) Channel Power Spectrum. d) Channel Power Spectrum after interference cancellation.

The speed performance is an important aspect in the DSP implementation. Table 2 and 3 show the benchmarks. We only studied the 128, 64, 32 channels filter banks with the roll-off factor ρ =1 and 40~50 dB stopband attenuation (overlapping factor K = 5, 4, 3). The interference detection algorithm uses the block length of 2048 samples to process the signal.

Table 2. Execution time (Cycles)

	M=128	*M=64*	*M=32*
K=5	**126708**	**71322**	**48392**
K=4	**112151**	**62330**	**41362**
K=3	**96629**	**52317**	**34471**

Table 3. Sampling rates (M samples per second)

	M=128	*M=64*	*M=32*
K=5	**9.23**	**8.20**	**6.04**
K=4	**10.43**	**9.38**	**7.07**
K=3	**12.10**	**11.18**	**8.48**

As we can see from Table 3, the maximum achievable sampling rate is over 12M samples per second. Considering we acquire 2048 samples each time, then the highest block acquisition rate is 6 kHz. Actually, detecting and suppressing interference is a recursive one, and the actual speed performance varies a little with the data sequences. In case of no interference, the implementation is faster.

5. CONCLUSION

In this paper, we have studied the structure of cosine and sine modulated filter bank based interference suppression and its fast implementation on a single DSP device C6414. Our aim was to find out what is the achievable sampling rate for different prototype filter banks on the target DSP. The performance was tested and optimized in the TI Code Composer Studio 2.0 environment. Over 12*MHz* sampling rate is achievable for the case of K = 3 and M = 128.

6. REFERENCE

[1] S. Glisic, B. Vucetic, Spread Spectrum CDMA Systems for Wireless Communications, Artech House, 1997

[2] R. A. Monzingo, T. W. Miller, Introduction to Adaptive Arrays. John Wiley and Sons, 1980

[3] P. P. Vaidyanathan, Multirate Systems and Filter Banks, Prentice Hall, NJ, 1993

[4] A. Viholainen, J. Alhava, M. Renfors, "Implementation of parallel cosine and sine modulated filter banks for equalized transmultiplexer systems," *ICASSP*, Salt Lake City, USA, May 2001

[5] A. Viholainen, T. Hidalgo S., J. Alhava, T. Ihalainen, M. Renfors, "Complex modulated critically sampled filter banks based cosine and sine modulation," accepted by *ISCAS 2002*, Arizona, USA

[6] T. Hidalgo Stitz and M. Renfors, "Filter bank based interference detection and suppression in spread spectrum systems", accepted by *ISCAS 2002*, Arizona, USA

[7] T. Saramäki, "Designing prototype filters for perfect reconstruction cosine modulated filter banks," *Proceeding IEEE International Conference on Circuits and Systems*, San Diego, USA, pp. 1605-1608, May 1992

[8] A. Viholainen, T. Saramäki, and M. Renfors, "Cosine modulated filter bank design for VDSL modems," *IEEE Int. Workshop on Intelligent Signal Processing and Communications Systems*, Melbourne, Australia, pp. 143-147, Nov. 1998

[9]H. S. Malvar, "Extended lapped transform: properties, application, and fast algorithms". *IEEE Transaction on Signal processing.* Vol.40, No. 11, November 1992

[10] Yuan Yang, Juuso Alhava, Markku. Renfors, "Implementation of perfect reconstruction cosine-modulated filter banks," in *Proc. The Third European DSP Education and Research Conference* Paris, France, Sept. 2000.

[11] T. J. Kumpumäki, A. Pouttu, J. K. Juntti, "Adaptive transform domain interference suppression in a hybrid DS/FH system," *Proceedings of ISSSTA' 98*

[12] Texas Instruments, TMS320C6000 Optimizing C Compiler User's Guide, (*SPRU187E*), Feb. 1999

[13] Texas Instruments, Auto-scaling Radix-4 FFT for TMS320C6000 DSP, (*SPRA654*), Sep. 2000

Tampereen teknillinen yliopisto
PL 527
33101 Tampere

Tampere University of Technology
P.O. Box 527
FIN-33101 Tampere, Finland